

8-6-2005

## RELIABILITY OF LIGHT-FRAME WOOD ROOF CONSTRUCTION UNDER EXTREME WIND LOADS

Daniel Meireles de Oliveriria Rocha

Follow this and additional works at: <https://scholarsjunction.msstate.edu/td>

---

### Recommended Citation

Rocha, Daniel Meireles de Oliveriria, "RELIABILITY OF LIGHT-FRAME WOOD ROOF CONSTRUCTION UNDER EXTREME WIND LOADS" (2005). *Theses and Dissertations*. 5307.  
<https://scholarsjunction.msstate.edu/td/5307>

This Graduate Thesis - Open Access is brought to you for free and open access by the Theses and Dissertations at Scholars Junction. It has been accepted for inclusion in Theses and Dissertations by an authorized administrator of Scholars Junction. For more information, please contact [scholcomm@msstate.libanswers.com](mailto:scholcomm@msstate.libanswers.com).

RELIABILITY OF LIGHT-FRAME WOOD ROOF CONSTRUCTION UNDER  
EXTREME WIND LOADS

By

Daniel Meireles de Oliveira Rocha

A Thesis  
Submitted to the Faculty of  
Mississippi State University  
in Partial Fulfillment of the Requirements  
for the Degree of Master of Science  
in Civil Engineering  
in the Department of Civil Engineering

Mississippi State, Mississippi

August 2005

Copyright by

Daniel Meireles de Oliveira Rocha

2005

RELIABILITY OF LIGHT-FRAME WOOD ROOF CONSTRUCTION UNDER  
EXTREME WIND LOADS

By

Daniel Meireles de Oliveira Rocha

Approved:

---

Dr. Christopher D. Eamon  
Assistant Professor of Civil Engineering  
(Director of Thesis and Committee Member)

---

Dr. William H. McAnally  
Associate Professor of Civil Engineering  
(Graduate Coordinator)

---

Dr. Masoud Rais-Rohani  
Professor of Aerospace Engineering  
(Committee Member)

---

Dr. Ralph R. Sinno  
Professor of Civil Engineering  
(Committee Member)

---

Dr. Kirk H. Schulz  
Dean of the Bagley College of Engineering

Name: Daniel Meireles de Oliveira Rocha

Date of Degree: August 6, 2005

Institution: Mississippi State University

Major Field: Civil Engineering

Major Professor: Dr. Christopher D. Eamon

Title of Study: RELIABILITY OF LIGHT-FRAME WOOD ROOF CONSTRUCTION  
UNDER EXTREME WIND LOADS

Pages in Study: 160

Candidate for Degree of Master of Science

Light-frame wood construction is frequently used in the U.S. High wind events, such as hurricanes, may cause severe damage to these structures by breaking the roof envelope. This study focuses on computing reliability indices of roof sheathing panels exposed to high wind events while considering a time and spatially varying wind load. A procedure is developed that links probabilistic and dynamic finite element analysis codes. The results show that a few critical panels are most susceptible to damage, while most panels have significantly higher reliability indices than previous studies based on simplified analyses have shown. By setting a target reliability index, panel nail spacing can be adjusted to provide a more uniform level of safety over the entire roof.

## DEDICATION

I would like to dedicate this work to my parents, Jose Carlos and Eliane, for all of their support and love. I would also like to dedicate this work to my (soon to be) wife, Kayla, whose patience, support and love has made this work much easier.

## ACKNOWLEDGEMENTS

I would like to acknowledge the following people for their help in during the completion of this project. First and foremost I would like to thank Dr. Christopher Eamon, my major advisor, for all the help, guidance and support.

I would also like to thank Dr. Ralph Sinno for all the help with the wind loads and for serving on my graduate committee. I want to extend my gratitude to Dr. Masoud Rais-Rohani, for serving my graduate committee.

I also want to thank Mr. Gaurav Savant for all the help with the many computer problems I have encountered, and Mr. Jeremy Lokits for the help with NASTRAN.

Last but not least, I would like to thank my fiancée, Kayla, for all the support, patience and encouragement.

## TABLE OF CONTENTS

	Page
DEDICATION .....	ii
ACKNOWLEDGEMENTS .....	iii
LIST OF TABLES .....	vi
LIST OF FIGURES .....	vii
CHAPTER	
I. INTRODUCTION .....	1
BACKGROUND .....	1
OBJECTIVES .....	3
SCOPE .....	4
II. LITERATURE REVIEW .....	6
WIND DAMAGE AND RESEARCH NEEDS.....	6
RELIABILITY OF LIGHT FRAME WOOD CONSTRUCTION .....	9
III. ROOF MODEL.....	22
TYPICAL SINGLE FAMILY HOUSE IN THE SOUTHERN U.S. ....	22
FEA MODELING OF LIGHT-FRAME WOOD STRUCTURES .....	31
FEA MODEL OF ROOF STRUCTURE .....	33
IV. WIND LOADS .....	50
INTRODUCTION .....	50
ASCE 7-02 WIND LOAD PROVISIONS .....	51
UWO WIND LOAD DATA.....	57
GLOBAL AND LOCAL WIND DISTRIBUTION .....	64



ASCE 7-02 AND DYNAMIC WIND LOAD COMPARISON .....	64
V. RELIABILITY ANALYSIS .....	67
INTRODUCTION .....	67
LIMIT STATE FUNCTIONS .....	68
LOAD AND RESISTANCE STATISTICS .....	69
SOLUTION METHOD .....	71
ANALYSIS PROCEDURE .....	77
COMPARISON WITH PREVIOUS RESEARCH RESULTS .....	79
VI. RESULTS AND CONCLUSIONS .....	81
RESULTS OF RELIABILIT ANALYSIS .....	81
SENSITIVITY ANALYSIS .....	84
COMPARISON WITH PREVIOUS RESULTS .....	88
CONCLUSIONS .....	91
RECOMMENDATIONS .....	93
RECOMMENDATIONS FOR FUTURE RESEARCH .....	94
REFERENCES .....	95
APPENDIX	
A. UWO WIND LOAD AND 20 POINT MOVING AVERAGE .....	99
B. SENSITIVITY CHARTS .....	134
C. NESSUS SAMPLE IMPUT FILE .....	143
D. MONTE CARLO SIMULATION RESULTS .....	158

## LIST OF TABLES

TABLE	Page
2.1 Wind load factor statistics [Rosowsky et al 2000].....	12
2.2 Wind speed statistics [Rosowsky and Cheng, 1999a] .....	14
2.3 Composite Wind Load Statistics.....	14
2.4 Resistance and Dead Load Statistics [Rosowsky and Cheng, 1999b].....	15
2.5 Summary of Results [Rosowsky and Cheng, 1999b] .....	18
3.1 Characteristics of Study House.....	24
3.2 Panel Lay-Up .....	26
3.3 Roof Nailing Schedule [UBC, 1997].....	28
3.4 Comparison Between Analysis Methods [Kasal et al. 2005] .....	32
3.5 Beam Elements (CBAR) used in FEA model.....	35
3.6 Plate Elements (CQUAD4) used in FEA model.....	39
3.7 Properties of Materials.....	44
3.8 Maximum panel forces (deterministic).....	49
4.1 Parameter for ASCE 7-02 wind loads calculations.....	54
4.2 ASCE 7-02 Uplift pressure for zones 1, 2 and 3.....	56
4.3 Summary of UWO wind load data (20 Hz) .....	58
4.4 Pressure distribution for load areas.....	63
4.5 Panel Forces .....	65
5.1 Summary of resistance statistics .....	70
5.2 Summary of dead load statistics .....	70
6.1 Results of Reliability Analyses.....	82

## LIST OF FIGURES

FIGURE	Page
2.1 Rosowsky and Cheng [1999b] Nail spacing for sheathing panels.....	16
2.2 Reliability Index for ASCE 7-95 (p.e.) [Rosowsky and Cheng, 1999b] .....	18
2.3 Details of test (1) [Schiff et al. 1996] .....	19
2.4 Details of test (2) [Schiff et al. 1996] .....	20
2.5 PDF of panel and single nail [Schiff et al. 1996].....	21
3.1 Isometric View of Study House.....	23
3.2 Properties of Structural Lumber.....	25
3.3 Detail of sheathing panel placement.....	27
3.4 Panel numbering and fastening zones.....	27
3.5 Roof fastening zones [UBC, 1997].....	28
3.6 Nail schedule for panels 2 and 4.....	29
3.7 Nail schedule for panels 1, 3, 6, and 8.....	30
3.8 Nail schedule for panels 5, 7, 9, 10, 11, 12, 14, and 16.....	30
3.9 Nail schedule for panels 13 and 15.....	31
3.10 CBAR element coordinates [Lee, 1997].....	34
3.11 CBAR element forces [Lee, 1997].....	34
3.12 Truss Elements (CBAR), X-Y view .....	35
3.13 Ridge Beam and Top Plate details.....	36
3.14 CQUAD element coordinates [Lee, 1997].....	37
3.15 CQUAD element forces [Lee, 1997] .....	38
3.16 Plate elements (CQUAD4) and Nail elements (CROD).....	40
3.17 Forces on CROD element.....	41
3.18 Fully meshed model with outline of panels.....	42

3.19	Element Connectivity.....	42
3.20	Plywood Modulus of Elasticity with respect to span.....	44
3.21	Detail of nail connectivity (Side View).....	45
3.22	Panels and corresponding nails.....	46
3.23	Nail stresses for panel #9, time step = 0.05 sec.....	48
3.24	Nail stresses for panel #9, time step = 1.0 sec.....	48
4.1	Wind load regions for ASCE 7-02.....	50
4.2	ASCE 7-02 external pressure coefficients [ASCE, 2002].....	55
4.3	Quarter roof section with ASCE 7-02 zones 1, 2 and 3.....	56
4.4	Placement of UWO wind load areas.....	59
4.5	Peak loads for UWO data (Area 1).....	61
4.6	Peak loads for 20 point moving average data (Area 1).....	61
5.1	Removal of panels of house in Florida, Hurricane Jeanne [USGS, 2005].....	68
5.2	Removal of panels of building in Florida, Hurricane Jeanne [USGS, 2005] ...	68
5.3	Wind load areas acting directly on Panel #2.....	76
6.1	Sensitivity factors (with respect to std. dev.) for panel #3.....	86
6.2	Sensitivity factors (with respect to std. dev.) for panel #4.....	86
6.3	Sensitivity factors (with respect to std. dev.) for panel #5.....	87
6.4	Sensitivity factors (with respect to std. dev.) for panel #6.....	87
6.5	Sensitivity factors (with respect to std. dev.) for panel #11.....	88
6.6	Results for Clemson 1 Structure using updated statistics.....	90
6.7	Results for 35 RV AFORM analysis.....	90
6.8	Panel nail spacing for target $\beta = 4.0$ .....	93
A.1	Peak loads for UWO data (Area 1).....	100
A.2	Peak loads for 20 point moving average data (Area 1).....	100
A.3	Peak loads for UWO data (Area 2).....	101
A.4	Peak loads for 20 point moving average data (Area 2).....	101
A.5	Peak loads for UWO data (Area 3).....	102
A.6	Peak loads for 20 point moving average data (Area 3).....	102

A.7 Peak loads for UWO data (Area 4).....	103
A.8 Peak loads for 20 point moving average data (Area 4).....	103
A.9 Peak loads for UWO data (Area 5).....	104
A.10 Peak loads for 20 point moving average data (Area 5).....	104
A.11 Peak loads for UWO data (Area 6).....	105
A.12 Peak loads for 20 point moving average data (Area 6).....	105
A.13 Peak loads for UWO data (Area 7).....	106
A.14 Peak loads for 20 point moving average data (Area 7).....	106
A.15 Peak loads for UWO data (Area 8).....	107
A.16 Peak loads for 20 point moving average data (Area 8).....	107
A.17 Peak loads for UWO data (Area 9).....	108
A.18 Peak loads for 20 point moving average data (Area 9).....	108
A.19 Peak loads for UWO data (Area 10).....	109
A.20 Peak loads for 20 point moving average data (Area 10).....	109
A.21 Peak loads for UWO data (Area 11).....	110
A.22 Peak loads for 20 point moving average data (Area 11).....	110
A.23 Peak loads for UWO data (Area 12).....	111
A.24 Peak loads for 20 point moving average data (Area 12).....	111
A.25 Peak loads for UWO data (Area 13).....	112
A.26 Peak loads for 20 point moving average data (Area 13).....	112
A.27 Peak loads for UWO data (Area 14).....	113
A.28 Peak loads for 20 point moving average data (Area 14).....	113
A.29 Peak loads for UWO data (Area 15).....	114
A.30 Peak loads for 20 point moving average data (Area 15).....	114
A.31 Peak loads for UWO data (Area 16).....	115
A.32 Peak loads for 20 point moving average data (Area 16).....	115
A.33 Peak loads for UWO data (Area 17).....	116
A.34 Peak loads for 20 point moving average data (Area 17).....	116
A.35 Peak loads for UWO data (Area 18).....	117

A.36 Peak loads for 20 point moving average data (Area 18).....	117
A.37 Peak loads for UWO data (Area 19) .....	118
A.38 Peak loads for 20 point moving average data (Area 19).....	118
A.39 Peak loads for UWO data (Area 20) .....	119
A.40 Peak loads for 20 point moving average data (Area 20).....	119
A.41 Peak loads for UWO data (Area 21) .....	120
A.42 Peak loads for 20 point moving average data (Area 21).....	120
A.43 Peak loads for UWO data (Area 22) .....	121
A.44 Peak loads for 20 point moving average data (Area 22).....	121
A.45 Peak loads for UWO data (Area 23) .....	122
A.46 Peak loads for 20 point moving average data (Area 23).....	122
A.47 Peak loads for UWO data (Area 24) .....	123
A.48 Peak loads for 20 point moving average data (Area 24).....	123
A.49 Peak loads for UWO data (Area 25) .....	124
A.50 Peak loads for 20 point moving average data (Area 25).....	124
A.51 Peak loads for UWO data (Area 26) .....	125
A.52 Peak loads for 20 point moving average data (Area 26).....	125
A.53 Peak loads for UWO data (Area 27) .....	126
A.54 Peak loads for 20 point moving average data (Area 27).....	126
A.55 Peak loads for UWO data (Area 28) .....	127
A.56 Peak loads for 20 point moving average data (Area 28).....	127
A.57 Peak loads for UWO data (Area 29) .....	128
A.58 Peak loads for 20 point moving average data (Area 29).....	128
A.59 Peak loads for UWO data (Area 30) .....	129
A.60 Peak loads for 20 point moving average data (Area 30).....	129
A.61 Peak loads for UWO data (Area 31) .....	130
A.62 Peak loads for 20 point moving average data (Area 31).....	130
A.63 Peak loads for UWO data (Area 32) .....	131
A.64 Peak loads for 20 point moving average data (Area 32).....	131

A.65 Peak loads for UWO data (Area 33) .....	132
A.66 Peak loads for 20 point moving average data (Area 33).....	132
A.67 Peak loads for UWO data (Area 34) .....	133
A.68 Peak loads for 20 point moving average data (Area 34).....	133
B.1 Sensitivity with respect to standard deviation for Panel #1 .....	135
B.2 Sensitivity with respect to standard deviation for Panel #2 .....	135
B.3 Sensitivity with respect to standard deviation for Panel #3 .....	136
B.4 Sensitivity with respect to standard deviation for Panel #4 .....	136
B.5 Sensitivity with respect to standard deviation for Panel #5 .....	137
B.6 Sensitivity with respect to standard deviation for Panel #6 .....	137
B.7 Sensitivity with respect to standard deviation for Panel #7 .....	138
B.8 Sensitivity with respect to standard deviation for Panel #8 .....	138
B.9 Sensitivity with respect to standard deviation for Panel #9 .....	139
B.10 Sensitivity with respect to standard deviation for Panel #10 .....	139
B.11 Sensitivity with respect to standard deviation for Panel #11 .....	140
B.12 Sensitivity with respect to standard deviation for Panel #12 .....	140
B.13 Sensitivity with respect to standard deviation for Panel #13 .....	141
B.14 Sensitivity with respect to standard deviation for Panel #14 .....	141
B.15 Sensitivity with respect to standard deviation for Panel #15 .....	142
B.16 Sensitivity with respect to standard deviation for Panel #16 .....	142
D.1 MCS results for panel #2 .....	159
D.2 MCS results for panel #3 .....	160

## CHAPTER I

### INTRODUCTION

#### **BACKGROUND**

The vast majority of the structures in the United States are residential structures. Light-frame wood construction is still used in most of the residential structures mainly due to straightforward framing methods, high availability of materials, and economy. Although light-frame residential structures are common, often insufficient engineering knowledge is used in their design, leading to construction irregularities and susceptibility to extreme wind hazards.

Although most current building codes (1997 Uniform Building Code, 2000 International Building Code, etc) provide certain guidelines for structural design in high wind zones (such as nailing schedules and minimum frame spacing), residential structures still experience significant damage caused by hurricanes and other extreme wind events. In 2004, Hurricane Ivan alone produced severe damage to structures in several states. In Mississippi, Alabama and Florida alone over four billion dollars were approved by the Federal Emergency Management Agency (FEMA) for disaster aid, of which over \$1.1 billion was designated for housing assistance. FEMA conducted inspections in one million homes to verify damages and 1.5 million people applied for



some type of disaster assistance [FEMA, 2005].

Light-frame wood houses may experience several different types of failure due to wind load. These failure modes include roof collapse (partial or complete) due to weak connections between roof and walls or loss of roof sheathing, racking failure caused by excessive wind-induced sway, and entire structure lift-off from the foundation. Although any of these failure modes may be experienced during a storm, research has shown that most damage occurs due to component failure of the building envelope. For example, over 50% of all insurance losses are resulted from wind driven rain while most of the residential structures do not experience complete collapse [Sparks et al, 1994]. Therefore it is important to maintain the roof system intact, because even partial removal of the sheathing can result in great damage due to rain.

In general, resistance of structural components and load distribution on structures are not known with certainty, therefore design codes may simplify these variables as deterministic for design purposes. In order to evaluate structural safety, probabilistic methods are required. Probabilistic methods take into account the statistical properties of a design variable (mean, coefficient of variation, probabilistic distribution, etc.) while deterministic methods do not [Cheng, 1998]. Design codes that use a probabilistic approach rely on reliability analysis for the calibration of the code. In the popular code format of Load and Resistance Factor Design (LRFD), design variables are multiplied by partial safety factors  $\phi$  (resistance factor) and  $\gamma$  (load factor) that must be calibrated based on the target reliability index ( $\beta$ ) assumed by the code. The reliability index is calculated using probabilistic methods.

Previous studies [Rosowsky and Cheng, 1999a and 1999b; Rosowsky and Huang, 2000] assessed structural reliability of light-frame components using simplified wind load models but experimental results have shown that significant response difference between actual wind load and simplified static wind load models [Sinno and Taylor, 1995; Fowler, 2001]. Therefore, in order to accurately determine reliability there is need to use better wind load models. Reliability a measure of safety and once reliability indices are accurately determined rational decisions can be made to improve current design procedures. Thus in regions where extreme wind events (such as hurricanes) are an issue, reliability analysis is necessary to determine design procedures that will account for partial failure of roof systems. Houses designed to resist partial roof collapse will experience much less internal damage, therefore reducing the high cost of insurance and repair.

## **OBJECTIVES**

The purpose of this research is to develop a reliability model that can be used to examine the reliability of roofs of light-frame residential construction and determine the reliability of the roof system. To meet these objectives the following tasks will be accomplished:

1. Develop structural model of the roof.
2. Form relevant probabilistic limit states.
3. Identify significant random variables and their statistical parameters.
4. Develop load and resistance models.
5. Develop the reliability model.

6. Conduct probabilistic sensitivity analysis.
7. Compute component and system reliability indices of the roof system.
8. Compare results to existing code design procedures and identify inconsistencies in reliability.
9. Make recommendations for improvement.

This study is unique because it uses detailed finite element model of a residential structure and realistic wind load data developed at the University of Western Ontario. The wind load simulates hurricane forces reaching speeds of 110 miles per hour.

## **SCOPE**

This study consists of developing a finite element model of a idealized house and applying realistic wind loads to the house in order to determine the reliability of the roof sheathing. The study house comprises of a single story structure similar in square footage and construction methods used in the Southern U.S. The house was also designed to meet code requirements (1997 UBC, 2000 IBC).

The roof system is assumed to fail when one single roof sheathing panel fails, as at this point the envelope is broken and rain can enter the building. Previous research at Clemson University has determined resistance statistics for the roof panels [Schiff et al., 1996]. Since sheathing panels normally not break during an extreme wind event, following previous research results, it assumed that pullout of the nails causes the removal of the panels.

The finite element analysis software NASTRAN was coupled with the reliability analysis software NESSUS in order to calculate reliability indices for each of the panels. A series system reliability model is then used to consider overall structural performance.

## CHAPTER II

### LITERATURE REVIEW

#### **WIND DAMAGE AND RESEARCH NEEDS**

Light-frame wood construction refers to structures whose support materials comprise mainly of dimensional lumber (2x4's, 2x6's, etc) and panel products, such as plywood or oriented strand board (OSB), connected together by nails, screws and bolts. This type of construction is extensively utilized in service establishments (such as gas station, hotels, and convenience stores), churches, schools and residential structures. The use of light-frame wood construction is particularly common in residential construction, where approximately 90% of all buildings in the U.S. are constructed using this method [Ellingwood, et al, 2004].

The economical development of regions where hurricane hazards is eminent (specially the southeastern U.S.) has created a need to develop less susceptible residential construction. Most of the damage claims after a major hurricane come from homeowners whose houses did not fully collapse. Sparks, et al. [1994] conducted extensive assessment of insurance claims resulted from hurricanes Hugo and Andrew. This study shows that over 50% of all damage costs resulted from damage to houses. Since most houses do not collapse during the hurricanes, it was observed that most of the insurance losses results

from water damage (caused by wind-driven rain). The study established that component failure, such as the loss of roof sheathing or a door, causes significant water damage to the structure as wind speed reaches 90 miles per hour (mph). As the wind speed reaches 155 mph, the average insurance loss is magnified by a factor of 2, and at 180 mph this factor rises to 9. The authors also discuss that while component failure may lead to collapse of the building in some occasions, the main need is to improve the performance of residential structures for economic rather than public safety reasons

Soltis [1984] observed the performance of low-rise wood structures subjected to extreme natural hazards. The impact of hurricane Camille to residential wood houses was emphasized, since 75000 people were left homeless. Much of the damage caused by Camille resulted from tides of up to 25 feet. However, in regions where water surge was not an issue, damage to the roof was the most frequent occurrence. The roof damage observed was caused by improper connection between roof and walls and damage to the roof covering. It was also observed that hip roofs experienced less damage than gable end roofs. The author also concludes that most of the structures that performed inadequately were marginally engineered or non-engineered structures.

Liu, et al. [1989], conducted research on problems, solutions and research needs to wood houses subjected to wind loads. The authors show that even though extensive damage to structures usually occur when wind speeds reach 100 mph, many buildings experience severe damage at much lower wind speeds. They also indicate that with an increase of 20% in total cost, a light-frame house could resist wind speeds up to 237 mph. The majority of the damage in the houses observed relates to some type of failure of the

roof system. Inadequate connections between roof rafters and top plate are the most common type of failure, followed by joint failure. The study shows that maintaining the integrity of the roof system is imperative in order to maintain a safe structure during an extreme wind event. In the rare event that a house experiences full collapse, it is observed that it is preceded collapse of the roof system. The authors also suggest some solutions using existing technology. Roof collapse usually occurs when a change in internal pressure, combined with exterior suction, causes failure of the roof to wall connection. Since changes in internal pressure during a hurricane occur after the loss of a window or door, it is important to use wind resistant cladding (windows and doors) to avoid the pressure increase. However, the use of wind resistant cladding alone is not enough to build adequate roof systems because roof sheathing is subjected to direct wind loading. The use of special clip connectors instead of toenails also increases the safety of roof systems. The authors conclude that future research is needed to create a greater understanding of the behavior of wood construction, including the experimental tests of wood components, fasteners and joints.

Liu, et al. [1990], suggest the need for developing analytical procedures to predict the effect of wind on light-frame wood houses. The procedures would take into account the several modes of failure observed from post-disaster investigations. The modes of failure include roof detachment from walls, racking failure due to extreme sway, door and window failure (which leads to an increase in internal pressures), and complete house assembly lift-off from its foundation.

## **RELIABILITY OF LIGHT-FRAME WOOD CONSTRUCTION**

The study of wood structures has evolved significantly in the past 20 years, but only recently have reliability concepts and finite element analysis taken a bigger role in the research of wood structures. Since the American Society of Civil Engineers (ASCE) and the National Forest Products Association (NFPA) fashioned the report “Load and Resistance Factor Design for Engineered Wood Construction” in 1988, a reliability based code for wood structures has been developed [Bulleit et. Al 1993]. The most recent version of the National Design Specifications for Wood Construction (NDS 2005) incorporates both allowable stress design (ADS) and load and resistance factor design (LRFD).

Bulleit et al. [1993] conducted an extensive literature review on the reliability of wood structural systems. The authors review past research in wood structures and discuss possible directions for the research on the reliability of wood structures. The behavior of wood systems was first investigated where a linear finite element analysis was used to model the system behavior wood joist floors. This procedure was later advanced to cover non-linear nail behavior. These procedures proved to be of great significance to the study of wood systems when large scale tests later validated analysis results. Further research included development of analytical and experimental procedures for analysis of sheathed stud walls and sheathed roof trusses. The authors emphasize the importance of the analysis of wood systems, whether for a design or research application, since most wood structures are composed of a repetitive series of members (such as roof trusses, floor joist, wall studs, etc). The effects of the sheathing used in many wood systems also play



an important part in the load-sharing mechanisms of these structures. Wood sheathing is responsible for the two primary load-shearing mechanisms in wood structures: two-way action and partial composite action. Two-way action takes place when sheathing is placed across parallel members, such as wood joists and roof trusses, potentially forming a perpendicular beam that reduces deflection and increases the stiffness of the members. The partial composite action takes place when sheathing and members interact in the same direction, essentially forming a T-beam. The increase of stiffness is directly related to the degree of bond between the sheathing and the member. Studies have shown that the increasing the sheathing stiffness and connection to the joist greatly decreases the deflection of joists. The behavior of sheathing and sheathing connection (e.g. nails) and the effects of their stiffening effects should be included in reliability based codes, since much of the behavior of wood systems depends on these elements.

Bulleit et al. also include discussions of the application of system reliability analysis to wood construction. Although the future of wood reliability research falls within system reliability, much research is still needed at both the system and component levels. The classical methods of system reliability, which classify systems as series or parallel, use formulations based on component level reliability to calculate system reliability. These methods need system level reliability information and specific definition of the structure to work properly. Most of the classical methods of analysis of wood structures use first member failure to define system failure (i.e. a series system), especially in low redundancy systems. Monte Carlo simulation has also been used to perform analysis of parallel system behavior. Most of the research on the parallel system

behavior of wood structures considers a limit state where two adjacent members failing leads to system failure [Bulleit et al, 1993]. The authors indicate that although system behavior will play a major role in the research of the reliability of wood systems, component level research is still needed in order to better understand the system behavior and to define appropriate limit states.

Rosowsky and Huang [2000] evaluated a set of wind load statistics for use in reliability analysis of light frame roof construction. The wind load statistics were calculated from wind speed data collected over numerous locations, wind speed data from ASCE 7-95 and statistical information on the various factors from the code specific wind load equation (eq. 2.1, ASCE 7-95).

$$W = 0.00256 \cdot K_z \cdot K_{zt} \cdot V^2 \cdot [(CG_p) - (CG_{pi})] \quad (2.1)$$

The various load factors and their definitions and statistical information are given in Table 2.1, while  $V$  is the wind speed collected in ten separate locations around the southeastern U.S. (NC, SC and FL). The authors then developed a composite set of wind-load statistics based on event-simulation using the Monte Carlo method. Monte Carlo simulation was used to generate statistical information (such as distribution type and statistical moments) for the wind load data collected at each of the ten sites.

Table 2.1 – Wind load factor statistics [Rosowsky et al, 2000]

Factor	Mean	Std. Dev.	Nominal Value	CDF
Exposure Factor, $K_z$	0.80	0.12	0.9	Normal
Topographic Factor, $K_{zt}$	1.0	-	1.0	Deterministic
Importance Factor, $I$	1.0	-	1.0	Deterministic
Gust Factor, $G$	0.82	0.08	0.85	Normal
Pressure Coefficient, $C_p$	-0.69	0.14	-0.7	Normal
Internal Pressure and Gust combined, $GC_{pi}$	0.15	0.05	0.18	Normal
External Pressure and Gust combined, $GC_p$	-1.61	0.19	-1.7	Normal
Wind Direction Factor (C & C)	0.89	0.14	-	Normal
Wind Direction Factor (MWFRS)	0.86	0.10	-	Normal

The average of the simulation results from each site determined the composite set of statistics. The results indicate that if a lognormal distribution is considered, a mean-to-nominal ratio (bias factor,  $\lambda$ ) of 0.53 and COV of 0.48 may be used assuming a 50 year maximum wind speed. If an extreme type I distribution is considered, a bias factor of 0.46 and COV of 0.64 are appropriate for 50 year maximum wind speed. These results are intended to be used for the reliability of light-frame wood construction.

Rosowsky and Cheng [1999a and 199b] performed extensive reliability analysis of light-frame roofs subjected to high winds. The study consisted of analyzing the safety of certain roof components using the Advanced First Order Second-Moment (AFOSM) technique. Three houses were selected to represent typical residential structures located in the southeastern U.S. The structures are similar in floor plan, but have different roof configurations. The houses differ in roof slope, number of stories, and amount of roof overhang.

The study calculated reliability indices for roof-to-wall connections and sheathing for the three baseline houses. The wind load applied to the structures was calculated

using code loads (ASCE 7-93, ASCE 7-95, 1995 SBC high wind edition, SBCCI standard for hurricane resistant residential construction) as nominal loads and a statistical data set of the wind loads was developed from observations in several locations. The nominal loads were calculated for each sheathing panel and 11 roof-to-wall connections, corresponding to one quarter of the roof of each house. Additionally, wind loads calculated using ASCE 7-93 [ASCE, 1993] and ASCE 7-95 [ASCE, 1995] were computed differently for the roof-to-wall connections and the sheathing panels. The roof-to-wall connections loads were calculated using the main wind force resisting system method and wind load for the sheathing panel were calculated using the components and cladding method.

Once the nominal loads for each component were calculated, a statistical analysis for the wind load was performed. The approach taken to analyze the wind loads was similar to the analysis performed by Ellingwood et al. [1980]. This method utilized the wind load statistics collected at several locations over a number of years. The extreme wind speed statistics are combined with the statistical parameter for the ASCE wind load equations (eq. 2.1) and the distribution of the wind load is determined using Monte Carlo simulation. Ellingwood et al. [1980] found the distribution in non-hurricane regions to fit an Extreme Type I distribution when fitted over the 90<sup>th</sup> percentile of the range (the region they assumed to be important for structural reliability analysis). For each site studied, a bias factor ( $\lambda$ ) and COV are determined. A composite set was then determined to have bias factor of 0.78 and COV of 0.37 (for non-hurricane regions). Rosowsky and Cheng [1999a] performed similar analysis using data collected in 5 locations in the

hurricane-prone region of the North and South Carolina coast. Table 2.2 illustrates the wind speed statistics collected from each site. The wind speed for each independent site is best described by an Extreme Type I distribution. [Rosowsky and Cheng, 1999a]

Table 2.2 – Wind speed statistics [Rosowsky and Cheng, 1999a]

Parameters	Location				
	Charleston 1	Cape Hatteras 1	Cape Hatteras 2	Wilmington 1	Wilmington 2
# of Years	35	37	105	24	105
Mean (mph)	57.68	64.02	69.03	58.54	61.71
Std Dev (mph)	9.89	12.08	14.23	10.84	13.45
COV	0.17	0.19	0.21	0.19	0.22

In order to determine the distribution of the 50-year maximum wind load the authors used Monte Carlo simulation. Subsequent exploration of the simulations results shows that the 50-year maximum wind load ( $W$  from eq. 2.1) was best described by a lognormal distribution. The authors fitted the results above the 90<sup>th</sup> percentile of the loads in order to obtain the lognormal distribution parameter, therefore utilizing the same methodology used by Ellingwood et al. [1980]. The results of the 50-year maximum wind load analysis yielded a single set of composite statistics (based on the five sites listed on Table 2.2) with characteristics listed on Table 2.3.

Table 2.3 – Composite Wind load Statistics

Distribution Type	Lognormal
Bias Factor ( $\lambda$ )	0.41
COV	0.41

Rosowsky and Cheng [1999b] finalized the study by performing a reliability analysis in each of the three baselines houses. The analysis was based on the limit state function listed below.

$$g(x) = R - (W - D) \quad (2.2)$$

Where  $x$  is the vector of random variables,  $R$  is the resistance of the component,  $W$  is the wind load and  $D$  is the dead load that acts upon the component. The resistance and dead load statistics are described in table 2.4. The sheathing panels used for the reliability are 4' X 4' and 4' X 8', 15/32 in. thick plywood panels as shown in figure 2.1.

Table 2.4 – Resistance and Dead Load Statistics [Rosowsky and Cheng, 1999b]

Resistance	Mean	COV	CDF
4' X 4' Panels	73.3 psf	0.20	Normal
4' X 8' Panels	57.7 psf	0.20	Normal
Roof-to-Wall Connection	1312 lb	0.10	Normal
Dead Load	Mean	COV	CDF
Dead Load on Sheathing	3.5 psf	0.10	Normal
Dead Load on Roof-to-Wall Connections	15 psf	0.10	Normal

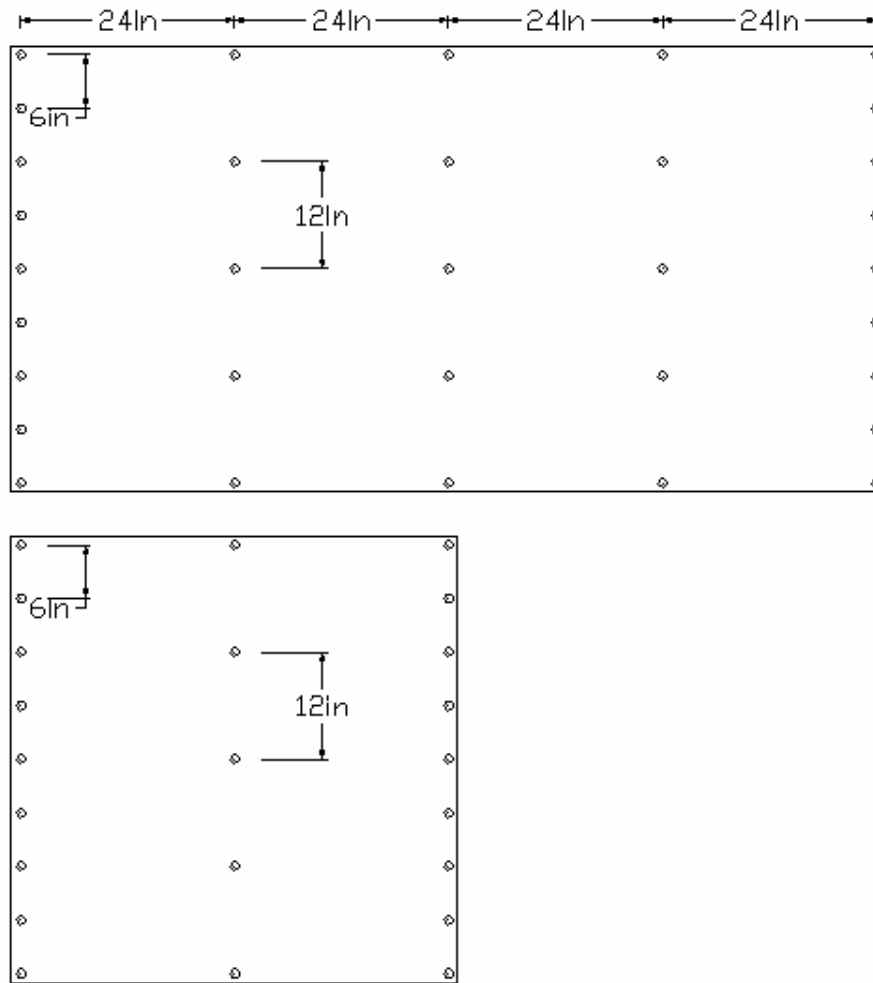


Figure 2.1 – Rosowsky and Cheng [1999b] Nail spacing for sheathing panels.

The resistance statistics are based on nail pullout. Thus, the number of nails in the panel is directly related to the resistance of the panel and the amount of force each nail experiences is directly related to the tributary area of the nail. In the case of the panels nailed as shown in figure 2.1 the mean resistance pressure of the panel 73.3 psf with a COV of 0.20 (for a 4' x 8' panel). The roof to wall connection is assumed to be made using Simpson H2.5 strap and its statistics were developed through a series of tests.

Although the roof-to-wall connections statistics are very specific to a type of connection, this is the type of connection preferred by builders and required by many codes.

The limit state function, defined in Eq. 2.2 contains random variables that have normal (dead load and resistance) and lognormal (wind load) distributions; therefore, AFOSM was then used to calculate reliability coefficients for each component. The analyses performed showed that the sheathing panels with the lowest reliability indices ( $\beta$ ) occurred near the gable end. This is expected since this is the region where the uplift loads are higher. The analyses also show that the lowest  $\beta$  for the roof-to-wall connection occur at the second or third connection from the gable end. This appears to take place because the first connection has only half of the tributary area of the second and third, and although is it located in the region of higher uplift it does not receive the highest loads. A sample of the reliability indices is presented in figure 2.2. It is important to note that when the Main Wind Force Resisting System method is used for design, reliability indices for the roof-to-wall are significantly higher (up to  $\beta = 10.0$ ). This is expected, since MWFRS calculations usually yield lower uplift forces when compared with the Components and Cladding method.



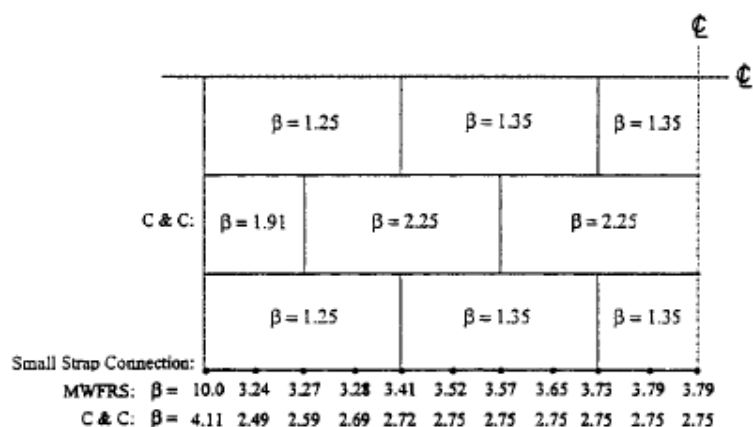


Figure 2.2 – Reliability indexed for ASCE7-95 (p.e.) [Rosowsky and Cheng, 1999b]

Table 2.5 – Summary of results [Rosowsky and Cheng, 1999b]

Structure	Code	Sheathing Panels					Roof-To-Wall Connections			
		Location (C&C only)					Location and Method			
		Soffit		Ridge		Interior	MWFRS		C&C	
	Edge	Interior	Edge	Interior	Roof	Gable	Interior	Gable	Interior	
Clemson 1	ASCE 7-93 c	1.92	2.03	1.92	2.03	3.30	10.0	10.0	3.55	4.11
	ASCE 7-95 c	1.81	1.93	1.81	1.93	3.22	10.0	10.0	3.42	3.81
	ASCE 7-93 p	1.61	1.71	1.61	1.71	2.72	4.42	4.42	2.99	3.30
	ASCE 7-95 p	1.25	1.35	1.25	1.35	3.25	3.24	3.79	2.49	2.75
	WFCM	2.68	2.77	2.68	2.77	3.76	10.0	10.0	-	-
	SSTD 10-93	-	-	-	-	-	10.0	10.0	-	-
NAHB 1	ASCE 7-93 c	1.92	2.04	-	2.26	3.30	10.0	10.0	3.17	3.61
	ASCE 7-95 c	0.57	0.66	-	0.83	1.55	4.42	10.0	1.58	1.61
	ASCE 7-93 p	1.61	1.71	-	1.87	2.72	3.62	3.62	2.60	2.96
	ASCE 7-95 p	0.21	0.29	-	0.43	1.02	2.27	3.22	0.99	1.09
	WFCM	2.68	2.77	-	2.95	3.76	10.0	10.0	-	-
	SSTD 10-93	-	-	-	-	-	10.0	10.0	-	-
NAHB 2	ASCE 7-93 c	2.69	2.71	-	2.87	2.97	10.0	10.0	3.58	3.75
	ASCE 7-95 c	0.42	0.51	-	1.01	1.39	3.16	10.0	1.44	1.54
	ASCE 7-93 p	2.18	2.20	-	2.34	2.43	3.51	3.51	2.88	2.97
	ASCE 7-95 p	0.09	0.17	-	0.55	0.86	2.17	2.94	0.86	0.97
	WFCM	2.19	2.29	-	2.83	3.29	4.17	10.0	-	-
	SSTD 10-93	-	-	-	-	-	4.17	10.0	-	-

Rosowsky and Cheng [1999b] conclude that a few roof components control the ultimate capacity of the roof system (refer to Table 2.5). Particularly, some components at the corners of the roof appear to be more susceptible to failure than interior components. The lowest reliability index found during the analysis was  $\beta = 0.09$ , which

implies a probability of failure  $P_f = 46.4\%$ . Although this number is very high, it is important to note that this structure was the most susceptible to high wind loads because it was the tallest (the only 2 story structure considered), widest (28 ft), largest roof slope (8:12) and had one foot of roof overhang.

Shiff et al. [1996] conducted a series of tests to evaluate the uplift capacity of nailed roof sheathing panels. Two types of tests were performed: (1) single fastener withdrawal tests and (2) Roof sheathing panel tests. Both tests considered the use of 8d smooth shank nails hand driven into southern pine framing members. The tests specimens were prepared one week prior to testing. Figures 2.3 and 2.4 show the details of tests (1) and (2).

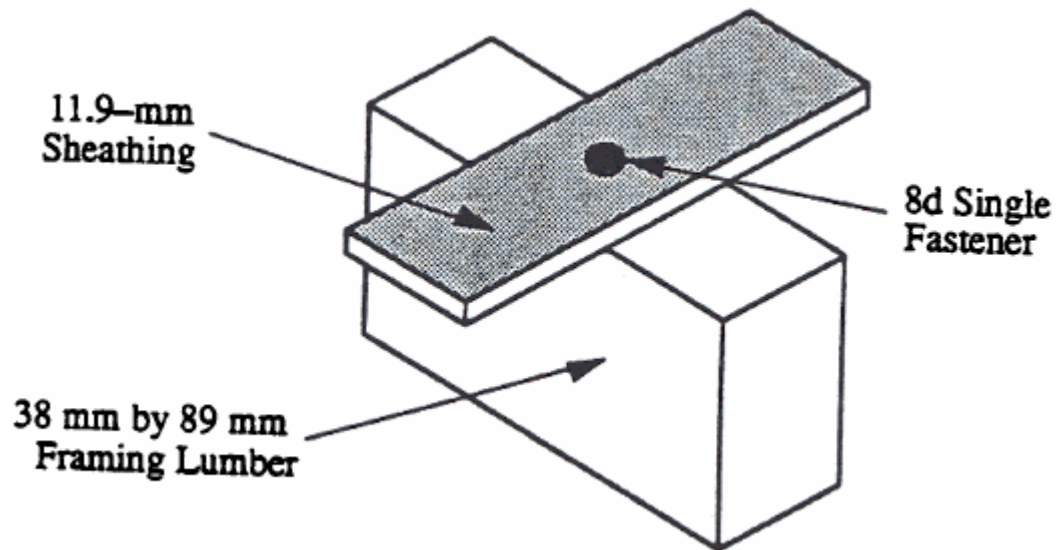


Figure 2.3 – Details of test (1) [Schiff et al. 1996]

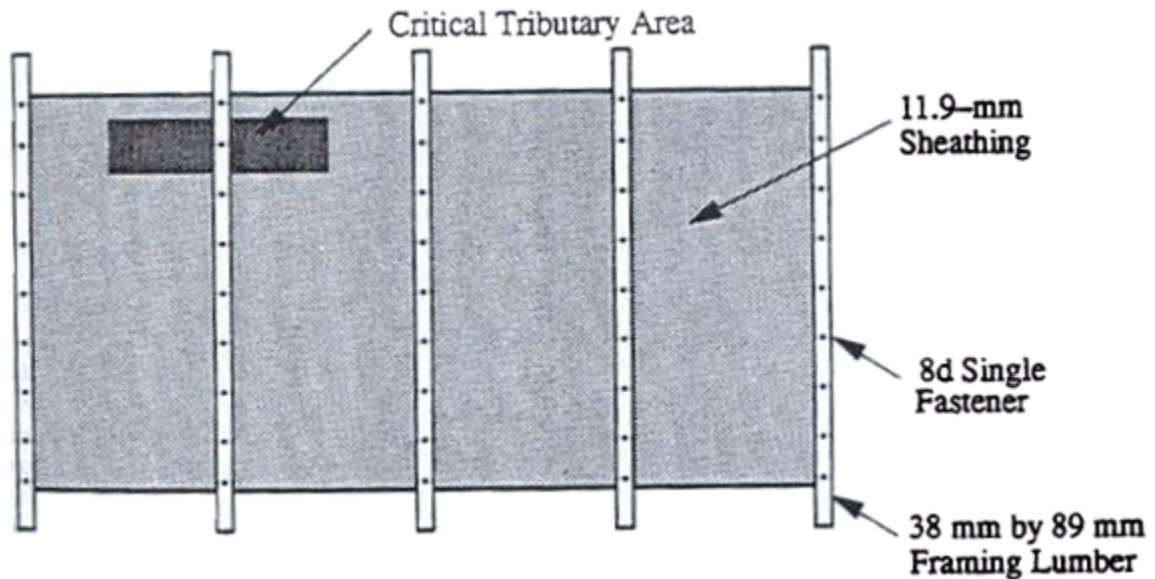


Figure 2.4 – Details of test (2) [Schiff et al. 1996]

Test (1) was conducted using a universal testing machine with cross head speed kept at 0.10 inches per minute. Each fastener was tested until failure. Failure took place either by pull-out or pull-through. Pull-out occurred when the nail is completely removed from the framing member. Pull-through occurred when the head of the nails broke through the sheathing. The authors note that pull-out occurred much more frequently than pull-through. The 40 tests conducted were best described by a Normal distribution with mean of 169 lb and COV of 0.41. The 5% exclusion value was 55 lb. Test (2) was conducted using 4 ft by 8 ft Oriented Strand Board (OSB) sheathing panels of 15/32 in thickness. The framing members consisted of 2" x 4" structural lumber (southern pine), the same size and type used during the single fastener withdrawal test. The fasteners were spaced 6 inches on centers. The sheathing panels were tested with the Building Research Establishment Real-Time Wind Uniform Load Follower (BRERWULF) at Clemson

University. The BRERWULF system has the capacity to apply positive or negative uniform (uplift) up to 209 psf. The panels were loaded with uniform uplift pressures that increased 1 psf every 1.5 seconds. The 30 tests conducted were best described by a Normal distribution with mean 131 psf and COV of 0.14. The 5% exclusion value was 101 psf. It was observed that when a panel was loaded to failure, noticeable separation of one or more nails takes place before complete panel failure. The authors also observed the panel failure occurred promptly after first nail failure. A series system approach to panel failure was suggested when using a critical tributary area of 1.10 ft. The PDF for the single nail withdrawal and the panel series system are shown in figure 2.5.

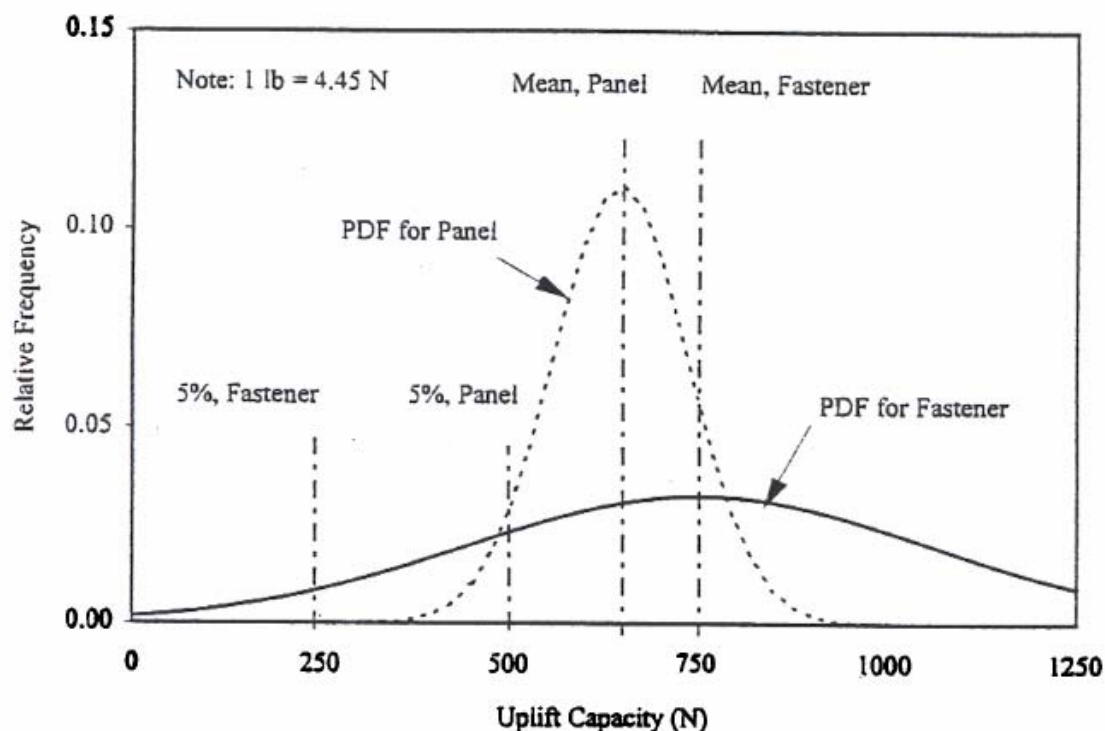


Figure 2.5 – PDF of panel and single nail [Schiff et al. 1996]

## CHAPTER III

### ROOF MODEL

#### **TYPICAL SINGLE FAMILY HOUSE IN THE SOUTHERN UNITED STATES**

The housing industry in the United States is known for the use of wood products. Although other materials, such as reinforced concrete and steel, have experienced an increase in use in this segment of the construction business, the vast majority of new residential construction in this country still uses wood as the material of choice. Light frame wood construction is widely used mainly because of familiar construction methods, low cost, and availability. This study focuses on single story, light-frame wood houses that represent a typical residence in the southern United States.

The study house was designed to meet both code requirements and typical construction in the state of Mississippi. The 1997 Uniform Building Code and 2000 International Building Code were used to establish minimum requirements. The American Plywood Association's (APA) Engineered Wood Construction Guide was used as a guideline for design. In addition to codes and guides, Dr. Harry Cole, PE (Professor of Civil Engineering) and Dr. David Lewis, AIA (Professor of Architecture) were consulted to ensure that the house conformed to common construction practices.

The study house is a single story idealized structure that is similar in construction to typical residences in the United States. The 2003 American Housing Survey for the

United States indicates that the average size for a residence in the U.S. is 1708 squared feet. Over 70% of all housing units are 1 or 2 stories tall and over 63% of all new residences have 1 or 2 stories. In order to represent a typical house in the state of Mississippi, Dr. David Lewis suggested that the size of the study house should be slightly smaller than 1700 sq. ft. and one story would be more representative than a two story dwelling. Dr. Harry Cole indicated that residential construction in Mississippi usually consists of 2x4 stud walls spaced 16 inches on center while roofs are typically composed of 2x6 rafters spaced 24 inches on center. These numbers are in accordance with the minimum requirements of the 1997 UBC, 2000 IBC and the Engineered Wood Construction Guide. Figure 3.1 shows an isometric view of the idealized structure and Table 3.1 summarizes the characteristic of the study house.

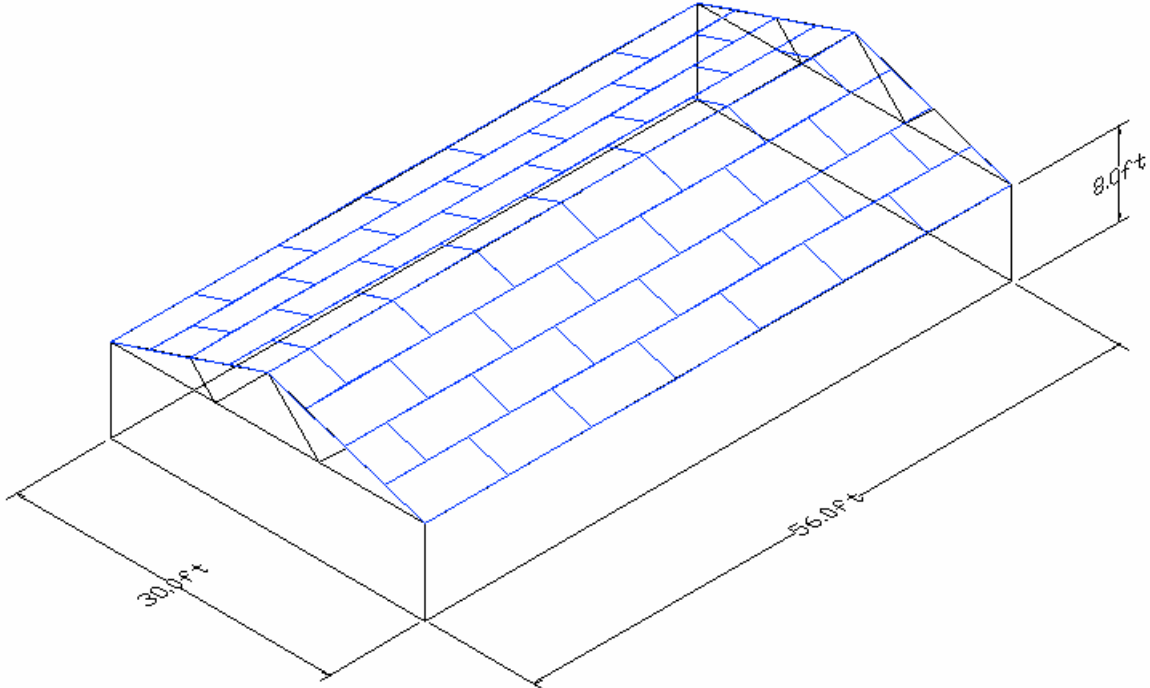
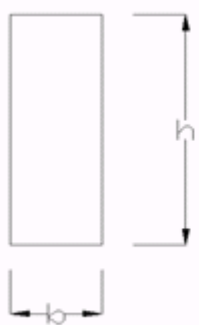


Figure 3.1 – Isometric View of Study House

Table 3.1 – Characteristics of Study House

Type	Wood Frame - Single Story
Wood Type	Southern Pine - Grade 3 or better
Dimensions	30 ft x 56 ft = 1680 sq. feet
Walls	2 x 4's 16" OC, 8' high. Double top plate composed of 2 2x4's attached together
Roof	Gable end, Truss type, Fink profile. All chords 2 x 6's 24" OC. 4:12 slope. Crest is 13' above ground level.
Roof Sheathing	4' x 8', ½" thick Plywood Panels.
Fasteners	8d common nails.

Since the roof is the main focus of this study, much attention to detail was included in the finite element model. The selection of a truss type roof is consistent with current research on wood houses and common construction practices. This type of roof consists of a series of roof trusses spaced according to a roof truss designer or fabricator. Roof trusses have grown in popularity recently because of their low cost, availability, easy installation, and durability. The most common roof trusses follow either a Fink (W) or Howe (K) profiles. Fink profiles usually span 16 to 33 feet and are very common in residential applications. Howe profiles usually span 24 to 36 feet and are used for large residences and commercial applications. The Fink profile was selected for the study house because it is more applicable to small residential applications. The trusses selected are made of 2x6's, commonly used in residential applications. The top-plate of the wall, which connects to one end of the roof trusses, were modeled as double 2x4's, creating a single member. The ridge beam consists of a 2x6 that is securely attached to the top of the truss system. The ridge beam is intended to connect all trusses together to form a continuous load path from the top of the roof all the way to the foundation.



Nominal Dimensions $b \times h$	True Dimensions	Area	Moment of Inertia ( $I_{zz}$ )	Moment of Inertia ( $I_{yy}$ )
in	in	in <sup>2</sup>	in <sup>4</sup>	in <sup>4</sup>
2 x 4	1.5 x 3.5	5.25	5.36	0.98
2 x 6	1.5 x 5.5	8.25	20.8	1.55

Figure 3.2 – Properties of Structural Lumber

The roof panels are of particular interest to this study. The typical house roof is constructed with plywood or Oriented Strand Board (OSB) sheathing connected to the roof rafters (or trusses) by nails. Typically, plywood and OSB panels are classified by type, grade and lay-up. The application of the plywood panel determines which type of panel should be selected. Plywood panels usually fit into two broad categories: Non-exterior and Exterior type. Exterior type panel is fabricated to be 100 percent water-resistant and should be used when weathering is an issue. Non-exterior panels are more applicable for indoor use. Although type of plywood is a concern for builders and architects, it becomes unimportant to this study because type does not affect structural strength. Grade is somewhat more important to structural performance. Plywood grades also indicate intended use, such as Structural I (commonly used for box beams and stresses skin panels) and APA-rated sheathing (commonly used for wall and roof sheathing). The study assumes APA-rated sheathing is used for the study house. Lay-up is the most important factor for specifying plywood panels. Lay-up is a common term that describes number of plies, number of layers, thickness of panel, span rating and



species of each ply. The characteristics of the panels used in this study are described in Table 3.2.

Table 3.2 – Panel Lay-up

Number of Plies	5
Number of Layers	3
Thickness of Panel	0.5 in
Span Rating	24/16
Species of each Ply	Southern Pine for all plies

Although it is important to have the stiffness properties of the plywood panels for this study, it has to be noted that they almost never rupture during wind events. Schiff et al. [1996] discuss that panels tested failed due to separation of the panels from the framing members and this occurs either pull-out (when the nails are removed from the framing) or pull-through (when the nail stays partially connected with the framing member). Also, Herzog [2005] indicates that plywood seldom fails during a wind storm, and as a rule fastener failure occurs prior to panel breakage. Therefore, panel pull-out will be considered for this study, but not panel rupture (i.e. bending failure). The sheathing panels are placed in a staggered manner, as shown in Figure 3.3. Although this is an optional procedure, almost all builders construct roofs this way. Since the house is symmetrical about two axes, only one quarter of the roof was modeled. Figure 4.4 shows the panel numbering and roof fastening zones.

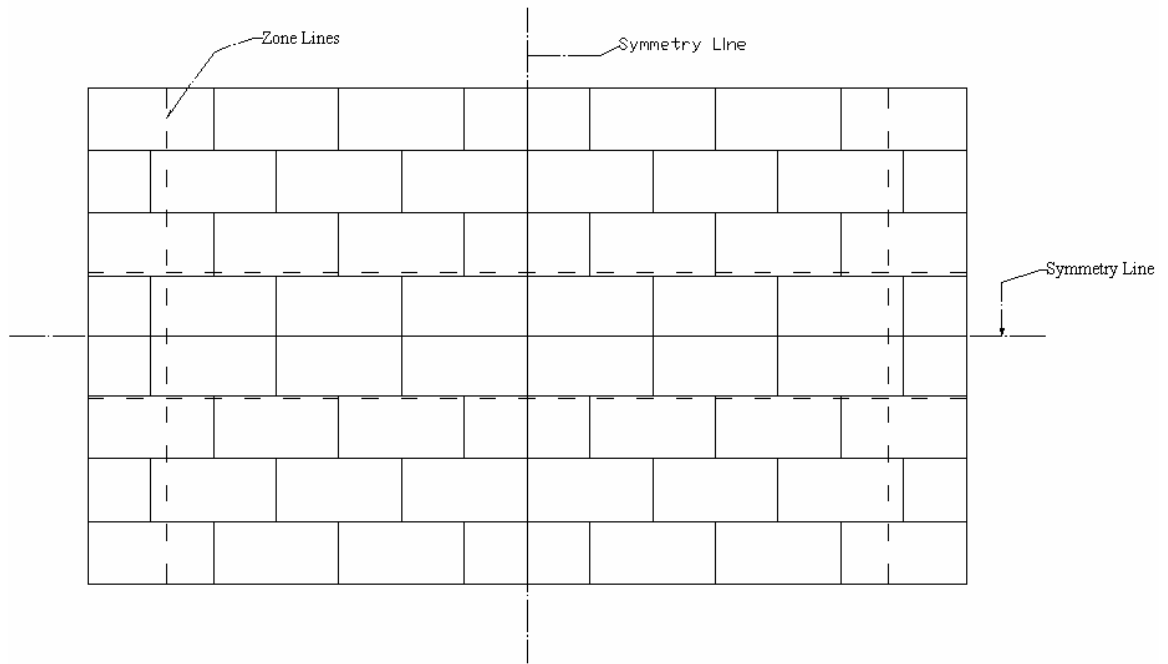


Figure 3.3 – Detail of sheathing panel placement

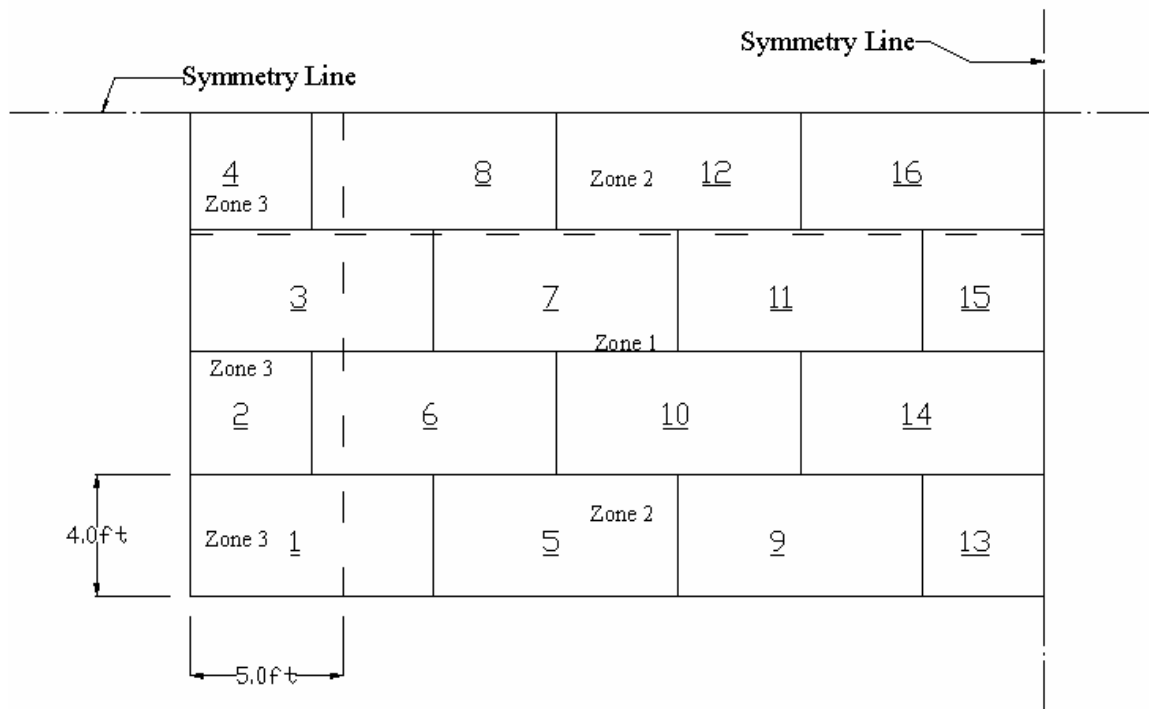


Figure 3.4 – Panel numbering and roof fastening zones

Houses are typically framed using common nails at spacing determined by code (nail schedule). 8d (eight penny) nails are very common for housing applications, and their use is recommended by many codes and standards. The fastening schedules for hurricane prone regions are identical for all the codes considered here (UBC 1997, IBC 2000, and APA 2003). The schedule divides the roof in three separate regions and assigns a nails spacing for each region. The nail schedule also recommends the type and size of nail to be used (8d nails in this case).

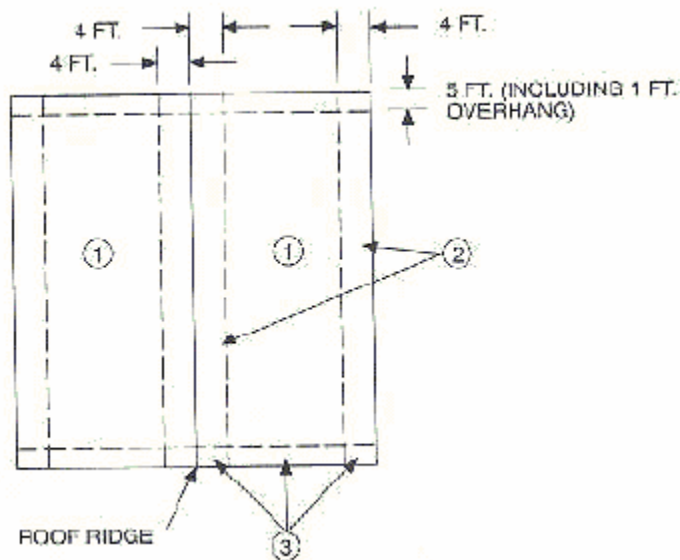


Figure 3.5 – Roof fastening zones [UBC, 1997]

Table 3.3 – Roof Nailing Schedule [UBC, 1997]

Wind Region	Nail Type	Panel Location	Roof Fastening Zone		
			1	2	3
			Nail Spacing (inches o.c.)		
(1) Greater than 90 mph	8d common	Edge	6	6	4
		Field	6	6	6
(2) Between 80 and 90 mph	8d common	Edge	6	6	4
		Field	12	6	6
(3) 80 mph or less	8d common	Edge	6	6	6
		Field	12	12	12

The roof fastening zones illustrated in Figure 3.5 were superimposed in Figure 3.4, where it can be observed that some panels fall within two separate nailing zones. The wind load used in this study was developed at the University of Western Ontario and it corresponds to 110 mph winds at 33 ft above ground [Fowler, 2001]. Table 3.3 specifies that the study structure falls within wind region greater than 90mph and should have fasteners spaced in wind region 1. Nail spacing for zones 1 and 2 are identical, regardless of edge or field location. Nails located in zone 3 should be spaced either 4 or 6 inches, depending on location. Refer to figures 3.6 though 3.9 for the nailing details of each panel.

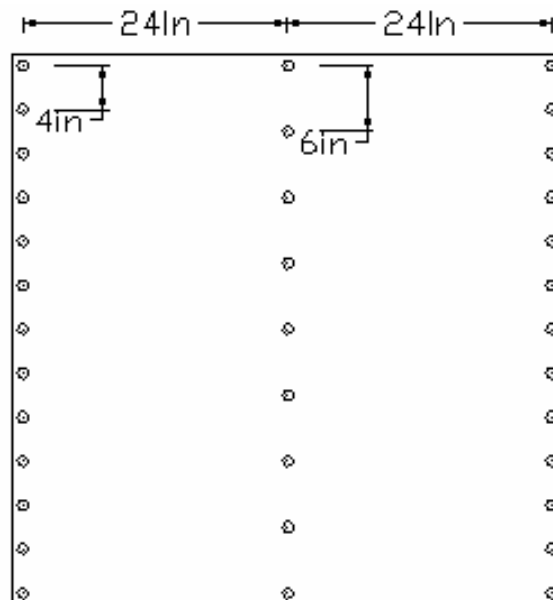


Figure 3.6 – Nail schedule for panels 2 and 4.

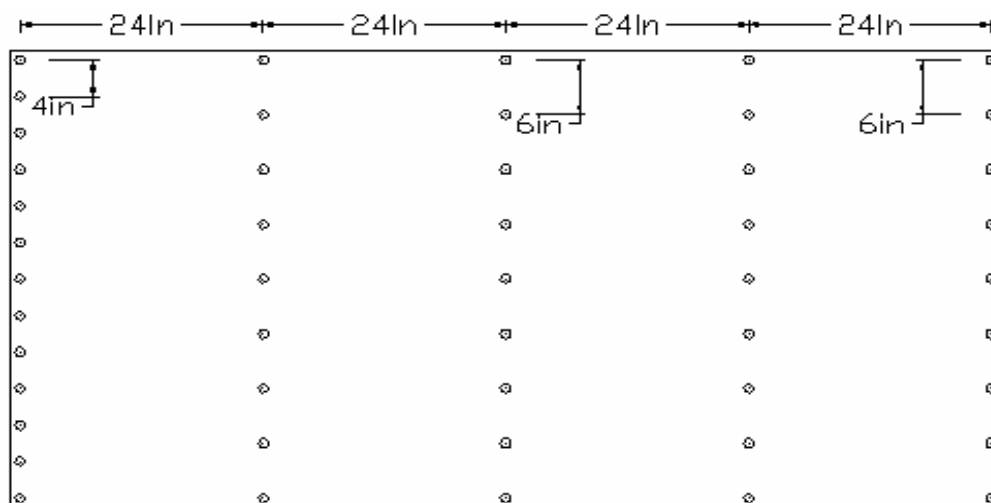


Figure 3.7 – Nail schedule for panels 1, 3, 6, and 8

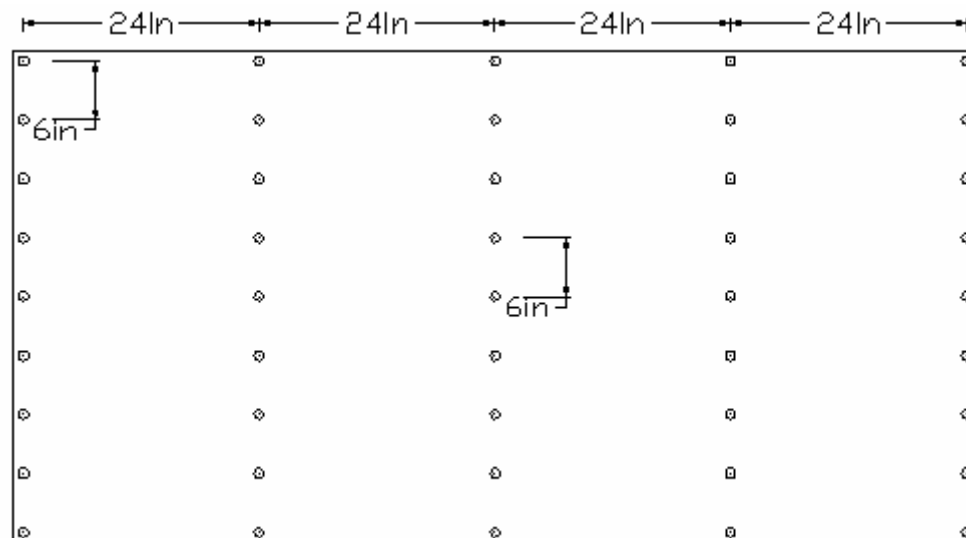


Figure 3.8 – Nail schedule for panels 5, 7, 9, 10, 11, 12, 14 and 16

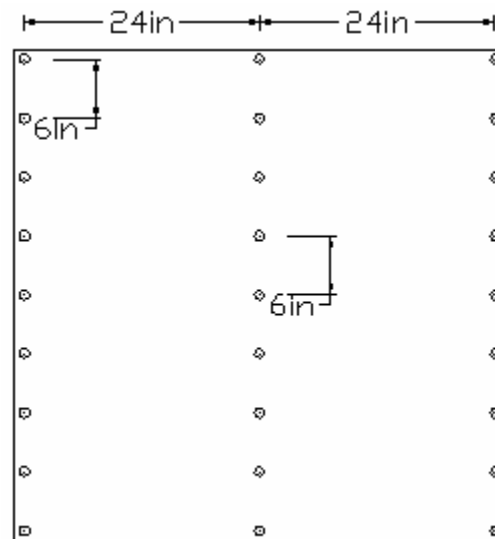


Figure 3.9 – Nail schedule for panels 13 and 15

### FEA MODELING OF LIGHT-FRAME WOOD STRUCTURES

The use of the finite element methods on wood structures is relatively new. Wood structures were built many years before sophisticated numerical methods were developed, and much of their analysis is based on traditional analytical methods. Although all of these analytical methods have their own merit, some of the assumptions made could lead to unrealistic results for research purposes. For example, the Total Shear Method [Kasal et al, 2004] of analysis of wood structures (for lateral loads) is highly dependent on the engineer's judgment. The method assumes that the total shear resisted by the walls must equal the total applied shear, but the load distribution is left to the designer. Clearly, the designer's experience and knowledge impacts the final load distributions [Kasal et al, 2005]. The Tributary Area Method [Kasal et al, 2004] assumes that load distribution is directly related to the tributary area of the particular member. This method does not

include the effects of member stiffness on the load distribution, which may produce inaccurate results [Kasal et al. 2004].

Kasal et al. [2004] conducted analysis on a single story, light frame wood house to determine which methods could better predict the true distribution of the wind loads applied to the structures. Eight of the most common methods for the analysis and design light frame wood structures were compared to the Finite Element Analysis (FEA) results, and then later compared to full scale testing. The analysis compared the wall reactions estimated by each method with the wall reactions obtained with the FEA analysis. The reactions at walls 1 through 4 (W1 – W4) are presented in Table 3.4.

Table 3.4 – Comparison Between Analysis Methods [Kasal et al. 2005]

Analysis Method	Calculated Reaction Force (kN)					% error from FEA			
	W1	W2	W3	W4	Total	W1	W2	W3	W4
Tributary Area	4.81	9.99	7.47	7.19	29.46	230	62	-49	-6
Relative Stiffness	0.86	6.79	13.58	8.48	29.71	-41	10	-7	11
Relative Stiffness w/ Torsion	1.18	8.41	13.25	6.66	29.50	-19	37	-9	-13
Simple Beam	3.30	9.89	11.55	4.96	29.70	126	61	-21	-35
Continuous Beam	1.55	11.40	13.22	3.50	29.67	6	85	-10	-54
Rigid Beam on Inelastic Springs	2.07	7.87	19.92	0.17	29.69	42	28	36	-102
Plate 1* (E = 11,300 Mpa)	1.22	4.81	17.05	6.62	29.70	-16	-22	17	-13
Plate 2* (E = 1,130 Mpa)	1.57	6.05	15.65	6.44	29.71	8	-2	7	-16
FEA	1.46	6.15	14.61	7.64	29.86	-	-	-	-

\* Plate 1 = Rigid Plate Method. Plate 2 = Flexible plate Method.

Once the eight methods were compared with the FEA analysis, the three methods that presented the closest results to FEA results (Rigid Beam Model, Plate Method 1 and 2) and the FEA method itself were compared with results obtained from a full scale testing of the structure using four separate tests. The full-scale tests applied prescribed

displacements to the structure and measured the wall reactions in 60 separate load cells. After the tests, it was determined that the FEA analysis predicted the reactions most accurately. In most cases the FEA analysis predicted results within 10% from the measured reactions, including some instances with 0% error. The other 3 methods also compared well to the measured reactions (usually within 20% of the measured reaction), and their use could be justified by their relatively simple procedures. The method most commonly used, the Tributary area method, performed very poorly compared with the FEA method. This method may over-predict loads by as much as 130% (leading to uneconomical designs) or under-predict loads by as much as 60% (leading to unsafe designs). The authors also point out that a FEA analysis is worthwhile for light-frame wood structures, since it tends to lead to safe and economical designs.

### **FEA MODEL OF ROOF STRUCTURE**

The finite element model is used to replicate in detail the roof structure described previously (Figures 3.1, 3.3, 3.4, 3.6, 3.7, 3.8, and 3.9). The model consist of rod, beam and plate elements intended to model the behavior of each component of the roof system. The commercial finite element code MSC/NASTRAN v. 2001 was used for the analysis.

The roof rafters and wall top-plate were modeled as two-node, beam elements (CBAR). CBAR stiffness matrix is derived from traditional (Euler) beam theory and assumes that plane cross-sections remain plane [Lee, 1997]. CBAR elements allow the user to define bending and shear stiffness characteristics in two perpendicular directions,



which allows for bending in two axes. Two nodes with six degrees of freedom each (three rotational and three translational) define the CBAR element (refer to Figure 3.10).

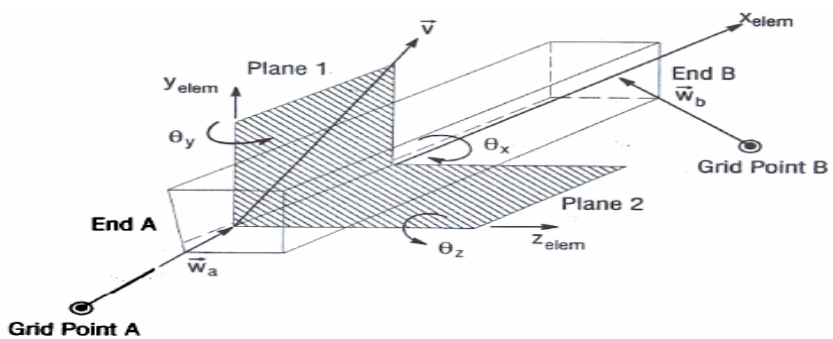


Figure 3.10 – CBAR element coordinates [Lee, 1997]

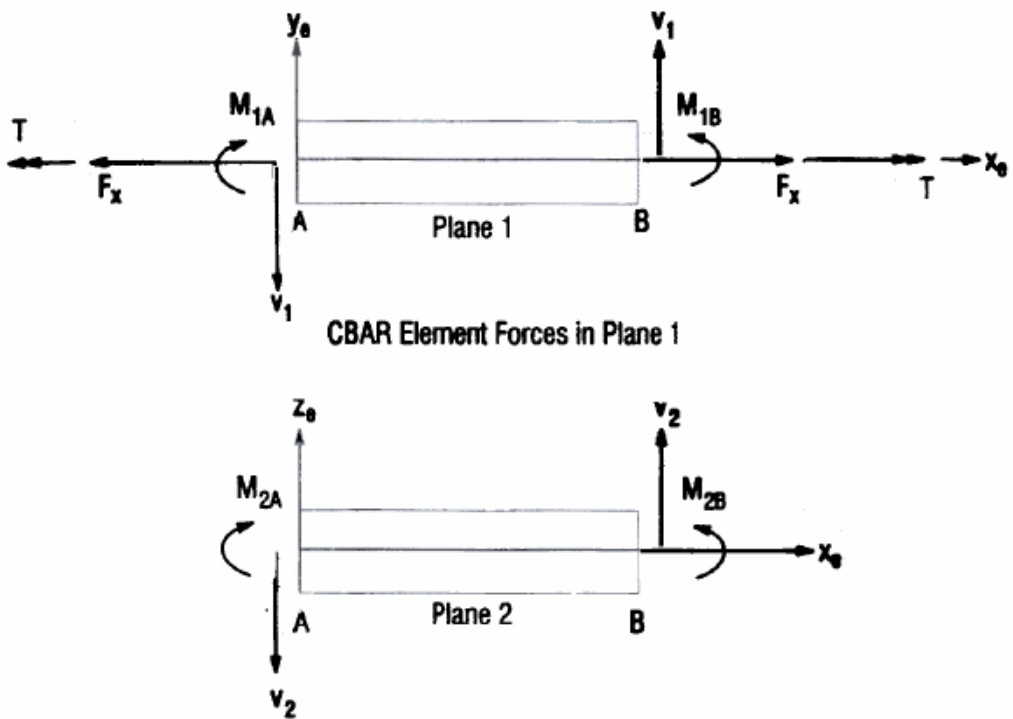


Figure 3.11 – CBAR element forces [Lee, 1997]

Planes 1 and 2 (Figures 3.10 and 3.11) represent the two perpendicular planes where bending and shear stiffness are defined. A total of 787 CBAR elements were used in the model. Three separate configurations were used: (1) Roof Truss , (1) Ridge Beam and (3) Top Plate.

Table 3.5 – Beam Elements (CBAR) used in FEA model

CBAR Configuration	# of elements	Cross Section	Orientation Vector
(1) Roof Truss	759	2x6	$\langle 0, 1, 0 \rangle$
(2) Ridge Beam	14	2x6	$\langle 1, 0, 0 \rangle$
(3) Top Plate	14	Double 2x4	$\langle 1, 0, 0 \rangle$

The majority of the CBAR elements are a part of the roof truss (1), which consist of 2x6 cross section (fig 3.2) and are oriented such that the element's strong axis falls within the X-Y plane (refer to figure 3.12 and 3.13).

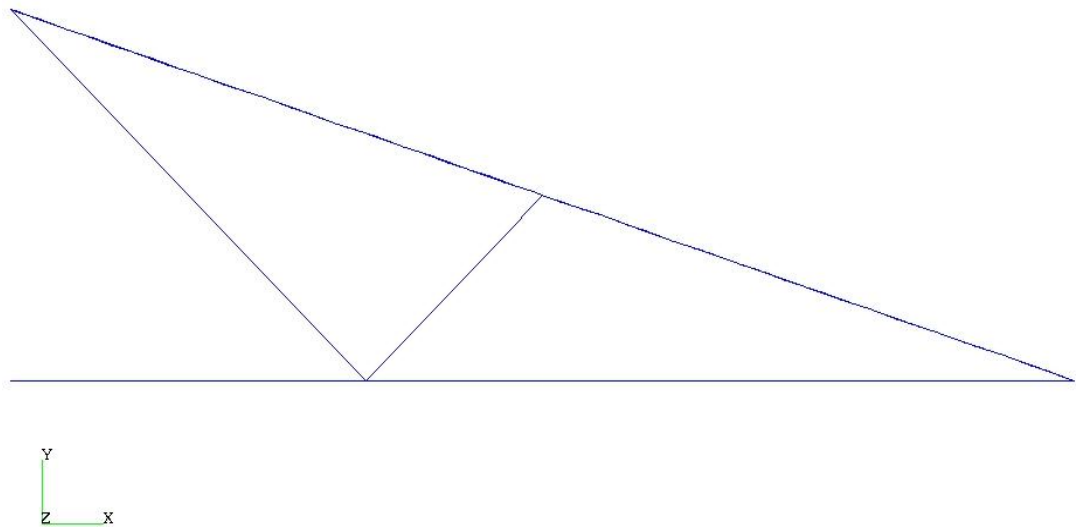


Fig 3.12 – Truss Elements (CBAR), X-Y view

The remaining 28 CBAR elements divided into 14 Ridge beam elements and 14 Top plate elements. Both ridge beam and top plate elements are oriented so the element's long axis is aligned with Z-axis. These elements differ in size and location. Ridge beam elements are positioned along the top (ridge) of the roof and consist of 2x6 sections with strong axis falling within the Y-Z plane. Top Plate elements are positioned at the bottom of the trusses (along the top of a wall) and consist of double 2x4 sections with strong axis falling within the Y-Z plane. Figures 3.13 illustrate the detail of these elements.

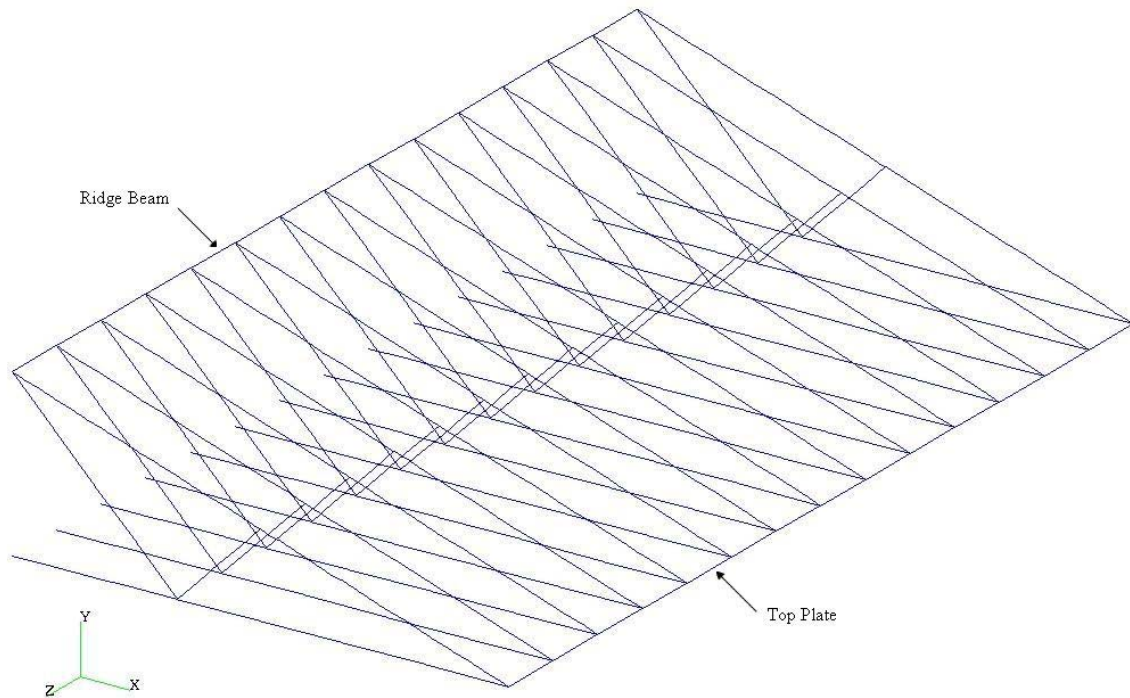


Figure 3.13 – Ridge Beam and Top Plate details

The sheathing panels were modeled as four-node, two dimensional plate elements (CQUAD4). Plate elements are intended to carry bending and shear, when in-plane

conditions are sufficient. MSC/NASTRAN offers several types of higher order plate elements (such as CQUAD8) that include more nodes for better accuracy, but these are more computationally demanding. The main focus of this study is the load distribution to the nails; therefore CQUAD4 elements are ideal for the application described here. Four nodes with six degrees of freedom each (three rotational and three translational) define CQUAD4 elements. Figures 3.14 and 3.15 illustrate in detail the plate element.

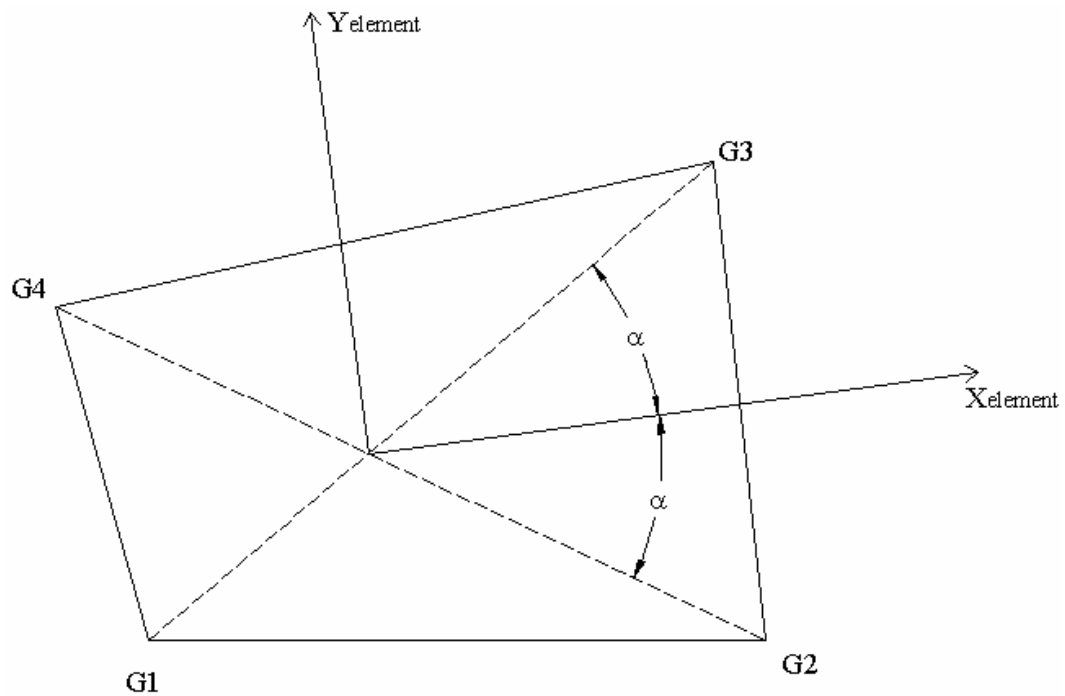


Figure 3.14 – CQUAD element coordinates. [Lee, 1997]

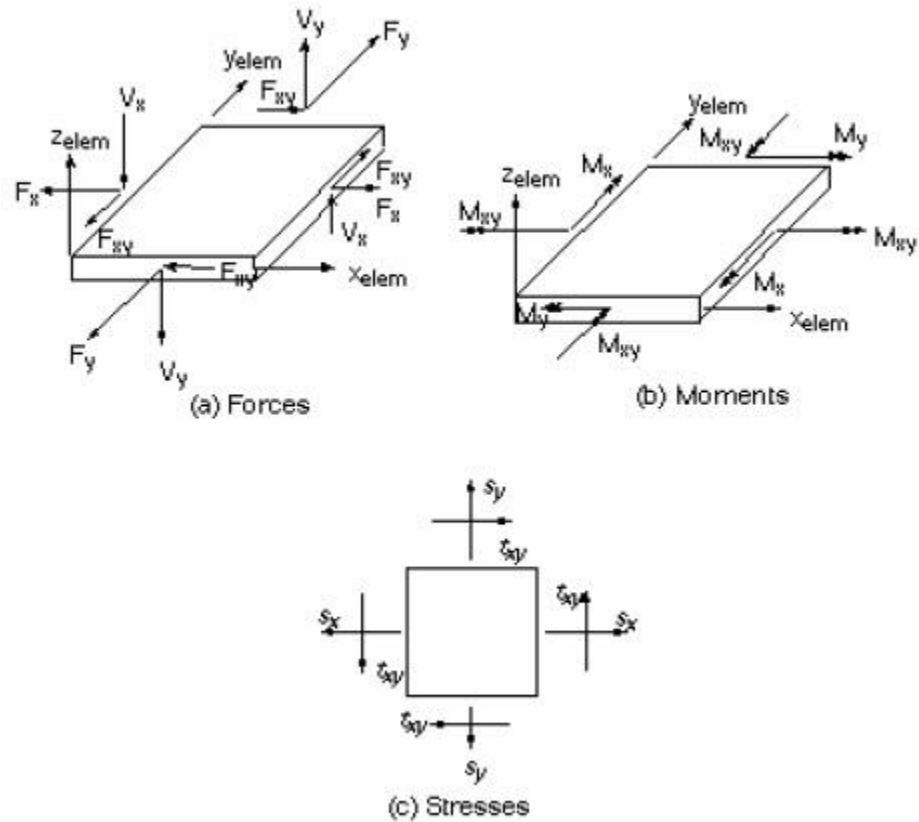


Figure 3.15 – CQUAD Element forces [Lee, 1997]

The position of the nodes (G1, G2, G3, and G4) is very important for the definition of the CQUAD4 element, especially when applying pressure loads [Lee, 1997]. The element's Z-axis is defined according to the right hand rule, so in figure 3.14 it would point out of the paper. The element's Z-axis defines the positive normal, therefore a positive pressure would be applied in the same direction of the Z-axis. The wind pressure loads developed at UWO (refer to Chapter 4) assumes that a negative pressure load corresponds to a panel uplift pressure; therefore, all of the plate elements were oriented so that the positive Z-axis points towards the structure.

A total of 2,184 plate elements were used in the roof model. All the elements have the same basic characteristics (such as thickness and material model), but the mesh density was selected based on the areas of interest. The panels that fall within region 3 (figure 3.5) require nails spaced 4 inches apart at the panel edges. In order to accommodate this, one node connecting the nails to the plate elements was required, therefore all panels that fell in this category were created using rectangular CQUAD4 elements (2 in X 6 in). In addition to the closer nail spacing, the panels located near the gable end were subjected to the 34 load areas, accordingly they require a finer mesh to properly account for the wind load effect.

Table 3.6 – Plate elements (CQUAD4) used in FEA model

CQUAD Element	# of elements	Thickness
Large Mesh (6" x 24")	352	0.5 in
Finer Mesh (2" x 6")	1832	0.5 in

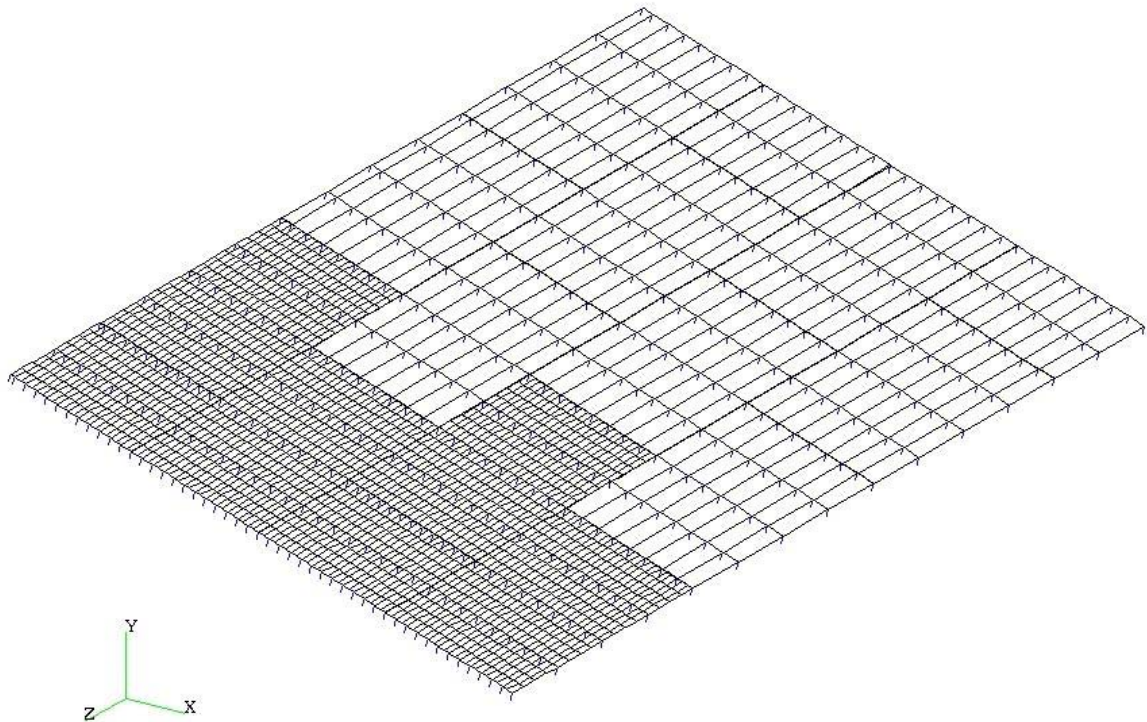


Figure 3.16 - Panel elements (CQUAD4) and Nail elements (CROD)

The mode of failure assumed for this analysis was panel failure due to fastener withdrawal, therefore correct modeling of the fasteners (8d nails) was critical when developing a FEA model for the roof system. Nail failure takes place when a nail is removed from the framing members [Schiff et al., 1996]. Given that fasteners failure models and tests are based on fasteners loaded axially, rod elements were the obvious choice when selecting an element type for the nails. Rod elements (CROD) are straight elements that carry only axial and torsional loads [Lee, 1997]. CROD elements are a good fit for modeling nails because these are intended to carry only axial load and have constant cross-section along the entire element span.

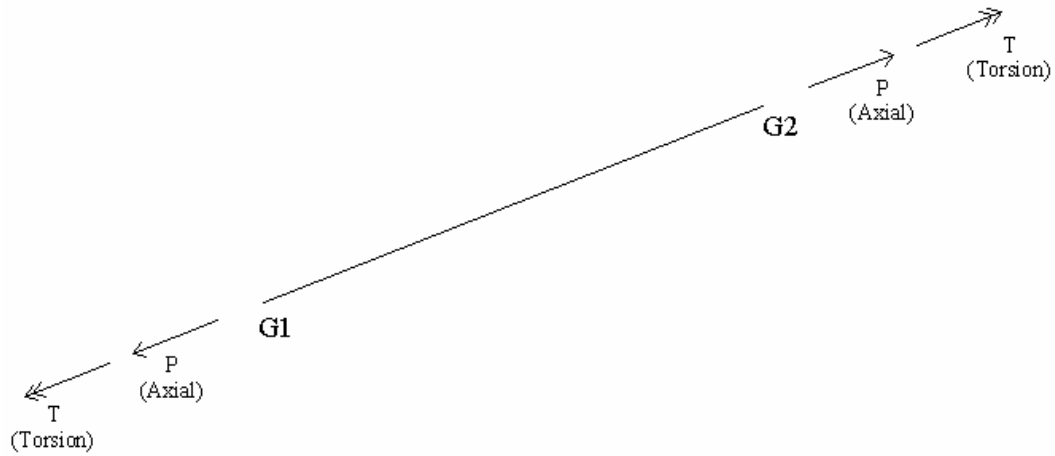


Figure 3.17 – Forces on a CROD element

A total of 680 CROD elements were used in the FEA model. Each element has the length (2.5 in) and diameter (0.131 in) of a true 8d nail and they connect a node from a Roof Truss element to a node on a Panel element. Figure 3.16 illustrates the positioning of the nail elements in relation to the panel elements and figures 3.18 and 3.19 illustrate the fully meshed model and how the elements connect.



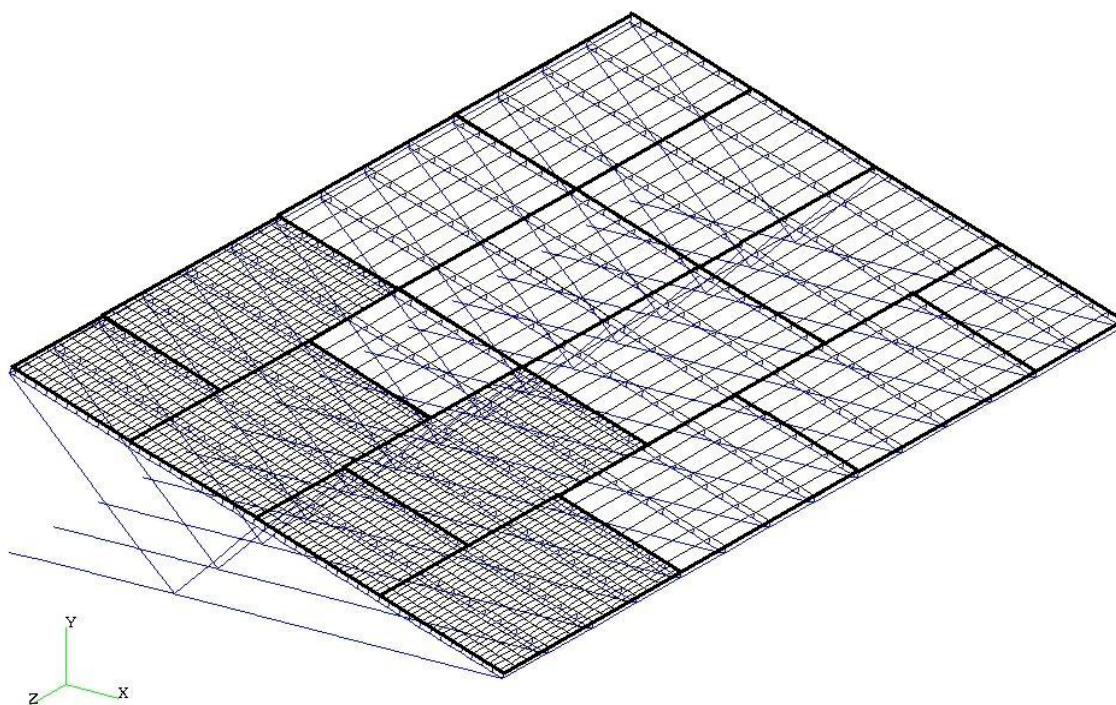


Figure 3.18 – Fully meshed model with outline of panels

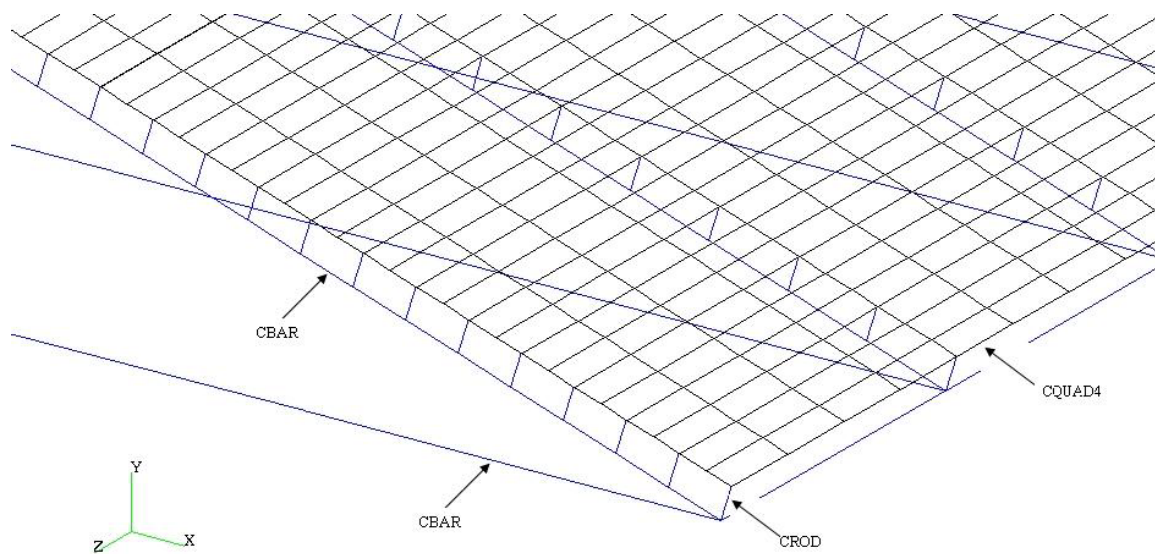


Figure 3.19 – Element connectivity.

Three basic material models were used: (1) structural lumber, (2) plywood, and (3) steel. For steel, the nail pull-out strength is significantly below yield (mean pull-out stress is almost 4 times smaller than yield strength of 50 ksi steel). For wood, although long term static loads may cause creep, behavior is linear-elastic until brittle failure. Under the short-term dynamic loads in this study, all material models are taken as linear elastic behavior. The material model used to describe the structural lumber was only applied to one dimensional elements (CBAR), therefore there a simple isotropic material model was used. Although plywood is an orthotropic material, it is layered symmetrically such that an isotropic material model can be used when considering stiffness. Thus, although plywood has different strength when stressed perpendicular or parallel to the face grain, its plywood's modulus of elasticity is the same as the same as long as the face grain is parallel or perpendicular to the span, refer to figure 3.20, [Smulski, 1997 and Faherty et al., 1999]. For the nails, material density was not included (each nail weights approximately 0.01 lb).

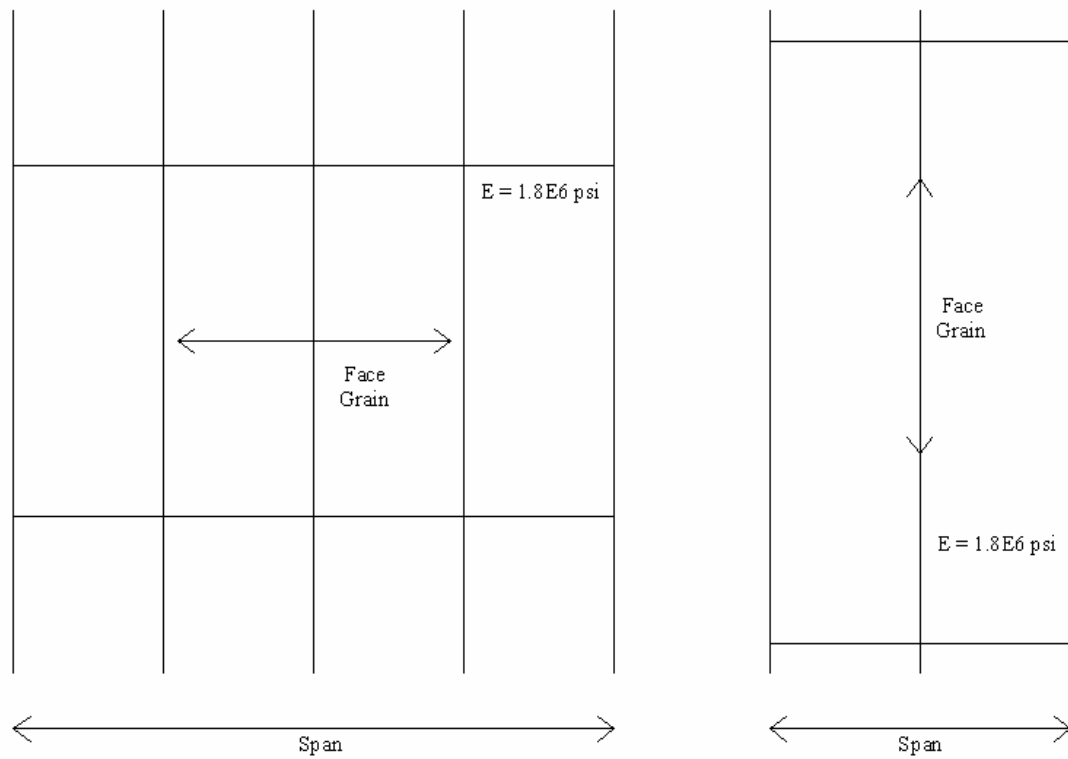


Figure 3.20 – Plywood Modulus of Elasticity with respect to span

The density of structural lumber was calculated from the Specific Density (G) of Southern Pine. Southern pine has a specific gravity of 0.55 [Faherty et al., 1999] and results in 0.5 inch thick panel weight of 1.5 pounds per square feet (of surface area). Refer to table 3.7 for material details.

Table 3.7 – Properties of Materials

Material Model	E (lb/in <sup>2</sup> )	$\rho$ (lb/in <sup>3</sup> )	Poisson Ration
(1) Structural Lumber	1750000	0.019861	-
(2) Plywood	1800000	0.020833	0.292
(3) Steel (nails)	29000000	-	-

Panel stability was another issue when modeling the roof system. From figures 3.8 through 3.9 it can be seen that each panel is nailed independently from each other. No nails are shared by any panel. To account for this effect a few CROD elements were duplicated and share the same spatial location, but have different nodes connecting the top end of the element. For example, nails 13 and 50 share the same spatial location but the top of the nails are connected to different nodes because nail 13 is a part of panel #1 but nail 50 is part a part of panel #2 (see figure 3.21). The nails share the same bottom node, but they allow the panel to behave independently from each other.

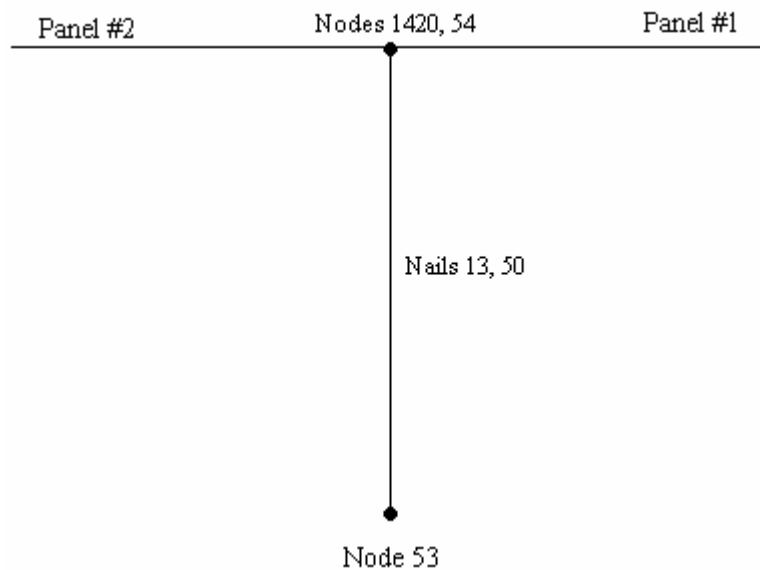


Figure 3.21 – Detail of nail connectivity (Side View)

Nails 134:168 <u>4</u>	Nails 308:356 <u>8</u>	Nails 492:536 <u>12</u>	Nails 636:680 <u>16</u>
Nails 85:133 <u>3</u>	Nails 263:307 <u>7</u>	Nails 447:491 <u>11</u>	Nails 609:635 <u>15</u>
Nails 50:84 <u>2</u>	Nails 214:262 <u>6</u>	Nails 402:446 <u>10</u>	Nails 564:608 <u>14</u>
Nails 1:49 <u>1</u>	Nails 169:213 <u>5</u>	Nails 357:401 <u>9</u>	Nails 537:563 <u>13</u>

Figure 3.22 –Panels and corresponding nails

The panel's independent behavior presented a problem of panel stability. Since there was not connectivity between the panels and they were linked to the roof truss only by the axial force in the CROD elements, there was a need to restrict the panels to avoid instability in the model. Each panel was restricted for lateral translation (X and Y directions) at on corner node, but the panels were free to move in Z direction. As the response is based on small deformations (no geometric non-linearity), this simple solution provided stability to the panel with minimal interference with the results. These panel reactions were significantly smaller than any single nail force. For example, in panel 16 the reactions were in the order of 1.0 lb, while the total panel response was about 702 lb. All of the panel's reactions (at any time step) were responsible for less than 0.5% of the total panel response.

By including density ( $\rho$ ) in the analysis, the mass matrix is generated by NASTRAN when a transient analysis is requested. Damping effects were not included in this analysis, mainly because there is very little information available regarding damping of light-frame wood structures. A series of deterministic analysis using damping coefficients of 15% were performed in order to verify that it was not necessary to include damping effects. Analysis with response frequencies ranging from 1 to 2000 Hz was tested, but no significant result was observed (when compared with an analysis performed without the use of damping). The difference in nail forces was less than 1% in all analysis. This is expected because the model is loaded at all time-steps, therefore there are very little damping effects actually taking place.

Modeling only one quarter of the roof was also justified by performing several analyses using a full roof model and comparing results with the quarter roof model. Difference in nail forces between the full roof analysis and the quarter roof analyses ranged from 1% to 2%, therefore only one quarter of the roof was modeled for the reliability analysis.

The selection of the appropriate time-step was based on a trial and error solution. Several analyses were performed using different time-step values, and the results (axial stress of the nails) were compared. Given that there is a major difference in total analysis time depending on the size of the time-step, the largest value that provides accurate results was selected. The largest value used for the time step was 1 second, while the smallest was 0.05 sec. Figures 3.23 and 3.24 show the difference in stress results and analysis duration for panel #9.

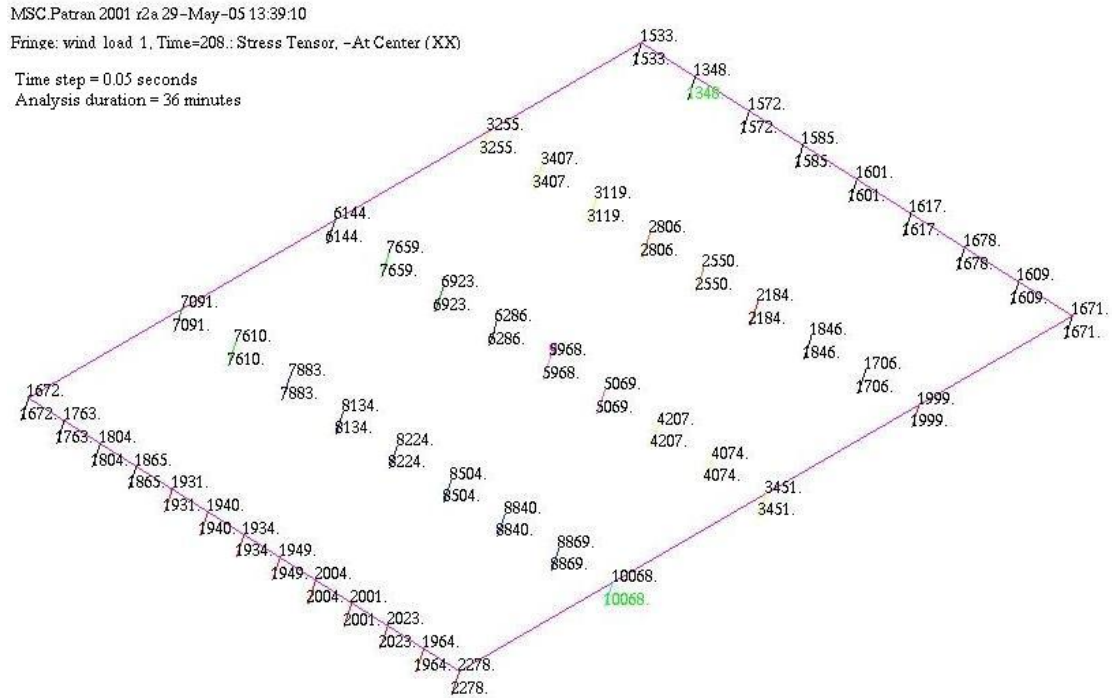


Figure 3.23 – Nail stresses for panel #9, time step = 0.05 sec

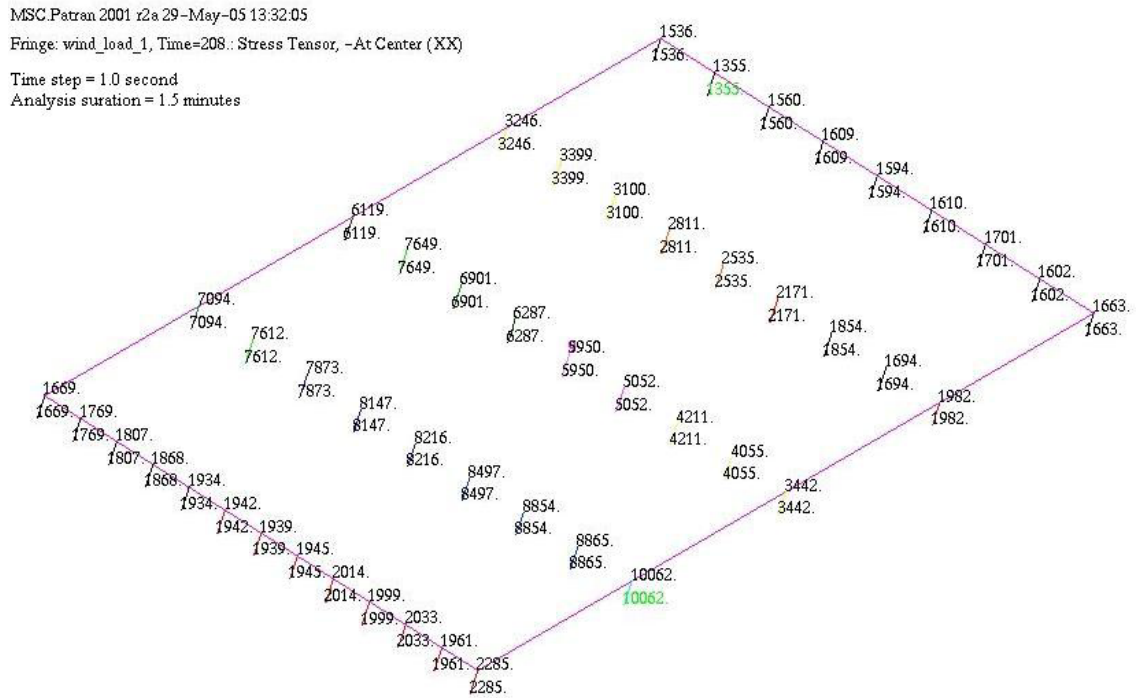


Figure 3.24 - Nail stresses for panel #9, time step = 1.0 sec

From figures 3.23 and 3.24 it can be observed that the difference in stress is minimal (less than 1% difference), but there is a significant difference in the duration of the analysis (1.5 minutes for the 1 sec time-step against 36 minutes for the 0.05 sec time step). Since the stress difference is so small, the selection of a 1 sec time-step provides for an accurate model that runs relatively fast. Table 3.8 shows the resulting panel maximum panel forces for the deterministic wind load analysis.

Table 3.8 – Maximum panel forces (deterministic)

Panel	Maximum Force (lb)	Time
1	1207.3	185
2	837.5	52
3	1412.5	180
4	743.9	229
5	732.8	267
6	751.1	139
7	733.8	240
8	1629.2	36
9	732.8	66
10	732.9	3
11	738.9	282
12	1490.1	244
13	366.5	3
14	732.9	3
15	366.6	3
16	702.5	278



## CHAPTER IV

### WIND LOADS

#### INTRODUCTION

Current design codes and standards treat wind loads on low-rise buildings as static pressures applied in certain regions of the structure. The calculation of design nominal loads on buildings depends on several factors that include type of structure, geographical location, building loading zone, building surroundings, slope of the roof, and other factors.

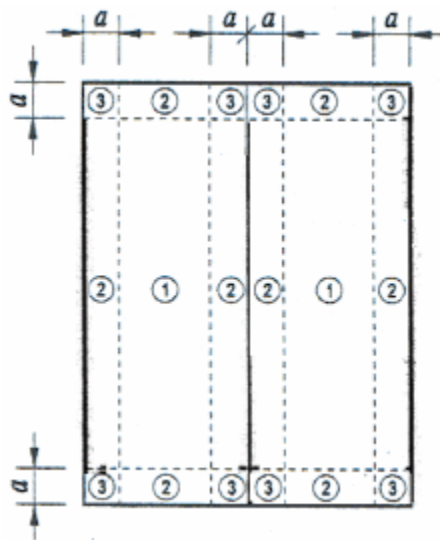


Figure 4.1 – Wind load regions for ASCE 7-02

Most codes that include wind load provisions apply these loads in a similar manner. For example, ASCE 7 [ASCE, 2003] considers 3 separate wind load regions on

the roof structure, namely: (1) interior; (2) edge; and (3) corner regions (refer to Figure 4.1). The Metal Building Manufacturers Association (MBMA) Manual also divides the roof structure into the same three regions. The difference between the codes is the values for the pressure coefficients, which are slightly larger in ASCE 7 when compared to MBMA coefficients [Sinno et al., 1993]. The ASCE 7-02 provisions for wind load on the study house are described in the following section.

### **ASCE 7-02 WIND LOAD PROVISIONS**

The American Society of Civil Engineers (ASCE) publishes the standard ASCE 7-02 “Minimum Design Loads for Buildings and Other Structures”, which supplies provisions for loads to be used in the design of civil engineering structure. The standard covers common design loads such as gravity loads, seismic effects, wind loads.

Section 6.0 of ASCE 7-02 governs the application of wind loads to structures. In this section several parameters concerning the design and analysis of structures to resist wind action are presented. ASCE 7-02 recognizes three methods of analyses: (1) Simplified procedure, (2) Analytical Procedure, and (3) Wind-Tunnel Procedure. The first method (Simplified Procedure) does not require any complex calculations, and most of the pressure coefficients are obtained from simple graphs, tables and figures. This method may only be used when the building fits certain requirements as described below:

- The building must be classified as low-rise (mean roof height less than 60 ft).
- The building must be classified as enclosed (assumes no breakage of doors or windows).

- The building must have a regular shape, must be classified a simple diaphragm, and have no expansion or separation joints.
- The building must not be classified as flexible (natural frequency less than 1 Hz).
- The building must not fall within a special wind or topographical region.
- The building must be approximately symmetrical in shape and have roof slopes of 45° or less.

Method 1 is very useful for design purposes, given the structure meets all of the requirements, but it is not used for research purposes. Method 3 is based on wind-tunnel analysis and is not presented here in detail.

Method 2 (Analytical Procedure) has been used in research for many years. This method uses the two equation listed below to evaluate design wind load. Equation 4.1 is used to calculate the velocity pressure coefficient, and Equation. 4.2 is used to calculate the total pressure applied to a certain surface.

$$q_z = 0.00256 \cdot K_z \cdot K_{zt} \cdot K_d \cdot V^2 \cdot I \quad (4.1)$$

$$p = q_h [(GC_p) - GC_{pi}] \quad (4.2)$$

Where,

$z$  = height above ground (here the mean roof height  $h = 10.5$  ft)

$V$  = Basic wind speed (mph)

$K_z$  = Velocity pressure exposure coefficient (0.85 for Components and Cladding, exposure C and  $h < 15$ ft)

$K_{zt}$  = Topographic Factor (here taken as 1.0 for simplicity)

$K_d$  = Wind directionality factor (here taken as 1.0 for simplicity)

$q_h$  = Velocity pressure coefficient evaluated at mean roof height  $h$

$GC_p$  = External pressure coefficient

$GC_{pi}$  = Internal pressure coefficient

All of these factors are functions of the building type, location and structural classification (open, partially enclosed, or enclosed). It is important to define what type of element is being used: (1) Main Wind Force Resisting System (MWFRS) or (1) Components and Cladding (C&C). MWFRS elements are classified as elements that provide overall stability and support the building [ASCE, 2002], while C&C are classified as elements that receive direct wind loads and do not qualify as MWFRS [ASCE, 2002]. The design procedure is very similar for both MWFRS and C&C; however, MWFRS typically results in lower applied wind load pressures, because the method assumes some load redistribution within the MWFRS components [Cheng, 1998]. For the purpose of the study house, the plywood panels are considered to fit in C&C category because the removal of panels by themselves usually does not result in full collapse of the house. It is also important to classify the structure as open, partially-enclosed or enclosed. Open structures have at least 80% of each wall open (exposed). Partially-enclosed structures assume the loss of one window or door. Enclosed structures assume the windows and doors remains intact. The study house was assumed to be an enclosed structure, because the effects of loss of cladding are not studied here. Basic wind is determined directly from the wind speed map in ASCE 7-02 (map not included here). For this analysis the wind speed of 110 mph was selected to match the wind speed data developed at the University of Western Ontario (UWO). The building

classification has a direct influence on the importance factor (I). ASCE 7-02 classifies all single family residential structures as Category II, and all buildings in this category have an importance factor of 1.0. The parameter  $K_{zt}$  is a topographic factor that depends on the terrain where the structure is located. For simplicity, the study house is assumed to be located in a region that does not have any hills or escarpments. The parameter  $K_d$  is only used when load combinations are used; therefore, it is set equal to 1.0 for this study. The exposure category parameter directly influences the  $K_z$  factor. For a structure with mean roof height up to 15 ft and, located on exposure category “C” region, and using to C&C method,  $K_z$  is taken as 0.85. Other factors needed for determining wind loads are summarized in table 4.1.

Table 4.1 – Parameters for ASCE 7-02 wind loads calculations

ASCE 7-02 Parameters	
Basic Wind Speed	110 mph
Building Classification	Category II
Importance Factor	1.0
Exposure Category	C

With all of the parameters determined, the velocity pressure coefficient ( $q_h$ ) may be calculated using equation 4.1 above.

$$q_h = 0.00256 \cdot (0.85) \cdot (110)^2 \cdot (1.0) = 26.33 \text{ psf} \quad (4.3)$$

With the wind velocity pressure computed, the pressure in each zone may be calculated. The internal pressure coefficients (GC<sub>pi</sub>) for an enclosed building are -0.18 and +0.18 (use either to obtain maximum pressures). The external pressure coefficients

are determined from figure 4.2 below, and it depends on the tributary area of each fastener. Since the tributary area of a fastener is between 1 and 2 ft<sup>2</sup> [Cheng, 1998], the coefficients for zones 1, 2 and 3 are -0.9, -1.7 and -2.6, respectively.

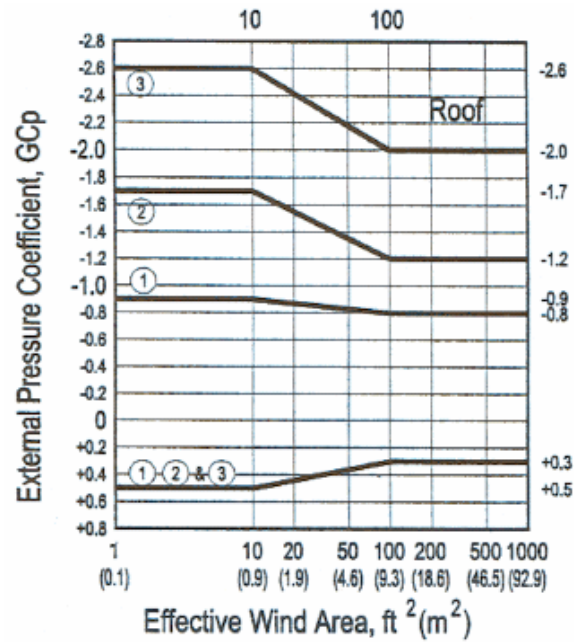


Figure 4.2 – ASCE 7-02 external pressure coefficients [ASCE, 2002]

Zones 1, 2 and 3 are determined from figure 4.1, where the distance  $a$  is 10% of the least horizontal dimension of the study house (from Figure 3.1, this would be 10% of 30 ft) or  $0.4h$ , whichever is smaller (but no less than 3 ft). For the study house,  $a = 3.0$  ft. The pressures applied for each zone are presented in figure 4.3 and Table 4.2.

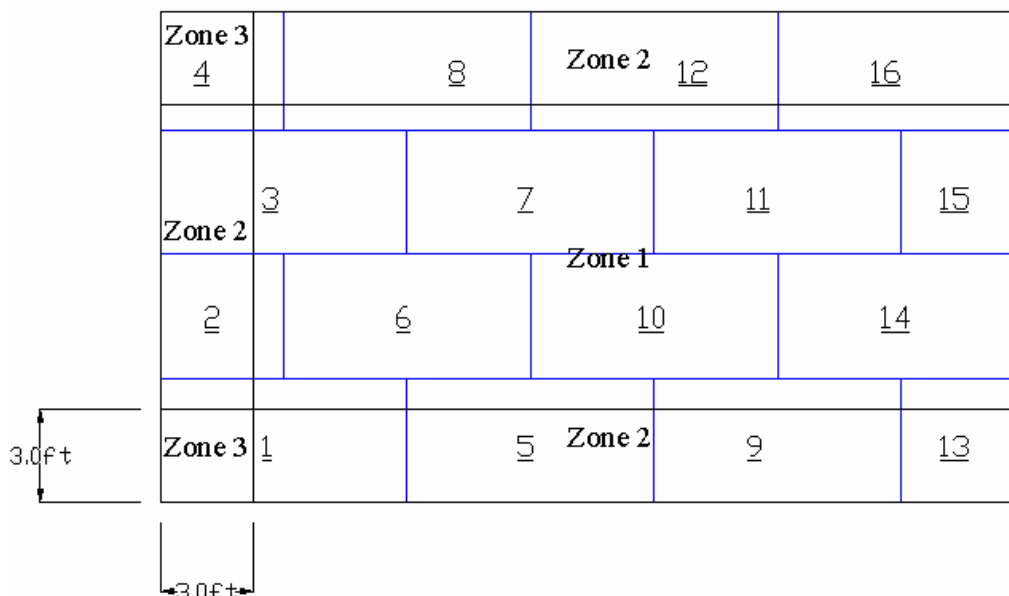


Figure 4.3 – Quarter roof section with ASCE 7-02 zones 1, 2 and 3

Table 4.2 – ASCE 7-02 Uplift pressure for zones 1, 2 and 3

Zone	Uplift Pressure (psf) - Sloped Roof	Uplift Pressure (psf) - Flat Roof
1	-28.44	-31.07
2	-49.5	-52.13
3	-73.2	-78.46

The results presented in table 4.2 demonstrate how the pressure would increase if a flat roof of similar dimensions was used. Comparing the results of sloped roof and flat roof reveal that the uplift pressures increase in regions 1, 2 and 3 by 8.5%, 5.1% and 6.7% respectively. ASCE 7-02 treats gable roof with a slope of  $7^\circ$  or less as a flat roof. Roofs with slope between  $7^\circ$  and  $25^\circ$  are also treated in the same category. The procedure presented is a common and code-required method to compute design wind loads on the study house.

## **UWO WIND LOAD DATA**

The wind load used in this study was developed at the University of Western Ontario (UWO) boundary layer wind tunnel [Sinno and Taylor, 1993].

The wind load data used here was developed to simulate a typical storm with winds of 110 mph at 33 ft above ground with an angle of incidence of  $45^\circ$  (critical angle). It is also important to note that the data are representative for a building life-span of 50 years [Sinno and Taylor, 1995]. The wind load data consists of pressures measured on a 1/50 scale model over a period of approximately 5 minutes. The time varying pressure data was developed of 34 loading areas with pressures recorded at a fidelity of 20 Hz. In addition to the 34 load areas, a uniform and constant uplift pressure (backing pressure) of 22.9 psf was present in the entire surface of the roof for the total duration of the wind tunnel test. Note that although the entire roof is loaded with 22.9 psf uplift, only a small portion of the roof is loaded with the high-pressure dynamic portion. This represents the most critical area. Other areas of the roof have an insignificant level of dynamic load, and thus these areas are left unloaded.

Table 4.4 shows a summary of the loads and Figure 4.4 shows the position of the load areas in the FEA model.



Table 4.3 – Summary of UWO wind load data (20 Hz)

Area Number	Dimensions (ft)	Surface Area (ft <sup>2</sup> )	Negative Peak Load (lb)	Negative Peak Load (psf)	Positive Peak Load (lb)	Positive Peak Load (psf)	Mean Load (lb)	Mean Load (psf)	% of time suction
1	1.5 X 1.5	2.25	-274.3	-121.9	43.7	19.4	-44.8	-19.9	93.9
2	1.0 x 1.5	1.5	-124.2	-82.8	31.8	21.2	-12.0	-8.0	69.6
3	1.0 x 1.5	1.5	-123.2	-82.1	34.3	22.9	-18.0	-12.0	75.8
4	1.0 x 1.5	1.5	-125.7	-83.8	31.5	21.0	-15.9	-10.6	74.0
5	1.0 x 1.5	1.5	-129.1	-86.1	30.6	20.4	-16.5	-11.0	74.7
6	1.5 x 1.0	1.5	-233.8	-155.9	31.4	20.9	-46.8	-31.2	96.0
7	1.0 x 1.0	1.0	-49.4	-49.4	24.7	24.7	6.2	6.2	19.2
8	1.5 x 1.0	1.5	-239.7	-159.8	26.8	17.9	-55.7	-37.1	98.5
9	1.0 x 1.0	1.0	-69.7	-69.7	26.2	26.2	6.0	6.0	17.3
10	1.5 x 1.0	1.5	-259.1	-172.7	24.6	16.4	-57.3	-38.2	98.6
11	1.0 x 1.0	1.0	-105.4	-105.4	24.6	24.6	-5.2	-5.2	56.3
12	1.5 x 1.0	1.5	-236.8	-157.9	24.2	16.1	-59.4	-39.6	99.0
13	1.0 x 1.0	1.0	-132.9	-132.9	24.1	24.1	-16.5	-16.5	84.0
14	1.5 x 1.0	1.5	-209.9	-139.9	22.6	15.1	-54.2	-36.1	99.2
15	1.0 x 1.0	1.0	-142.3	-142.3	22.0	22.0	-22.3	-22.3	92.5
16	1.0 x 1.0	1.0	-79.9	-79.9	26.9	26.9	4.9	4.9	25.2
17	1.5 X 1.5	2.25	-264.9	-117.7	36.1	16.0	-70.0	-31.1	99.0
18	1.0 x 1.5	1.5	-206.1	-137.4	29.1	19.4	-40.2	-26.8	95.7
19	1.0 x 1.5	1.5	-165.7	-110.5	40.4	26.9	-6.1	-4.1	51.1
20	1.0 x 1.5	1.5	-119.0	-79.3	13.6	9.1	13.6	9.1	17.9
21	1.0 x 1.5	1.5	-216.3	-144.2	33.6	22.4	-57.7	-38.5	98.5
22	1.0 x 1.5	1.5	-180.2	-120.1	27.5	18.3	-44.8	-29.9	97.9
23	1.0 x 1.5	1.5	-188.6	-125.7	37.6	25.1	-23.5	-15.7	80.3
24	1.0 x 1.5	1.5	-185.2	-123.5	46.1	30.7	-3.2	-2.1	44.9
25	1.5 X 1.5	2.25	-201.4	-89.5	36.7	16.3	-48.7	-21.6	97.5
26	1.0 x 1.5	1.5	-169.5	-113.0	27.6	18.4	-41.5	-27.7	98.4
27	1.0 x 1.5	1.5	-166.5	-111.0	34.6	23.1	-32.1	-21.4	91.1
28	1.0 x 1.5	1.5	-187.7	-125.1	41.7	27.8	-19.0	-12.7	68.1
29	1.0 x 1.5	1.5	-121.5	-81.0	40.3	26.9	-5.8	-3.9	57.4
30	1.5 X 1.5	2.25	-183.7	-81.6	38.9	17.3	-37.9	-16.8	94.0
31	1.0 x 1.5	1.5	-174.6	-116.4	29.4	19.6	-36.0	-24.0	97.7
32	1.0 x 1.5	1.5	-191.4	-127.6	32.2	21.5	-35.5	-23.7	94.7
33	1.0 x 1.5	1.5	-182.3	-121.5	43.4	28.9	-29.8	-19.9	82.8
34	1.0 x 1.5	1.5	-177.9	-118.6	42.1	28.1	-27.4	-18.3	81.3

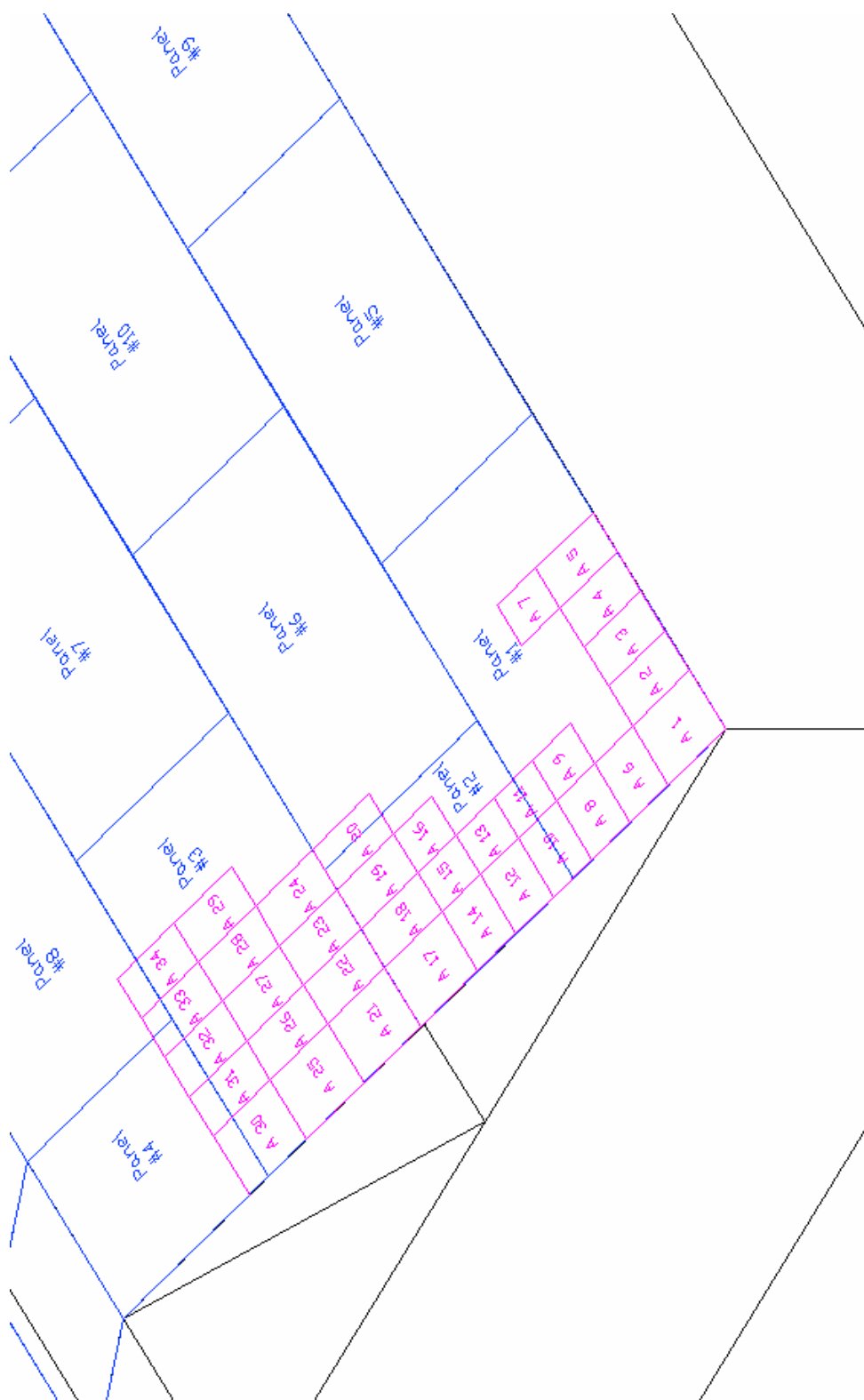


Figure 4.4 – Placement of UWO wind load areas

In recent findings, Sinno et al. [2003] have established that peaks with duration of less than one second do not get a significant response from the roof. In previous experimental studies [Sinno and Taylor, 1995; Sinno and Taylor, 1994] the peak loads were adjusted by performing a 10 point moving average of the data, therefore smoothing the load curve. The wind loads used here were averaged over 20 points in order to reduce the load data set to a computationally feasible size for transient dynamic analysis. This results in fidelity of 1 Hz, which is the minimum fidelity necessary for full roof response [Sinno et al, 2005]. Sinno et al [2003] found that dynamic loads under-predicted the roof response by 55% when compared to code uniform pressure model. Using the 1 Hz (20 point average) data, we also found about a 50% decrease in dynamic response when compared to code-applied uniform pressure response; thus the 1 Hz average is reasonable and verified (refer to the last section of this chapter). Moreover, the material models available in MSC/NASTRAN cannot track internal shock-wave response nor account for high strain rate effects, and thus using full load curve with 20 Hz peaks would result in greatly over-predicted roof forces. Figures 4.5 and 4.6 show the difference in peaks for area 1 when the 20 point moving average is applied. Refer to Appendix A for figures of wind loads for each area.

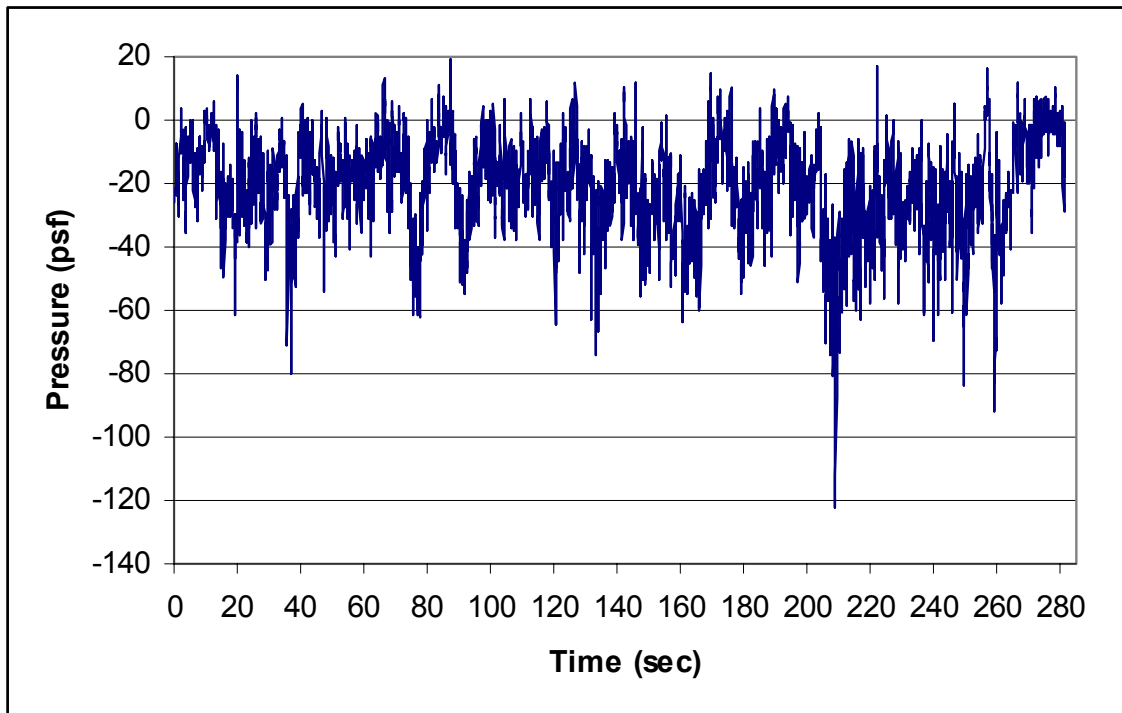


Figure 4.5 – Peak loads for UWO data (Area 1)

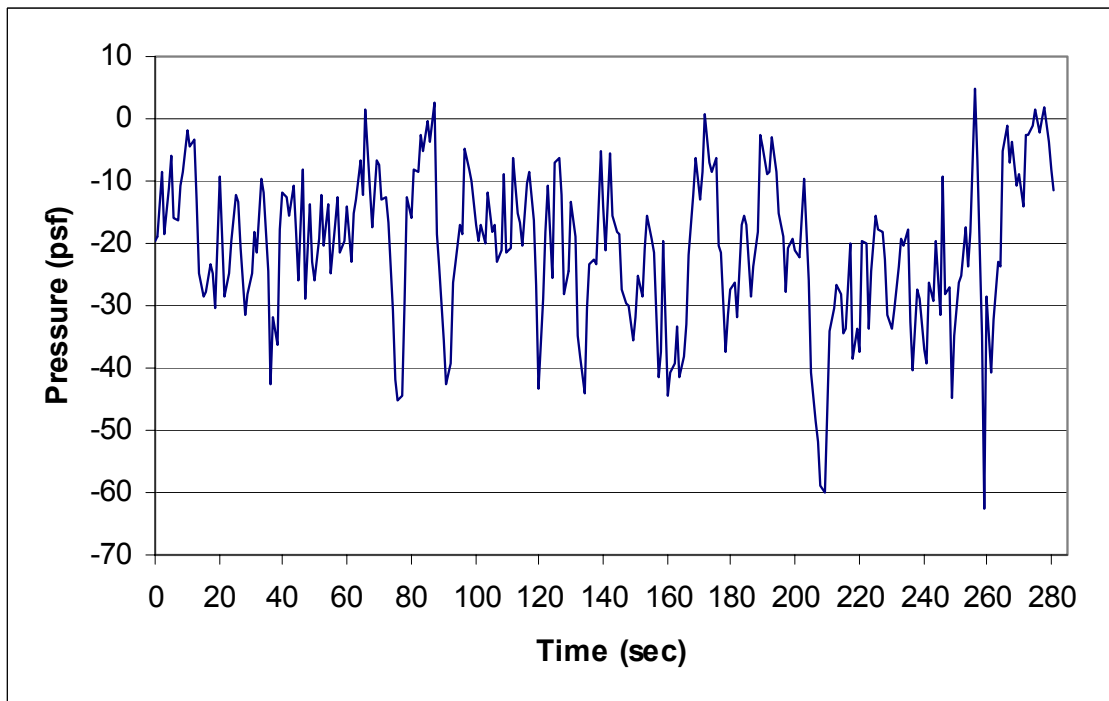


Figure 4.6 – Peak loads for 20 point moving average data (Area 1)

A structural reliability analysis requires probabilistic information of each random variable in order to accurately predict probability of failure. The magnitude of the pressure for each area of the 34 wind load areas is taken as a random variable (RV). Table 4.4 summarizes the wind load information for each loading area. Note that all of the loading areas have a normal load distribution.

Table 4.4– Pressure distribution for load areas

Area #	Mean	Std Dev	COV
1	-20.71	12.18	0.59
2	-8.67	11.07	1.28
3	-12.74	13.22	1.04
4	-11.30	12.57	1.11
5	-11.69	12.92	1.11
6	-32.11	18.87	0.59
7	5.81	6.85	1.18
8	-38.23	19.15	0.50
9	5.63	7.53	1.34
10	-39.26	19.83	0.51
11	-5.73	12.27	2.14
12	-40.66	19.96	0.49
13	-17.16	14.97	0.87
14	-37.18	18.32	0.49
15	-23.13	15.94	0.69
16	4.53	10.37	2.29
17	-32.13	16.36	0.51
18	-27.68	17.05	0.62
19	-4.59	13.58	2.96
20	8.64	10.55	1.22
21	-26.57	14.24	0.54
22	-30.76	17.02	0.55
23	-16.35	15.53	0.95
24	-2.67	15.37	5.76
25	-22.51	12.84	0.57
26	-28.58	15.62	0.55
27	-22.15	15.79	0.71
28	-13.30	17.22	1.29
29	-4.38	11.86	2.71
30	-17.64	11.60	0.66
31	-24.83	14.17	0.57
32	-24.43	15.50	0.63
33	-20.50	17.13	0.84
34	-18.89	16.60	0.88

## **GLOBAL AND LOCAL WIND DISTRIBUTION**

The wind load distribution was also divided into two distinct categories: global and local. The global distribution governs overall wind speed that strikes the roof while the local distribution governs spread in time versus pressure data for a particular loading area on the roof.

The global distribution used here was developed by Rosowsky and Cheng [1999a] using methodology developed by Ellingwood [1980]. The full description of these loads is available in Chapter II. Rosowsky and Cheng [1999a] used data collected in 5 different locations (in North and South Carolina coast) and Monte Carlo establish a composite set of wind load statistics. The resulting of the 50-year maximum wind load analysis determined that wind loads applied to roofs have a bias factor of 0.41 and COV of 0.41, with a lognormal distribution (in hurricane prone regions). The local wind load model used here is taken from the UWO wind-tunnel data and is summarized in table 4.4.

Because the local wind load data was developed for a flat roof, an investigation had to be made regarding the applicability of these loads to a sloped roof. Tables 4.2 shows the predicted difference in wind load uplift between the sloped roof used in this study and a flat roof of similar proportions. Since the loads on the sloped roof are 5% to 8% smaller, it was assumed that using the using UWO data as presented would provide slightly conservative results.

## **ASCE 7-02 AND DYNAMIC WIND LOAD COMPARISON**

Experimental results have shown that, when a metal roof is loaded under dynamic loads, the maximum measured force in the roof fasteners was only 55% of the load

measured in the fasteners when the roof had failed in the static test of uniform pressure meant to replicate the same wind pressure [Sinno et al., 2003]. Although this study deals with wood roofs, a finding of similar magnitude would be expected. Thus, a static analysis applying 55% of the uplift forces obtained from ASCE 7-02 (refer to Table 4.2) was performed. The results of this analysis was compared with the results from the deterministic analysis using 1-Hz data (refer to Table 3.7). Table 4.5 below shows the results from each analysis and the difference in response. Force results from the 1-Hz dynamic analysis are typically ~15% larger than expected experimental results. The analytical approach used here appears reasonable, if not slightly conservative. OF course exact comparisons are difficult as different roof systems are used.

Table 4.5 – Panel Forces

Panel #	Panel Force (lb)		% Difference
	Dynamic Analysis (using 1 Hz data)	Static Analysis (55% of ASCE 7)	
1	1207.3	1060.1	-12.2
2	837.5	714.3	-14.7
3	1412.5	1315.5	-6.9
4	743.9	846.4	13.8
5	732.8	825.5	12.7
6	751.1	620.2	-17.4
7	733.8	615.0	-16.2
8	1629.2	1519.6	-6.7
9	732.8	836.9	14.2
10	732.9	649.8	-11.3
11	738.9	638.4	-13.6
12	1490.1	1266.3	-15.0
13	366.5	420.0	14.6
14	732.9	635.4	-13.3
15	366.6	313.5	-14.5
16	702.5	801.8	14.1



Table 4.5 above shows that most areas were within  $\pm 15\%$  of the code loads (55% of ASCE 7-02), with the exception of panels #6 and 7, whose loads were slightly lower than 15%.

## CHAPTER V

### RELIABILITY ANALYSIS

#### **INTRODUCTION**

Performing a reliability analysis for light-frame wood construction can be a quite challenging task because these structures are not completely understood from a structural point of view. There is little research information available regarding load distribution, load statistics, component level performance, structural system level performance, and appropriate reliability analysis methods. There is a growing interest in analyzing these structures more precisely so better design methodologies may be implemented.

Extreme wind events are responsible for extensive damage to light-frame residential construction. Houses found in the path of hurricanes experience varying degrees of damage, but the most common cause of insurance loss is due to removal of roof sheathing [Sparks et al., 1994]. Thus, the reliability of these components is the focus of this study (refer to figures 5.1 and 5.2 for examples of roof sheathing failure). Chapter V describes the reliability principles applied to the study, which include method of analysis, limit states considered, resistance model, and load model.



Figure 5.1 – Removal of panels of house in Florida, Hurricane Jeanne [USGS, 2005]



Figure 5.2 – Removal of panels of building in Florida, Hurricane Jeanne [USGS, 2005]

## LIMIT STATE FUNCTIONS

The accuracy of a reliability analysis of a structure depends heavily on the quality of the probabilistic information and on the method of analysis. Probabilistic information of a Random Variable (RV) refers to the mean, coefficient of variation (COV), and probability distribution that most closely describe the RV in a statistical sense. Method of analysis refers to how these RV's are evaluated in order to estimate failure information (probability of failure or reliability index). The limit state ( $g$ ) includes all of the random variables, and represents the boundary between “failure” and “non-failure”. The two limit state functions used in this study are expressed as:

$$g(x) = R - Q \quad (5.1)$$

$$g(x) = R - Q + D \quad (5.2)$$

Where:

$x$  = vector containing all random variables

$R$  = resistance capacity of sheathing panel

$Q$  = wind load acting upon the panel; a function of 34 RV's (wind load areas)

$D$  = dead load on panel

$g(x)$  = limit state function.  $g(x) > 0$  indicates safety while  $g(x) < 0$  indicates failure.

This limit state function as a function of all RV's cannot be stated explicitly in this study because the wind load effects ( $Q$ ) is calculated using the finite element model described in Chapter III. To reduce computational effort, the effects of dead load (gravity) were not included directly in the finite element model, but rather they were taken to act against the wind uplift loads imposed on the panel in Eq. 5.2. Note that the inertial effects of mass were included in the FEA model, however. The next few sections of this chapter discuss the details of the resistance statistics, load statistics, and solution methodology applied in this study.

## **LOAD AND RESISTANCE STATISTICS**

The load and resistance statistics used in this study were previously discussed and are briefly summarized in this section. The resistance statistics used here was developed by Schiff et al. [1996] for plywood panels similar to the ones used in this study. The details of the resistance statistics is discussed in Chapter II. The panels tested assume a mean failure load of 131 psf with a COV of 0.14 (normally distributed). Since the failure occurs when the fasteners experience pull-out from the framing member and each

fastener is loaded relatively uniformly, the pressure load may be taken as a single pull-out force applied to the panel. The mean panel failure force is, thus, obtained by multiplying the total panel area by the uplift pressure (refer to table 5.1 below).

Table 5.1 - Summary of resistance statistics

Panel Size	Panel Area	Mean Uplift Pressure	Mean Uplift Force	COV
4 ft X 8 ft	32 ft <sup>2</sup>	131 psf	4192 lb	0.14
4 ft X 4 ft	16 ft <sup>2</sup>	131 psf	2096 lb	0.14

The wind load statistics are described in detail in Chapter IV, and the dead load statistics are described in Chapter II. Rosowsky and Cheng [1999b] provide dead load statistics for the panel in the form of applied pressure (psf), thus can be converted into a dead load force (lb) per panel. The dead load (DL) presented here includes the weight of the sheathing panels and other roofing materials (roof shingles, nails and straps, insulation, and others). The summary of the dead loads is presented in table 5.2.

Table 5.2 - Summary of dead load statistics

Panel Size	Panel Area	Mean DL Pressure	Mean DL Force	COV
4 ft X 8 ft	32 ft <sup>2</sup>	3.5 psf	112 lb	0.10
4 ft X 4 ft	16 ft <sup>2</sup>	3.5 psf	56 lb	0.10

## SOLUTION METHODS

The solution of the limit state functions (Eqs. 5.1 and 5.2) can be quite complex and this was proven true during the course of this research. The analysis of the roof structure requires the combined use of different software packages to perform different functions. The finite element analysis (FEA) software MSC/NASTRAN was used to compute the forces in each nail of the model. The in-house FORTRAN program FASTPANEL was used to determine the maximum loads in each panel (sum of the nail forces in the panel) and the probabilistic analysis package NESSUS was used to perturb the RV's and calculate the reliability index ( $\beta$ ) for each panel.

NESSUS allows the user to select from several analysis methods, including the first order reliability method (FORM), second order reliability method (SORM), advanced FORM (AFORM), Monte Carlo simulation and Advanced Mean Value Method (AMV+). The first method considered for this study was AMV+, but this method would not converge to an answer. At each iteration, the method would bounce between two  $\beta$  values for a particular panel, but it would not converge. For example, in panel #1 the method would skip between a  $\beta$  of 4.3 and 9.7, but no answer was determined. Since the search algorithm NESSUS uses to find the most probable point on the failure surface is similar in AMV + and other methods, the variance reduction methods (such as Importance Sampling) would be expected to experience similar convergence problems. The direct sampling methods, such as Monte Carlo simulation and Latin Hypercube sampling, would require too many simulations to be feasible and capture some of the

failure probabilities expected. Thus, the AFORM method was used, which could converge to a solution.

The advanced first order reliability method (or Rackwitz-Fiessler) requires knowledge of the distribution of each random variable. The method uses an algorithm that modifies the mean and standard deviation of non-normal random variables into “equivalent normal” values via Eqs. 5.3 and 5.4 [Nowak and Collins, 2000].

$$\mu_X^e = x' - \sigma_X^e \cdot [\Phi^{-1}(F_X(x'))] \quad (5.3)$$

$$\sigma_X^e = \frac{1}{f_x(x')} \phi\left(\frac{x' - \mu_X^e}{\sigma_X^e}\right) = \frac{1}{f_x(x')} \phi[\Phi^{-1}(F_X(x'))] \quad (5.4)$$

Where:

$\mu_X^e$  = equivalent normal mean

$\sigma_X^e$  = equivalent normal standard deviation

$F_x$  = true cumulative distribution of x

$\phi$  = PDF of standard normal distribution

$\Phi$  = CDF of standard normal distribution

$x'$  = Design point (mean value of x is usually a reasonable choice for initial design point)

This analysis procedure is an iterative procedure for non-linear cases, or cases that involve non-normal RV's, because the most probable point (MPP), or design-point, is not known prior to analysis. This analysis procedure has been used extensively in literature and is time-tested, however it may sometimes overestimate the reliability index in non-linear problems with many RV's (this fact must be considered when making conclusions

about this analysis). Analyses assuming the wind load RV's are uncorrelated and fully correlated were performed. The Rackwitz-Fiessler iterative procedure is described in detail below.

AFORM iterative procedure [Nowak and Collins, 2000]

1. Formulate limit state function ( $g$ ) and acquire the statistical parameters (mean, COV and distribution) for each of the random variables  $X_i$  ( $i = 1, 2, \dots, n$ ).
2. Assume design points for  $n-1$  of the RV's and determine the design point for the last RV by solving  $g = 0$  to ensure a design point at the failure boundary.
3. For each RV with a non-normal distribution, use Eqs. 5.3 and 5.4 to compute "equivalent normal" parameters.
4. Compute the reduced variables  $\{z'_i\}$  using Eq. 5.5 below

$$z'_i = \frac{x'_i - \mu_{X_i}^e}{\sigma_{X_i}^e} \quad (5.5)$$

5. Compute the partial derivative of  $g$  with respect to  $z'_i$  using Eq. 5.6 below

$$\frac{\partial g}{\partial z'_i} = \frac{\partial g}{\partial x'_i} \sigma_{X_i}^e \quad (5.6)$$



6. Compute the column vector  $\{G\}$  using Eqs. 5.7 and 5.8 below

$$G_i = - \left. \frac{\partial g}{\partial z'_i} \right|_{design\_point} \quad (5.7)$$

$$\{G\} = \begin{bmatrix} G_1 \\ G_2 \\ G_3 \\ \cdot \\ \cdot \\ \cdot \\ G_n \end{bmatrix} \quad (5.8)$$

7. Estimate  $\beta$  using Eq. 5.9 below.  $\{z'\}$  is the column vector containing all of the reduced variables

$$\beta = \frac{\{G\}^T \{z'\}}{\sqrt{\{G\}^T \{G\}}} \quad (5.9)$$

8. Compute the column vector of sensitivities ( $\alpha$ ) using Eq. 5.10 below

$$\alpha = \frac{\{G\}^T}{\sqrt{\{G\}^T \{G\}}} \quad (5.10)$$

9. Compute new design points for n-1 variable (in reduced variables format) using Eq. 5.11 below

$$z'_i = \alpha_i \cdot \beta \quad (5.11)$$

10. Compute the design points in original coordinates (for n-1 variables) using Eq. 5.12 below

$$x'_i = \mu_{Xi}^e + z'_i \sigma_{Xi}^e \quad (5.12)$$

11. Repeat steps 2-10 until  $\beta$  and design points (most probable point) converge.

Using the procedure described above, panel #2 was found to be the most problematic of all panels. None of the methods used, including AFORM, could converge to a solution. One of the factors affecting the solution procedures for this panel is the extensive number of loading areas present on this panel. 83% of the panel's surface area is covered by wind load areas (refer to figure 5.3). In order to circumvent the problem a Monte Carlo simulation was performed to estimate the reliability index of this particular panel. As noted, the computational requirements of Monte Carlo simulation prevent its use for all panels on the study house.

For comparison purposes the reliability, index of each panel was also calculated using a simple FORM analysis with simplified assumptions. The primary simplification is representing the 34 wind load RV's as a single RV with mean equal to the panel force (i.e. sum of nail forces) found from a deterministic analysis and considering a COV of 0.41. Four simplified analyses were performed:

1. FORM analysis using limit state from Eq. 5.1 (2 RV's problem).
2. AFORM analysis using limit state from Eq. 5.1 and assuming R is normally distributed and Q is lognormal (2 RV's problem).
3. FORM analysis using limit state from Eq. 5.2 (3 RV's problem).
4. AFORM analysis using limit state from Eq. 5.2 and assuming R and D are normally distributed and Q is lognormal (3 RV's problem).

Note that the FORM analysis does not include any information regarding the distribution of the RV's. First Order reliability index is calculated using the equations below 5.13 (2 RV's case) and 5.14 (3 RV's case) below:

$$\beta = \frac{\mu_R - \mu_Q}{\sqrt{\sigma_R^2 + \sigma_Q^2}} \quad (5.13)$$

$$\beta = \frac{\mu_R - \mu_Q + \mu_D}{\sqrt{\sigma_R^2 + \sigma_Q^2 + \sigma_D^2}} \quad (5.14)$$

Where:

$\mu_R, \mu_Q, \mu_D$  = Mean value for R, Q and D respectively

$\sigma_R, \sigma_Q, \sigma_D$  = Standard Deviation value for R, Q and D respectively

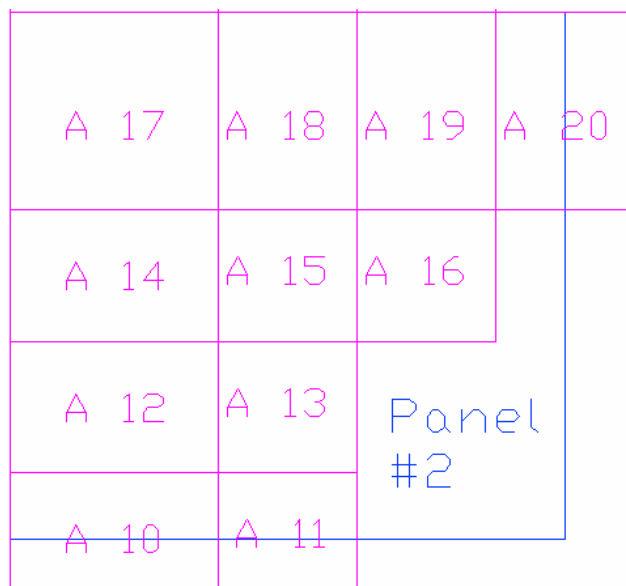


Figure 5.3 – Wind load areas acting directly on Panel #2.

Once the reliability index of each panel is obtained, a simple series (weakest-link) system model using uncorrelated and fully correlated cases is performed. This system allows the probability of failure of the entire roof to be estimated based on the probability of failure for each of the sixteen panels. A series system is appropriate as roof “failure” will occur if any panel is removed and thus compromises the house envelope [Sparks et al, 1994]. Note this is not equivalent to structural collapse.

### **ANALYSIS PROCEDURE**

The solution method described in the previous section details the actual reliability analysis method used to solve the limit states shown in Eqs. 5.1 and 5.2. The analysis procedure is described in detail in this section. The procedure involves the combination of the three programs used in the analysis (NASTRAN, NESSUS and FASTPANEL) to evaluate the limit state function. Conceptually, the process requires several calls to the FEA model in order to estimate  $\beta$  for each panel.

#### Conceptual Procedure

1. Perturb the RV values according to the reliability method used
2. Insert perturbed values into FEA input file
3. Perform finite element analysis of the roof model
4. Extract results from FEA output file
5. Evaluate limit state function
6. Repeat steps 1-5 until there are enough samples to estimate  $\beta$  for each panel.

The numerical procedure described below is what NESSUS, NASTRAN and FASTPANEL need to accomplish the task of calculating  $\beta$  values for each of the 16 panels in the roof system.

### Numerical Procedure

1. Based on global wind statistics (mean, COV, distribution), NESSUS inserts perturbed RV values into the wind load statistics file (windload.inc).
2. NESSUS calls the in-house program FASTPANEL. FASTPANEL reads the perturbed data file (windload.inc) and calculates a ratio of perturbed mean/base mean (pm/bm). The base mean is the actual mean wind load value of the RV in question. Each load area pressure data is then factored up or down by the (pm/bm) ratio. A perturbed load curve file (LCF) based on the factored pressure is then generated for each area. Thus, only the magnitudes of the wind load time history for each load area are proportionally changed. This keeps the local wind load COV's unchanged and preserves the correlations among the areas on the entire roof (i.e. the time wind peaks occur on a particular location on the roof is not altered).
3. NASTRAN conducts the analysis using the LCF for each of the 34 load areas.
4. Once NASTRAN finishes the FEA analysis, FASTPANEL searches through the NASTRAN output file and adds up the force in each nail element of each panel. It does this for each time-step. A total of 4512 panel force values is recorded (16 panels X 282 time-steps).

5. Once all of the force values are obtained, FASTPANEL searches for the maximum panel force in any time-step. The maximum force and associated time of each panel is recorded in the output file (panelmaxout.txt)
6. NESUSS opens panelmaxout.txt and extracts the maximum force for the panel being analyzed. This force value corresponds to  $Q$  in the limit state function.
7. NESSUS evaluates the limit state function based on  $Q$  and the perturbed value of  $R$  (and  $D$ , if used) and the Rackwitz-Fiessler method (AFORM). This process serves as one sample.
8. Steps 1-7 are repeated until a sufficient number of samples (determined by the AFORM algorithm) is taken and the reliability index for the panel in question is calculated.
9. Steps 1-8 are repeated for each of the 16 panels.

## **COMPARISON WITH PREVIOUS RESEARCH RESULTS**

Rosowsky and Cheng [1999a, 1999b], performed a reliability analysis on a series of sheathing panels and roof-to-wall connections. In order to compare results with the results obtained from that study, a simple analysis using the structure Clemson 1 (refer to Chapter II) was performed. The wind loads used in that study correspond to wind loads of 100 and 125 mph, therefore the ASCE 7-02 wind loads (110 mph) calculated in Chapter IV (refer to Table 4.1) were applied to the structure in the same way. Load statistics had a COV of 0.41, bias factor of 0.41, and lognormal distribution. Panel that fell within two or more load zones had nominal loads based on a weighted average of the uplift pressures.

Resistance statistics were also significantly lower in Rosowsky and Chang's study, therefore the resistance of the panels was increased to the same values used in this study (mean of 131 psf, COV of 0.41, and normal distribution). The new analysis provides comparable results with the ones obtained from this study.

## CHAPTER VI

### RESULTS AND CONCLUSIONS

#### **RESULTS OF RELIABILITY ANALYSIS**

The results of the reliability analyses are presented in Table 6.1. The first order reliability method (FORM) results consider 2 RV's (R and Q) or 3 RV's (R, Q and D). In this analysis, R is taken as panel pull-out capacity (with statistics given in Table 5.1) and Q is taken as total maximum panel force applied to the panel, with mean value found from the deterministic analysis (refer to Table 3.7) and COV taken as 0.41. Statistics for D can be found in Table 5.2. The advanced first order reliability method (AFORM) results consider 34 load random variables and one resistance random variable, and are calculated by the numerical procedure described in Chapter V. The probability of failure ( $P_f$ ) reported relates to the AFORM (35 RV's) analyses. Note that for panel #2 a Monte Carlo Simulation (MCS) was performed to obtain the results.



Table 6.1 – Results of Reliability Analyses

Panel #	Reliability Index (b)					Pf (%)
	Dead Load Included (g = R - Q + D)		Dead Load not Included (g = R - Q)			
	FORM (3 RV's)	AFORM (3 RV's)	FORM (2 RV's)	AFORM (2 RV's)	AFORM (35 RV's)	
1	4.03	3.18	3.90	3.10	4.55	2.74E-04
2	2.91	2.41	2.80	2.33	2.88*	1.99E-01
3	3.61	2.81	3.50	2.73	3.41	3.20E-02
4	3.33	2.69	3.20	2.61	4.35	6.68E-04
5	5.42	4.33	5.30	4.25	5.89	1.88E-07
6	5.36	4.27	5.20	4.19	5.85	2.45E-07
7	5.41	4.33	5.20	4.25	5.89	1.90E-07
8	3.01	2.50	2.90	2.41	4.10	2.10E-03
9	5.42	4.33	5.30	4.25	5.89	1.88E-07
10	5.42	4.33	5.30	4.25	5.89	1.88E-07
11	5.40	4.32	5.20	4.23	5.89	1.94E-07
12	3.32	2.68	3.20	2.60	4.06	2.42E-03
13	5.42	4.33	5.30	4.24	5.89	1.89E-07
14	5.42	4.33	5.30	4.25	5.89	1.88E-07
15	5.41	4.33	5.30	4.24	5.89	1.89E-07
16	5.51	4.42	5.40	4.34	5.95	1.37E-07

\*Computed Using Monte Carlo Simulation

Probability of failure in Table 4.1 above was approximated using equation 6.1

below:

$$P_f = \Phi(-\beta) \quad (6.1)$$

Where:

$\beta$  = Reliability Index of component

$\Phi$  = CDF of Standard Normal Distribution

Panel #2 has the lowest  $\beta$  in all analyses. Except for panel #12, all panels away from the dynamic loading region had reliability indices significantly higher than panels directly loaded, as shown in Figure 4.4. Panels #1, 2, 3, 4, 8 were those directly loaded with the wind load areas. Panel #12 was not directly loaded with the dynamic load but it also had a significantly lower  $\beta$  value. This is expected since Panel #12 also had relatively higher deterministic panel loads (see Table 3.7). Dead load (D) was

conservatively excluded (as D resists wind uplift) as a random variable from the 35 RV's AFORM analysis because its inclusion made little difference to in the simplified analyses results, and it would only add computational complexity to the 35 RV's AFORM analysis.

Assuming the entire roof (all 16 panels) to be a series system (weakest-link), the reliability index of the roof may be obtained using the following upper (Eq. 6.2) and lower (Eq. 6.3) bounds:

$$\beta_{system} = \beta (\text{lowest of any panels}) = 2.88 \quad (6.2)$$

Or

$$\beta_{system} = -\Phi^{-1} \left[ 1 - \prod_{i=1}^{16} (1 - P_{fi}) \right] = 2.83 \quad (6.3)$$

Where:

$\beta$  = Reliability Index of component

$\beta_{system}$  = Reliability Index of system

$\Phi$  = CDF of Standard Normal Variable

$P_{fi}$  =  $\Phi(-\beta)$  = Probability of failure of component (roof panel) i

Equation 6.2 assumes full correlation among panel resistances while Equation 6.3 assumes panels are uncorrelated. The actual degree of correlation is unknown. However, as the bounds are relatively narrow, this information is not needed.

A series system is used since failure of any panel breaks the roof envelope and allows water entry, thus constituting "failure" as defined in this study. A reliability index

of 2.83 corresponds to a probability of failure for the entire roof system of approximately 0.233% (1 in 429).

## SENSITIVITY ANALYSIS

The sensitivity analysis results for a few key panels are presented in the next few pages. A complete set of results is presented in Appendix B. Sensitivity derivatives are computed numerically using the dimensionless ratio (Eq. 6.4) and normalized to the largest value.

$$S = \frac{\partial \beta}{\partial \sigma} \cdot \left( \frac{\sigma}{\beta} \right) \quad (6.4)$$

Where:

S = Sensitivity Factor

$\beta$  = Reliability Index

$\sigma$  = Standard Deviation of RV in question

Random variables on the charts refer to wind load areas as numbered in Figure 4.4. Resistance importance is significantly higher than load importance, and it is not included in the figures for clarity. Although this is the case, inclusion of load RV's is necessary for accurate results. If the wind load is taken as deterministic, as suggested by sensitivities, significant differences in analysis results appear. For example, an analysis of panel #1 that considers only one RV (panel resistance) and takes wind load to be deterministic (substituting constant results from Table 3.7), a  $\beta$  value of 5.08 is obtained. This is significantly larger than 4.54 from the 35 RV's AFORM analysis (see Table 6.1).

Similarly, a deterministic wind load reliability analysis for panel #3 results a  $\beta$  of 4.73 compared to 3.41 from the 35 RV's AFORM analysis (see Table 6.1).

Figures 6.1-6.5 illustrate the sensitivity analysis results for panels #3, 4, 5, 6 and 11. Panel #3, 4 and 6 are directly affected by the dynamic load areas, while panels 5 and 11 are representative of panels away of dynamic loading areas. It was expected that the areas directly over the panel would have higher influence on the reliability results than other area. For example, in panel #3 areas 21-34 were expected to have higher sensitivity values; in panel #4 areas 30-33 were expected to have higher sensitivity values; and in panel #6 areas 20 was expected to have higher sensitivity values. Panels #5 and 11 were expected to be little influenced by any loading area.

The expected results were not generally matched by the outcome of the sensitivity analysis. Panel #6 was the only one showed here that showed some similarity in outcome and expected results. All the other panels behaved very differently than expected. Panel #3 and 5 showed relatively uniform sensitivity for all RV's. Panel #4 is most highly influenced by areas 8, 17, 21 and 22. Panel #11 was only influenced by area 17. The quite unexpected sensitivity results most probably resulted from numerical error. The sensitivity chart for panel #2 (Figure B.2) was obtained by Monte Carlo Simulation (MCS). The resistance RV sensitivity was so much larger than any other sensitivity that the outcome may have been influenced by its large magnitude. Other methods of analysis that included MCS a sensitivity calculation using loads from the same time step also yielded similar results. It is possible that numerical error caused the inconsistencies in the sensitivity analysis results.

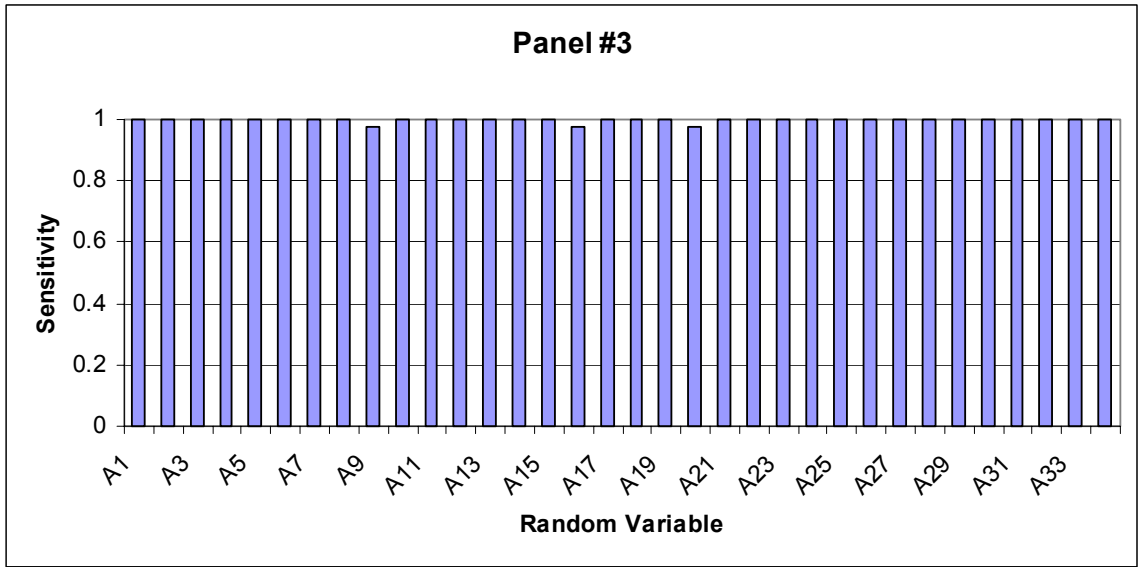


Figure 6.1 – Sensitivity factors (with respect to std. dev.) for panel #3

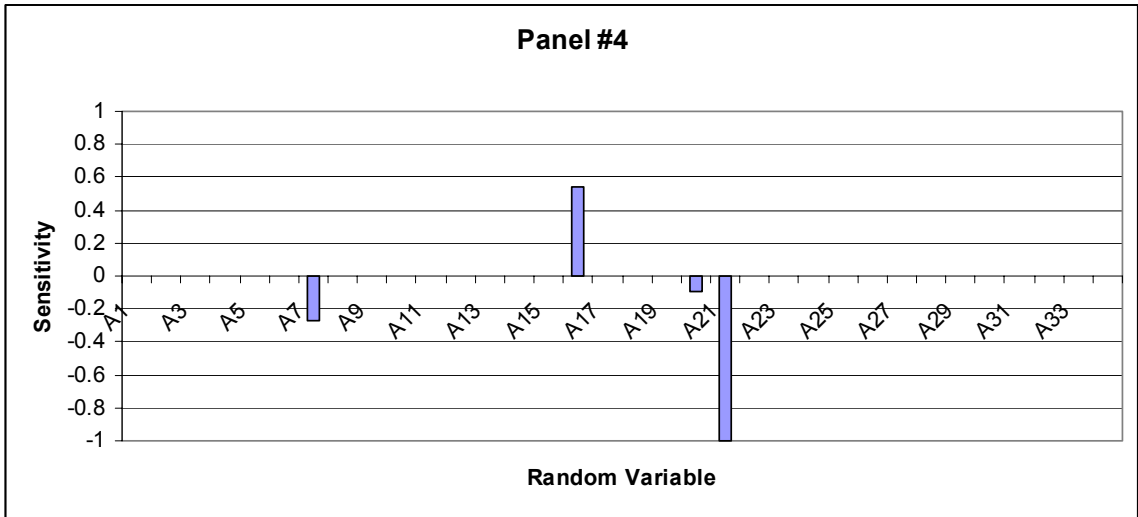


Figure 6.2 – Sensitivity factors (with respect to std. dev.) for panel #4

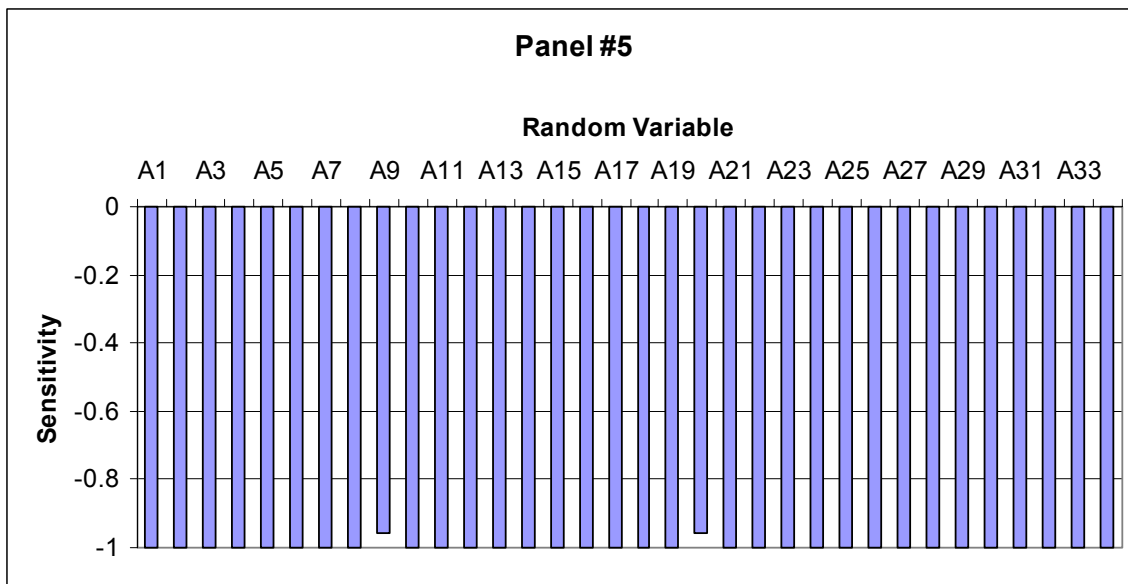


Figure 6.3 – Sensitivity factors (with respect to std. dev.) for panel #5

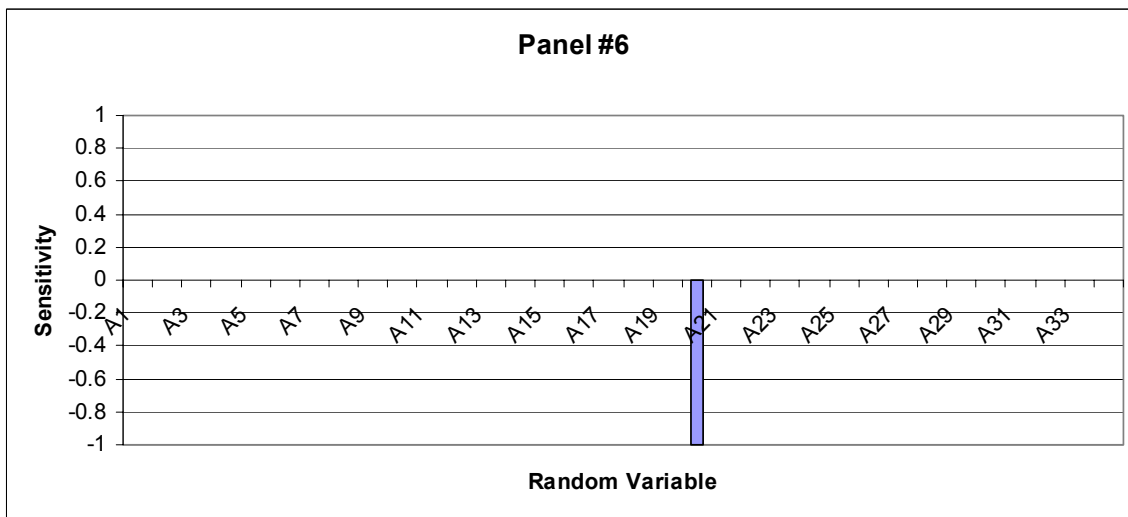


Figure 6.4 – Sensitivity factors (with respect to std. dev.) for panel #6

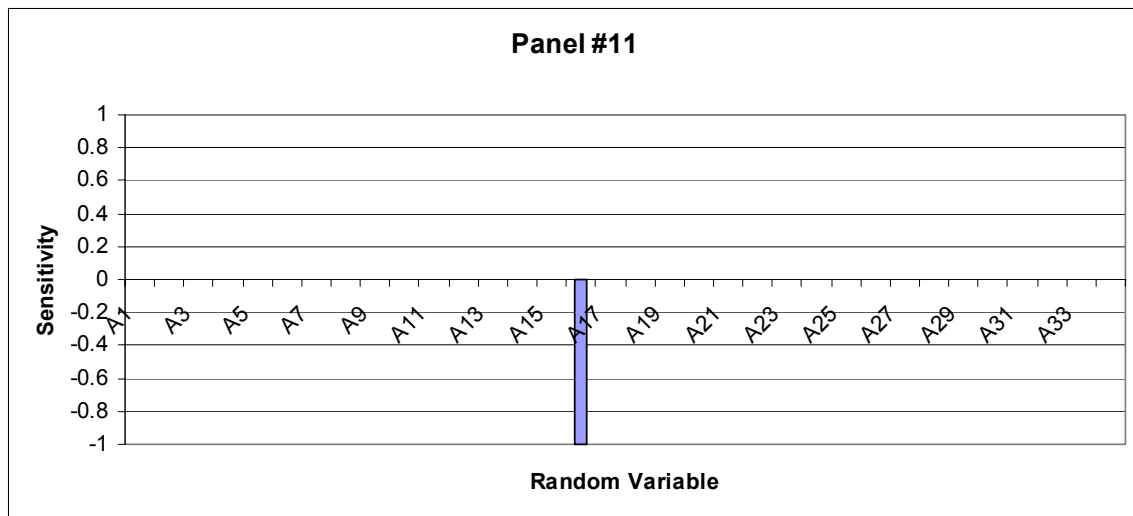


Figure 6.5 – Sensitivity factors (with respect to std. dev.) for panel #11

## COMPARISON WITH PREVIOUS RESULTS

As discussed in Chapter IV, since the deterministic dynamic load effects are significantly lower (~50%) than the assumed equivalent uniform pressure loads, it is expected that the reliability indices of the panels calculated with the dynamic loads are significantly higher than reliability indices using the simplified uniform load model. This may be verified by comparing  $\beta$  values obtained in this analysis and  $\beta$  values from previous research.

This expectation is verified as Rosowsky and Cheng [1999b] obtained significantly lower reliability indices for a house of similar proportions using a uniform wind load model (refer to Table 2.5). Clemson 1 is a structure similar to the one used in this study (similar height, roof slope, roof overhang, dimensions). The minimum reliability index for that structure is 1.25 ( $P_f = 10.6\%$ ) while the maximum reliability

index is 3.76 ( $P_f = 0.0085\%$ ). In this study, the minimum reliability index found is 2.88 ( $P_f = 0.199\%$ ) while the maximum reliability index is 5.95 ( $P_f = 1.34E-07\%$ )

Note, however, that there are two differences in Rosowsky and Cheng's work that need to be accounted for to compare results accurately.

1. The panels used in this study are significantly stronger than the panels used by Rosowsky and Cheng because more fasteners are used in each panel. This would bias the  $\beta$ 's upwards in this study relative to Rosowsky and Cheng's work.
2. The wind load used in Rosowsky and Cheng is based on a 125 mph wind, while those in this study are based on a 110 mph wind. This would bias the results in this study upwards.

Figure 6.6 present results from Rosowsky and Cheng that has increased panel resistance (by adding more nails) and proportionally lower uniform wind load to a 110 mph equivalent. In this case, since resistance and wind speed are identical, only the more realistic dynamic wind load model and refined analysis technique used here impacts the results.

As expected from the deterministic analysis, Figures 6.6 and 6.6 show that panels in similar locations in this study have significantly higher reliability indices than reliability indices from the modified Clemson 1 analysis. Interior panels have  $\beta = 2.28$  in Clemson 1, while interior panels have  $\beta = 5.89$  in this study. The panels in Clemson 1 that governs the roof reliability are the two corner panels, with  $\beta = 2.08$ . In contrast, the panels with lowest  $\beta$  in this study are the interior panels at the gable end (with  $\beta = 2.88$  and 3.41).



This occurs because panels are loaded highest in that region (see Figure 4.4). The corner panels have reliability indices of 4.55 and 4.35.

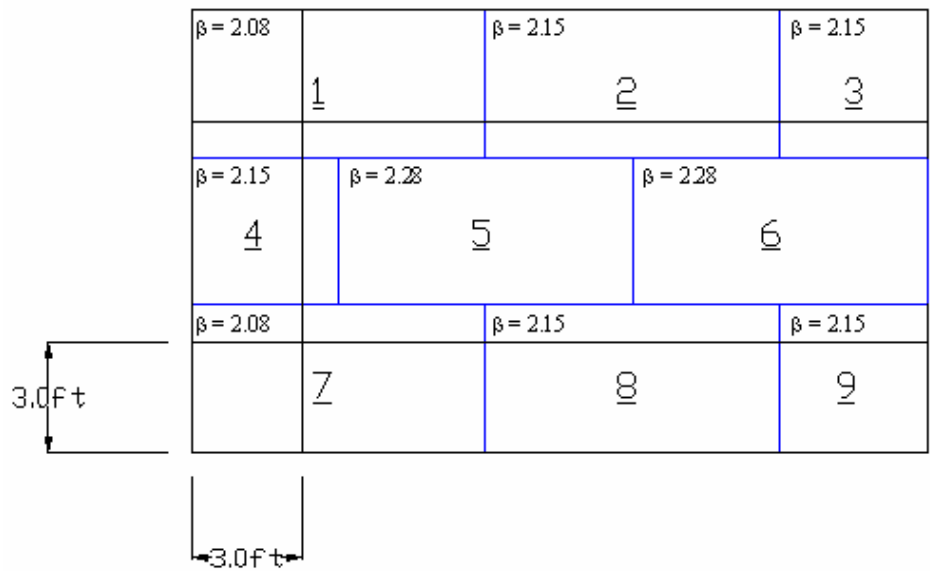


Figure 6.6 – Results for Clemson 1 Structure using updated statistics

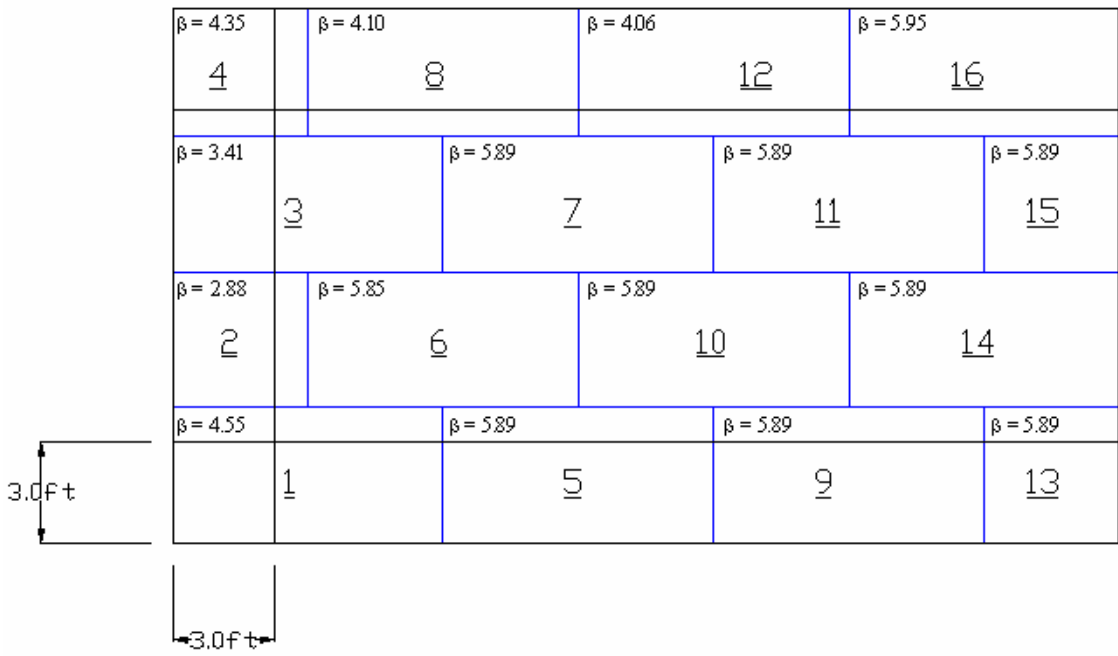


Figure 6.7 – Results for 35 RV AFORM analysis

## CONCLUSIONS

From the analyses performed in this study the following conclusions can be reached:

1. For some panels, reliability indices are significantly higher here than computed in previous studies.
2. Reliability indices are significantly different from panel to panel, ranging from 2.88 to 5.95. Therefore, there is significant under and/or over-design for wind loads using the current code procedures. A reliability calibration is needed.
3. The location of the governing panels appear to be the exterior edge rather than the corners, as previously thought using the uniform wind load model.
4. The limit state surface is very complex. This is evident by the fact that the most-probable-point (or design point) is very difficult to find. The AMV+ method was unable to converge for most panel limit states in this study. AFORM was unable to converge for panel #2. This poses computational difficulties for future reliability studies, as sophisticated variance reduction techniques such as importance sampling, rely on most-probable-point for solution. If the MPP cannot be located, a crude simulation method, that is computationally expensive, such as Monte Carlo Simulation of Latin Hypercube, must be used solution in some cases.
5. Using AFORM and 34 load random higher  $\beta$ 's than those calculated using one load random variable. The use of 1 load random variable provides significantly more conservative designs. For example, interior panels analyzed with one load

RV had  $\beta$ 's around 4.2, while the 34 load analysis yielded  $\beta$ 's around 5.9 for the same interior panels.

6. Dead load is a minor contribution to panel reliability and can be conservatively disregarded.
7. As expected, changing the load probabilistic distribution to normal results in higher reliability indices. In most cases, the difference is significant (for example, in panel #3,  $\beta$  changes from 2.73 to 3.50) and should be accounted for.
8. The results from the MCS for panels #2 and #3 have shown that the AFORM method is valid for this analysis. Panel #2 had the lowest reliability index (as expected) and MCS results for panel #3 shows a  $\beta = 3.21$ , very close to 3.41 obtained from the AFORM analysis (See Appendix D).

## RECOMMENDATIONS

By setting a target reliability index of 4.0, the nails spacing for each panel, as shown in figure 6.8, results in a uniform design. The probability of failure of each panel is almost the same; therefore economy and safety are improved.

$\beta = 4.35$ <u>4</u> S = 6 in Field 4 in Edge	$\beta = 4.10$ <u>8</u> Spacing = 6 in	$\beta = 4.06$ <u>12</u> Spacing = 6 in	$\beta = 4.01$ <u>16</u> Spacing = 12 in
$\beta = 4.31$ <u>3</u> Spacing = 4 in	$\beta = 4.01$ <u>7</u> Spacing = 12 in	$\beta = 4.01$ <u>11</u> Spacing = 12 in	$\beta = 4.01$ <u>15</u> Spacing = 12 in
$\beta = 3.96$ <u>2</u> S = 4 in Field 3 in Edge	$\beta = 4.01$ <u>6</u> Spacing = 12 in	$\beta = 4.01$ <u>10</u> Spacing = 12 in	$\beta = 4.01$ <u>14</u> Spacing = 12 in
$\beta = 4.55$ <u>1</u> Spacing = 6 in Field 4 in Edge	$\beta = 4.01$ <u>5</u> Spacing = 12 in	$\beta = 4.01$ <u>9</u> Spacing = 12 in	$\beta = 4.01$ <u>13</u> Spacing = 12 in

Figure 6.8 – Panel nail spacing for target  $\beta = 4.0$ .

## RECOMMENDATIONS FOR FUTURE RESEARCH

From the analyses performed in this study, the following recommendations for future research can be made:

1. Further advance the research on wind loads applied to roofs with different slopes and geometric configuration to provide a better understanding of load distribution and wind load uplift pressures.
2. Conduct additional tests to determine the statistical parameter for resistance of panels considering different thickness, type of wood, ply lay-up, and number of nails per panel.
3. Determine panel clip behavior. Panel clips tend to increase the strength of panels but little is known about their structural contribution. The results obtained in this study are conservative because they do not include the effects of panel clips.
4. Conduct reliability analysis with a simulation-based technique to verify findings. Such techniques, however, are generally associated with high computational costs.
5. Conduct further investigations on the importance and sensitivity of each random variable.
6. Conduct reliability research that includes error in the computation of the resistance of the panels.

## REFERENCES

1. ASCE (1993). *Minimum Design Loads for Buildings and Other Structures*. ASCE 7-93, American Society of Civil Engineers, Reston, VA.
  2. ASCE (1995). *Minimum Design Loads for Buildings and Other Structures*. ASCE 7-95, American Society of Civil Engineers, Reston, VA.
  3. ASCE (2003). *Minimum Design Loads for Buildings and Other Structures*. ASCE 7-02, American Society of Civil Engineers, Reston, VA.
  4. Bulleit, W.M., Rosowsky, D.V., Fridley, K.J, and Criswell, M.E (1993). "Reliability of Wood Structural Systems". *ASCE Journal of Structural Engineering*, v 119, n 9, 2629-2641.
  5. Cheng, N. (1998). "Reliability of Light-Frame Roof Systems Subject to Wind Uplift." MS Thesis, Department of Civil Engineering, Clemson University, Clemson, SC.
  6. Cole, H. A. (2004), Personal communication.
  7. Eamon, C.D. (2004). "CE 4693: Reliability of Structures." *Class Notes*. Mississippi State University.
- Ellingwood, B., Galambos, T.V., MacGregor, J.G. and Cornell, C.A. (1980). *Development of a Probability Based Load Criterion for American National Standard A58*, NBS Special Publication 577, U.S. Department of Commerce, National Bureau of Standards, Washington, D.C.

8. Ellingwood, B.R., Rosowsky, D.V., Li, Y., and Kim, J.H. (2004). "Fragility Assessment of Light-Frame Wood Construction Subjected to Wind and Earthquake Hazards." *ASCE Journal of Structural Engineering*, v 130, n 12, 1921-1930.
9. Faherty, K.F and Williamson, T.G. (1999). *Wood Engineering and Construction Handbook*, McGraw-Hill Companies, New York, NY.
10. Federal Emergency Management Administration ([www.fema.gov](http://www.fema.gov)). January 2005.
11. Fowler, S.L. (2001). "Clip Reactions in Standing Seam Roofs of Metal Buildings." MS Thesis, Department of Civil Engineering, Mississippi State University, Mississippi State, MS.
12. Herzog, B. (2005), Personal communication.
13. "International Residential Code for One- and Two-Family Dwellings" (2000). International Code Council, Falls Church, VA.
14. Kasal, B., Collins, M.S., Paevere, P., and Foliente, G.C. (2004). "Design Models of Light Frame Wood Buildings under Lateral Loads." *ASCE Journal of Structural Engineering*, v 130, n 8, 1263-1271.
15. Lee, J. M. (1997) *MSC/NASTRAN Linear Static Analysis User's Guide* (v 69+). MacNeal-Schwendler Corporation, Los Angeles, CA.
16. Lee, S.H. (1992) *MSC/NASTRAN Nonlinear Analysis Handbook Volume 1* (v 67). MacNeal-Schwendler Corporation, Los Angeles, CA.
17. Lee, S.H. (1992) *MSC/NASTRAN Nonlinear Analysis Handbook Volume 2* (v 67). MacNeal-Schwendler Corporation, Los Angeles, CA.
18. Lewis, D. (2004), Personal communication.
19. Liu, H., Saffir, H.S., Sparks, P.R. (1989). "Wind Damage to Wood-Frame Houses: Problems, Solutions and Research Needs." *ASCE Journal of Structural Engineering*, v 2, n 2, 57-70.
20. Liu, H., Gopalaratnam, V.S., Nateghi, F. (1990). "Improving Resistance of Wood-Frame Houses." *Journal of Wind Engineering and Industrial Aerodynamics*, v 36, 669-707.

21. MSC/NASTRAN *Quick Reference Guide* (v 67). (1993). MacNeal-Schwendler Corporation, Los Angeles, CA.
22. Nowak, A.S. and Collins, K.R. (2000). *Reliability of Structures*. McGraw-Hill Companies, Inc., Boston, MA.
23. Nowak, A. S, Eamon, C. D., and Ritter, M. A. (2001). *LFRD Calibration of Wood Bridges*. Report Submitted to the US Department of Agriculture, Forest Services, Forest Products Laboratory. Ann Arbor, MI.
24. Riha, D. S., Thacker, B. H., Millwater, H. R., Wu, Y. T., and Enright, M.P. (2000). "Probabilistic Engineering Analysis Using the NESSUS Software." *41st Structural Dynamics and Materials Conference*, Paper 2000-1512, Atlanta, GA.
25. Rosowsky. D.V. and Cheng, N. (1999a) "Reliability of Light-Frame Roofs in High-Wind Regions. I: Wind Loads." *ASCE Journal of Structural Engineering*, v 125, n 7, 725-733.
26. Rosowsky. D.V. and Cheng, N. (1999b) "Reliability of Light-Frame Roofs in High-Wind Regions. II: Reliability Analysis." *ASCE Journal of Structural Engineering*, v 125, n 7, 734-739.
27. Rosowsky, D.V. and Huang, Z. (2000). "Wind Load Statistics for Reliability Analysis of Light-Frame Roof Components in Hurricane-Prone Regions." *Proceedings of the 8th ASCE Specialty Conference on Probabilistic Mechanics and Structural Reliability*, University of Notre Dame, Notre Dame, IN, July 24-26, 2000. CD-ROM proceedings, paper PMC2000-055.
28. Schiff, S.D., Mizzell, D.P., Zaits, M.D. (1994). "Uplift Resistance of Plywood and OSB roof Sheathing." *Proceedings of the Structures Congress XII 1994*, Atlanta, GA. 1054-1559.
29. Schiff, S.D., Rosowsky, D.V., Lee, A.E.C. (1996). "Uplift Capacity of nailed roof Sheathing Panels." *Proceedings of the International Wood Engineering Conference, New Orleans, LA*, v 4, 446-670.
30. Smulski, S. (1997). *Engineered Wood Products: A Guide for Specifiers, Designers, and Users*. PFS Research Foundation, Madison, WI.
31. Sinno, R.R. and Taylor, C.D. (1993) "Use of Magnetic Forces to Simulate Dynamic Variable Wind Uplift Forces." Report MBMA 701B-S3, Metal Building Manufacturers Association, Cleveland, OH.
32. Sinno, R.R. and Taylor, C.D. (1994) "Simulating Dynamic Non-Uniform Wind Uplift Pressures on Sheet Metal Roofing." Report MBMA 802-S8, Metal



Building Manufactures Association, Cleveland, OH.

33. Sinno, R.R. and Taylor, C.D. (1995) "Response of Standing Seam Metal Roofing to Non-Uniform Unsteady Uplift Pressures." Report MBMA 902-S8, Metal Building Manufactures Association, Cleveland, OH.
34. Sinno, R.R., Surry, D., Fowler, S. and Ho, T.C.E. (2003). "Testing of Metal Roofing Systems under Simulated Realistic Wind Loads." *11th International Conference on Wind Engineering*, Lubbock, TX.
35. Soltis, L.A (1984). "Low-Rise Timber Buildings Subjected to Seismic, Wind and Snow Loads." *ASCE Journal of Structural Engineering*, v 110, n 4, 744-753.
36. Sparks, P.R., Schiff, S.D., Reinhold, T.A. (1994). "Wind Damage to Envelopes of Houses and Consequent Insurance Losses." *Journal of Wind Engineering and Industrial Aerodynamics*, v 53, 145-155.
37. Sundararajan, C.R. (1995). *Probabilistic Structural Mechanics Handbook: Theory and Industrial Applications*. International Thompson Publishing Company, New York, NY.
38. "Uniform Building Code Volume 2: Structural Engineering Design Provisions" (1997). International Conference of Building Officials, Whittier, CA.
39. United States Geological Survey ([www.usgs.gov](http://www.usgs.gov)). March 2005.

APPENDIX A

UWO WIND LOAD AND 20 POINT MOVING AVERAGE

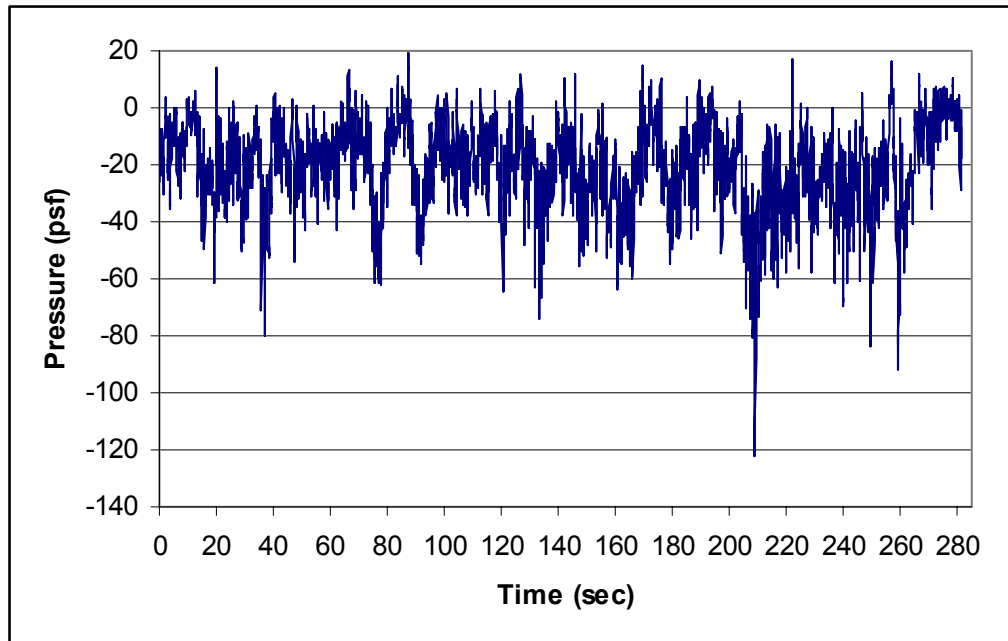


Figure A.1 - Peak loads for UWO data (Area 1)

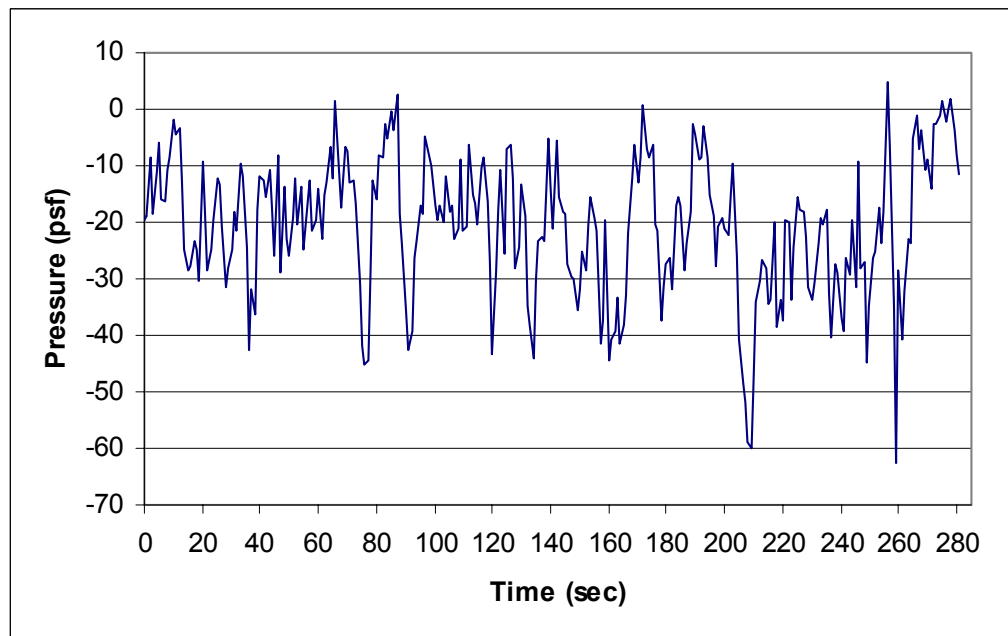


Figure A.2 – Peak loads for 20 point moving average data (Area 1)

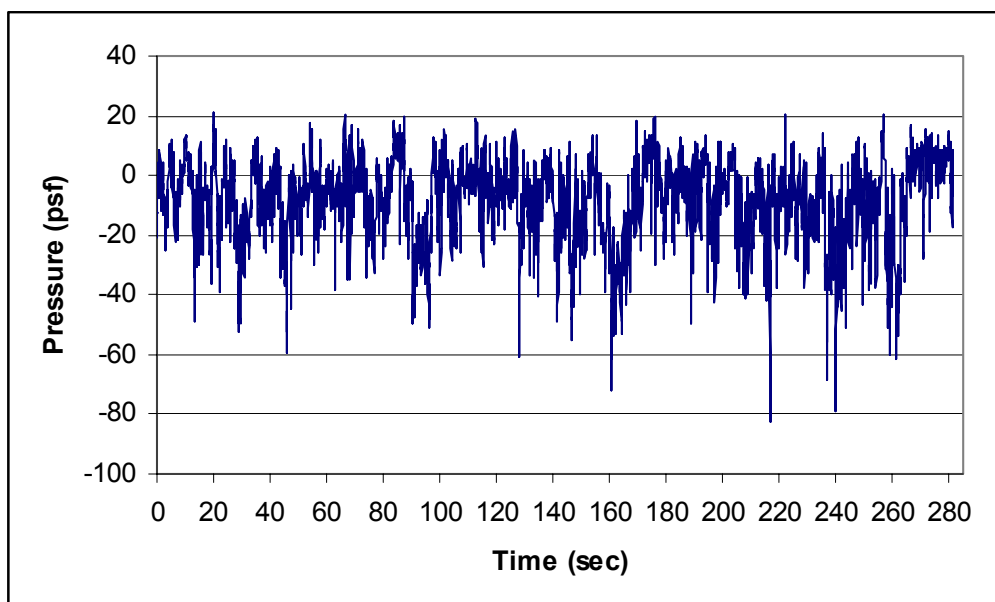


Figure A.3 – Peak loads for UWO data (Area 2)

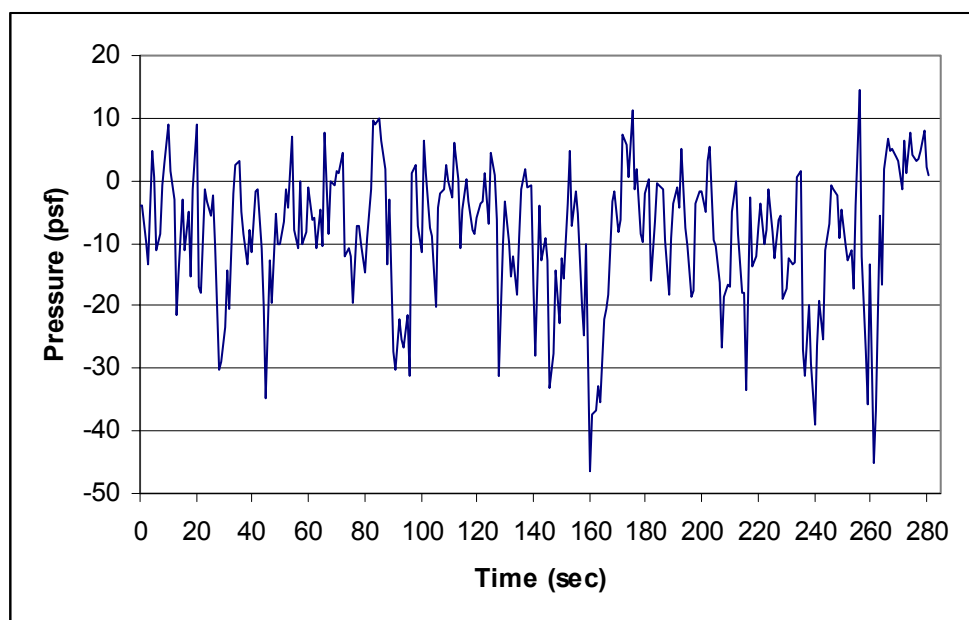


Figure A.4 – Peak loads for 20 point moving average data (Area 2)

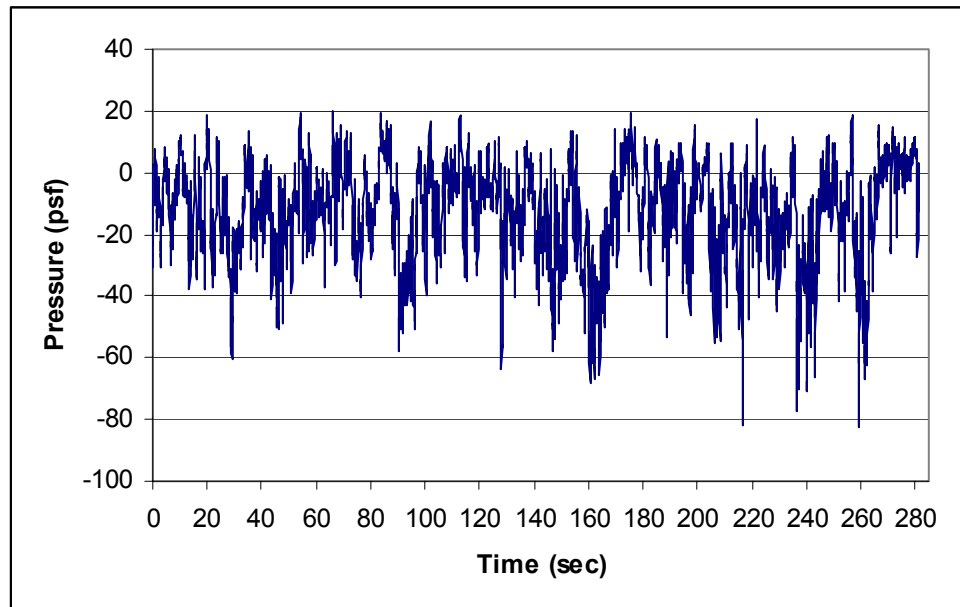


Figure A.5 – Peak loads for UWO data (Area 3)

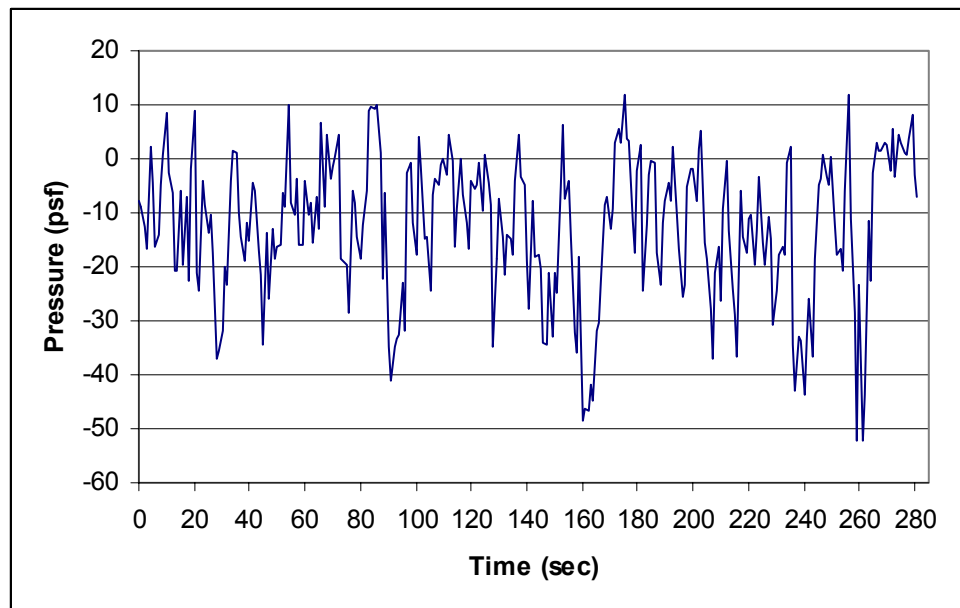


Figure A.6 – Peak loads for 20 point moving average data (Area 3)

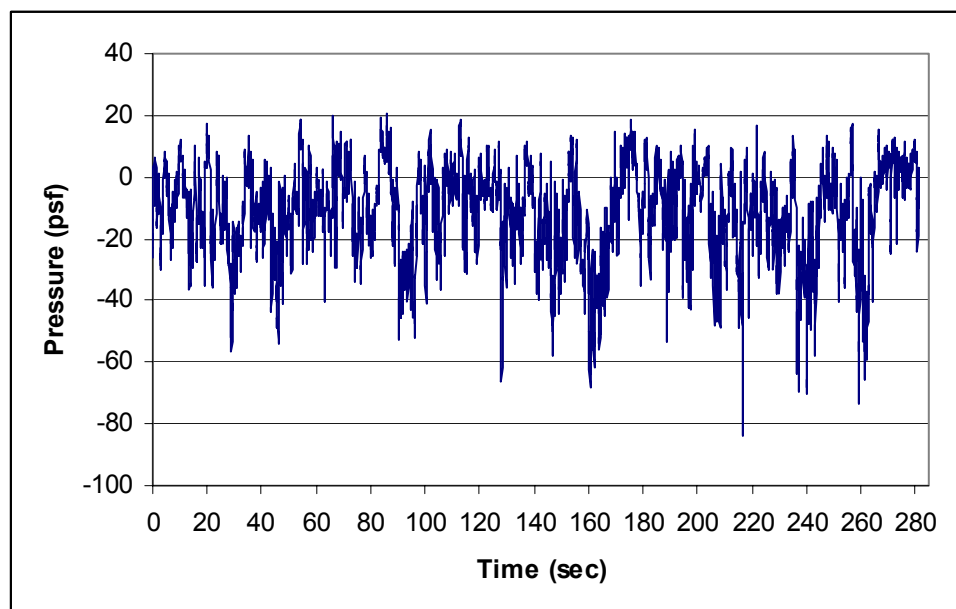


Figure A.7 – Peak loads for UWO data (Area 4)

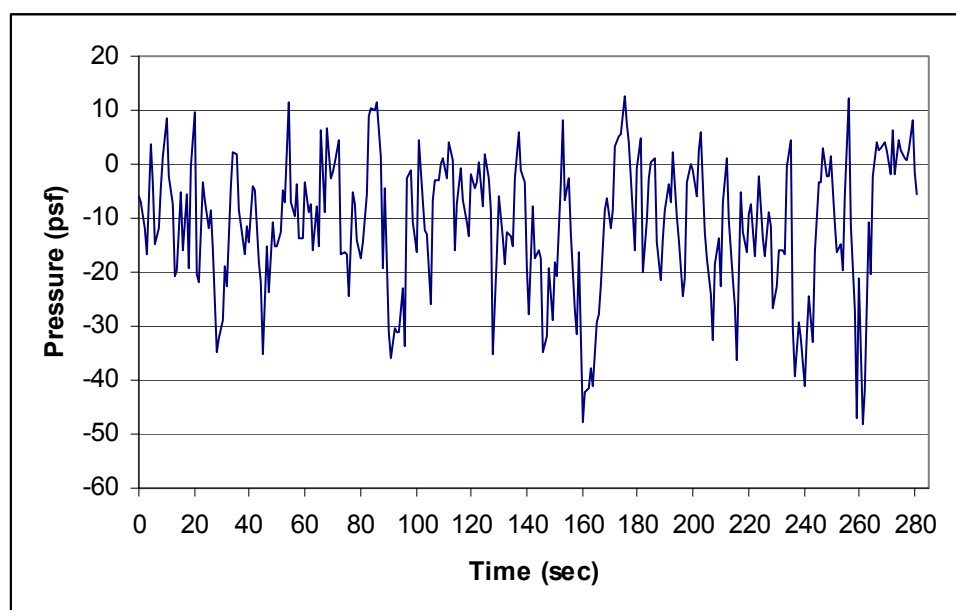


Figure A.8 – Peak loads for 20 point moving average data (Area 4)

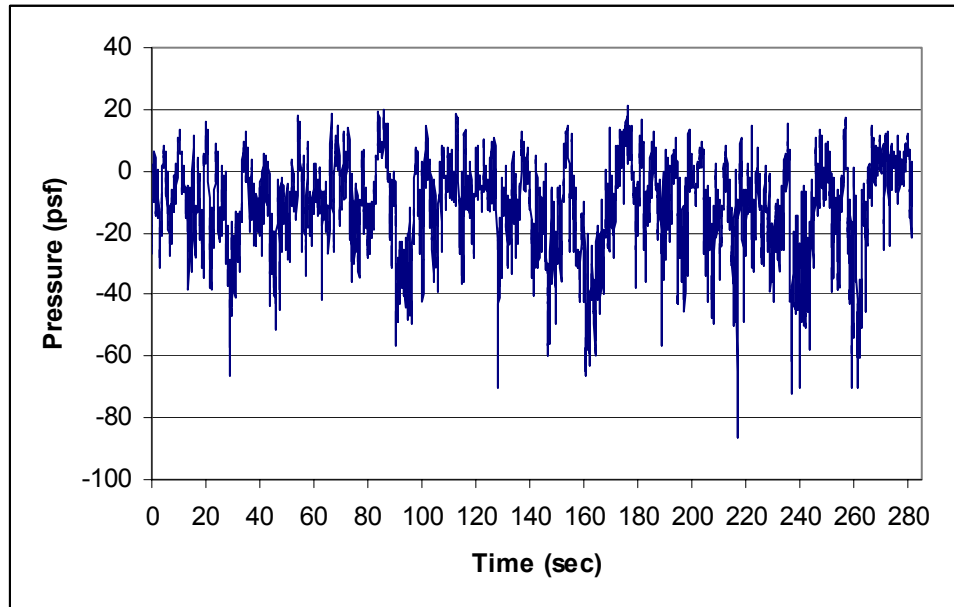


Figure A.9 – Peak loads for UWO data (Area 5)

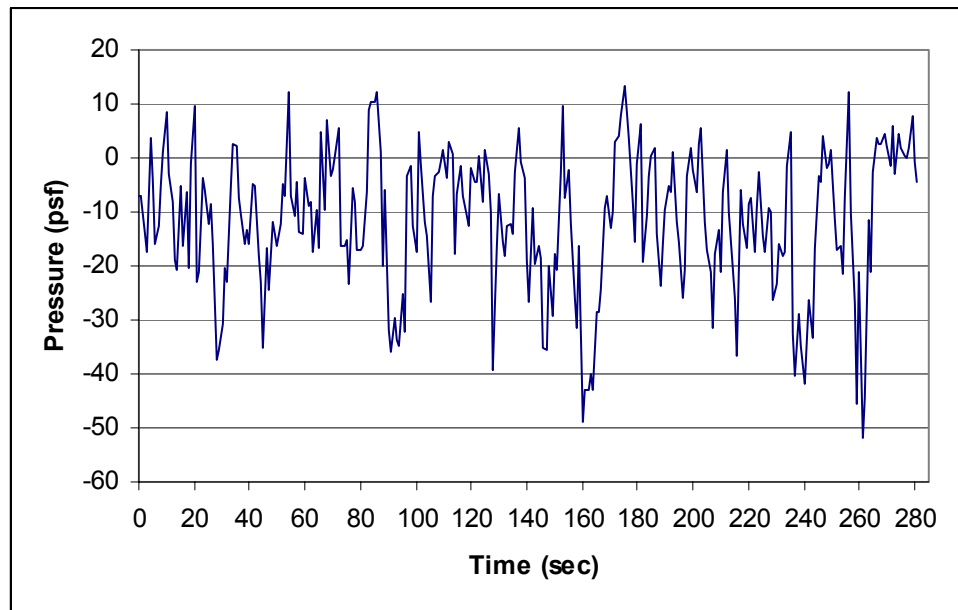


Figure A.10 – Peak loads for 20 point moving average data (Area 5)

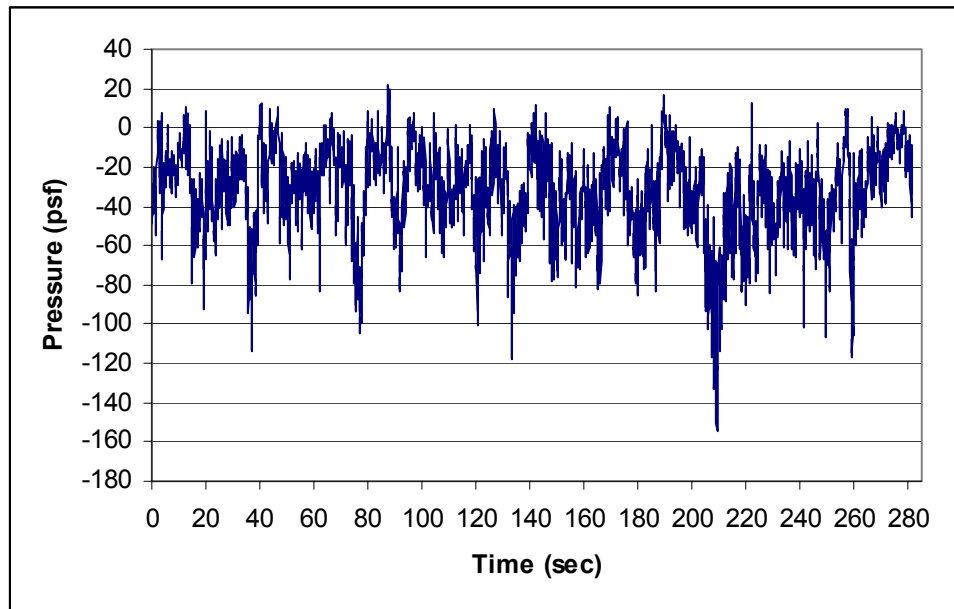


Figure A.11 – Peak loads for UWO data (Area 6)

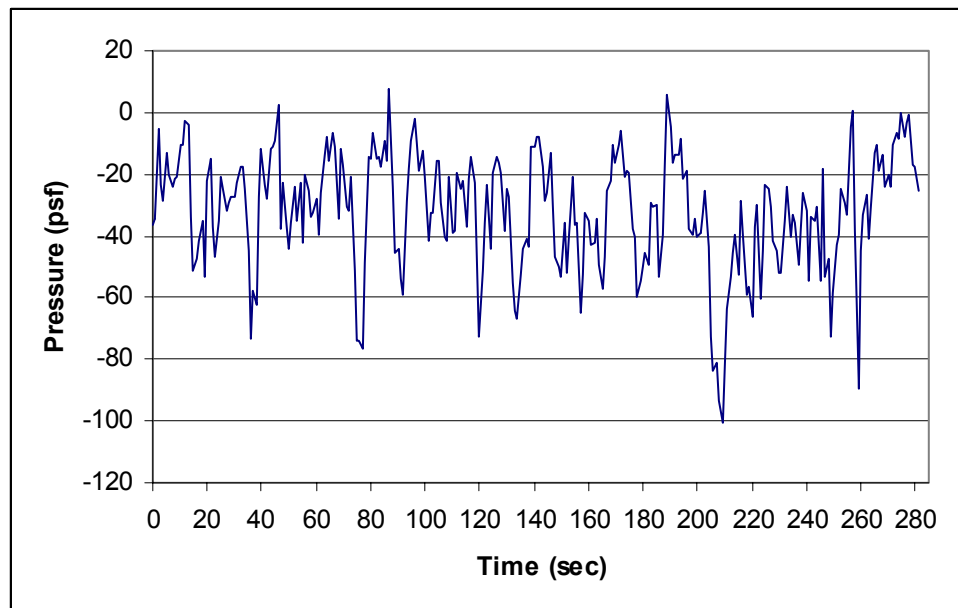


Figure A.12 – Peak loads for 20 point moving average data (Area 6)



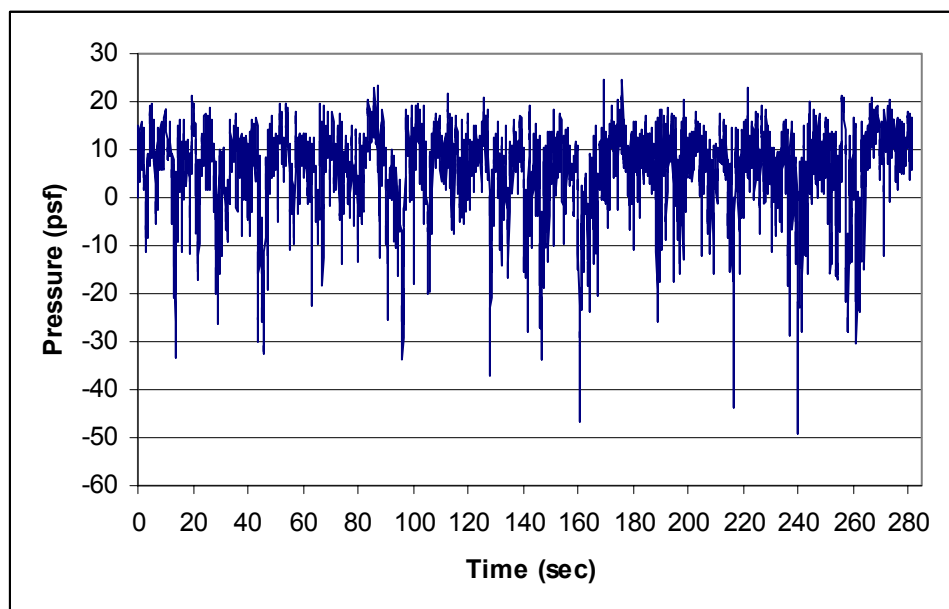


Figure A.13 – Peak loads for UWO data (Area 7)

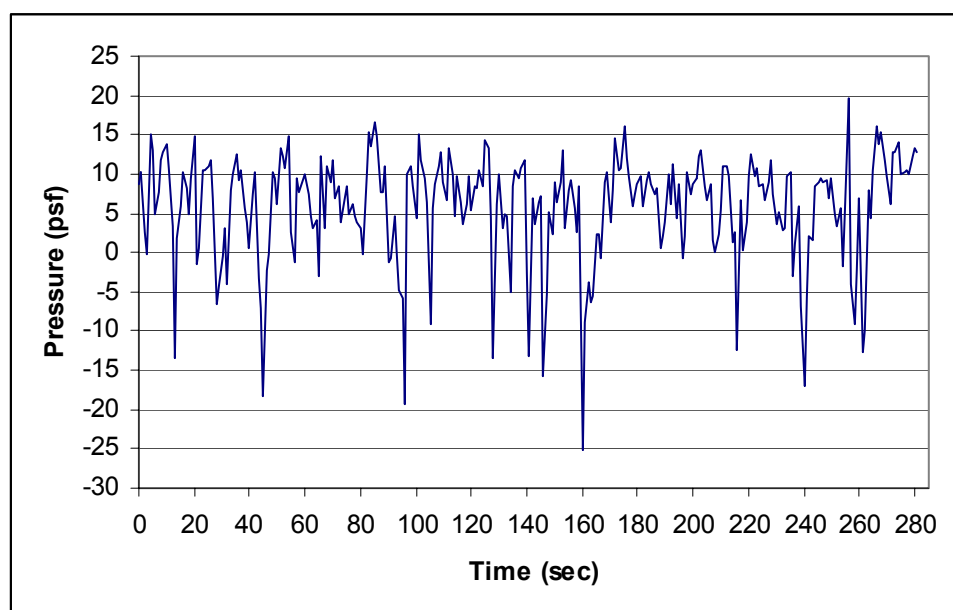


Figure A.14 – Peak loads for 20 point moving average data (Area 7)

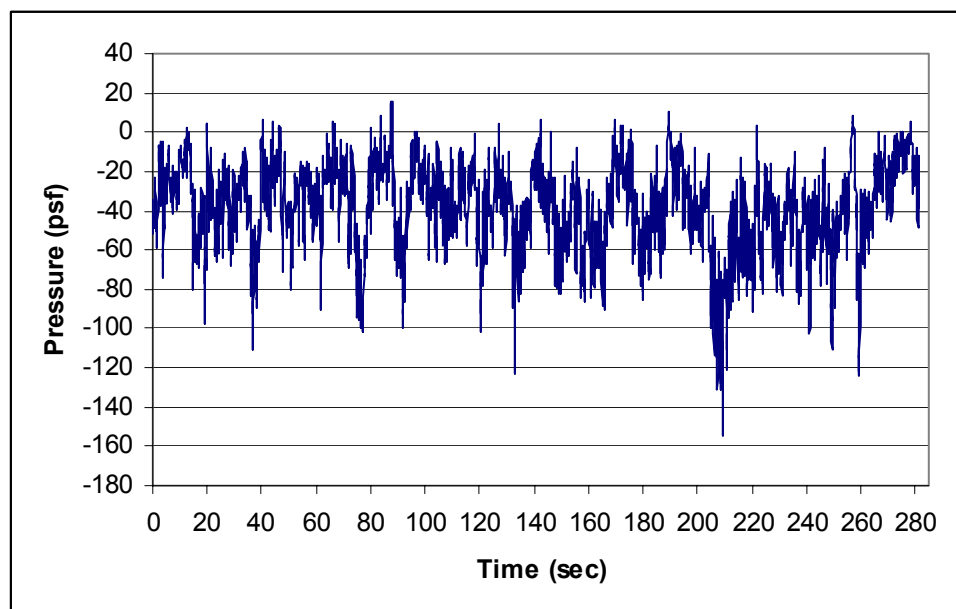


Figure A.15 – Peak loads for UWO data (Area 8)

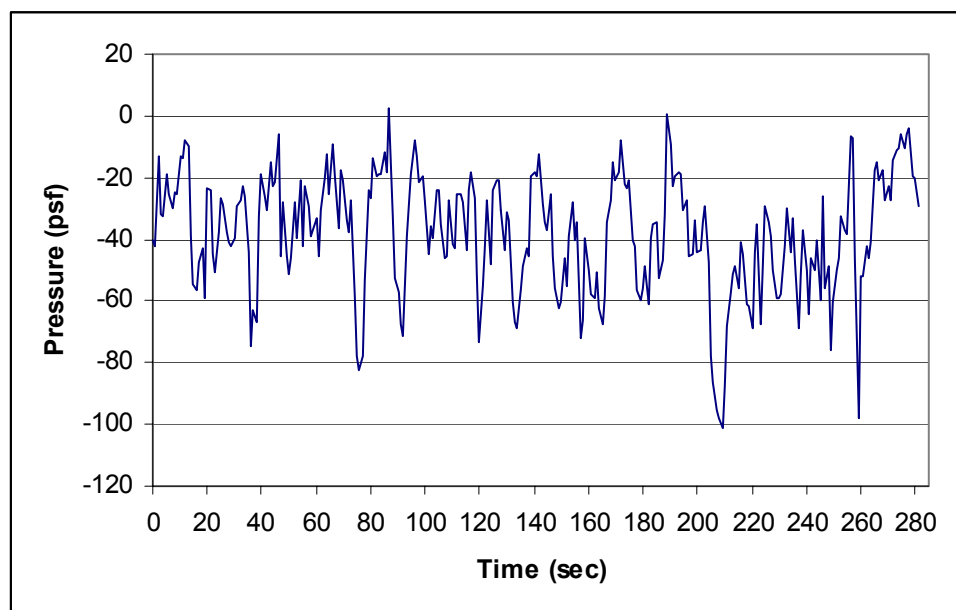


Figure A.16 – Peak loads for 20 point moving average data (Area 8)

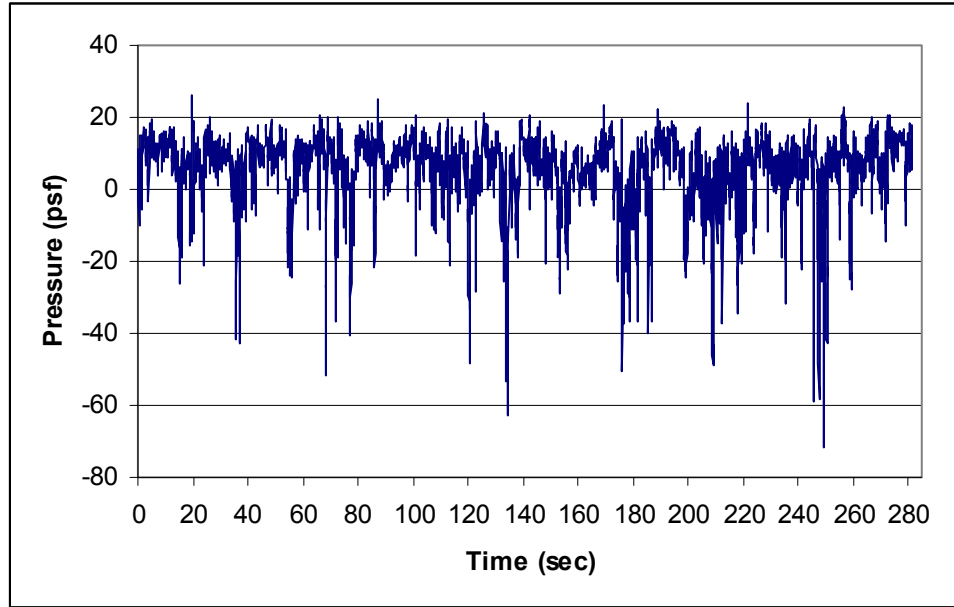


Figure A.17 – Peak loads for UWO data (Area 9)

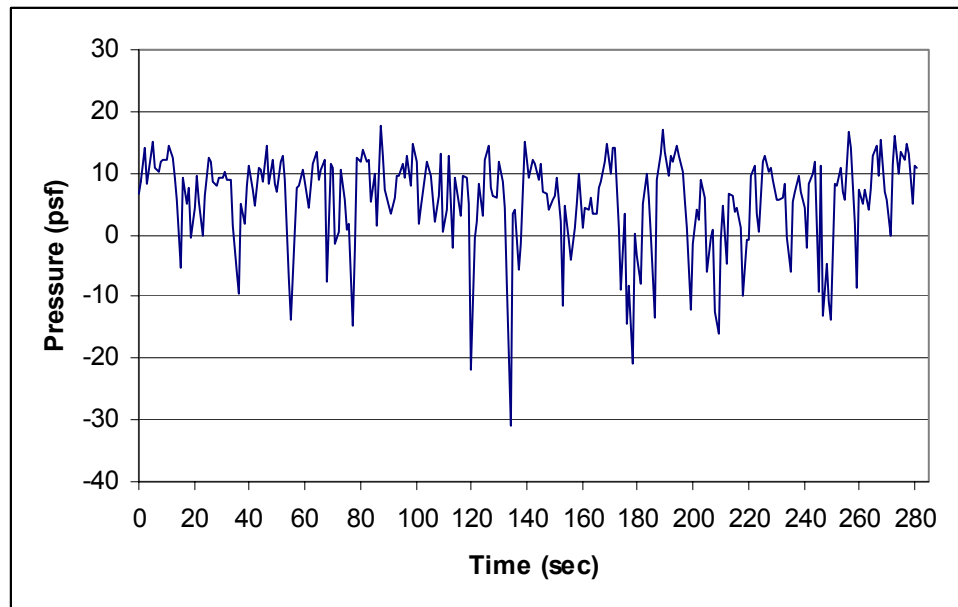


Figure A.18 – Peak loads for 20 point moving average data (Area 9)

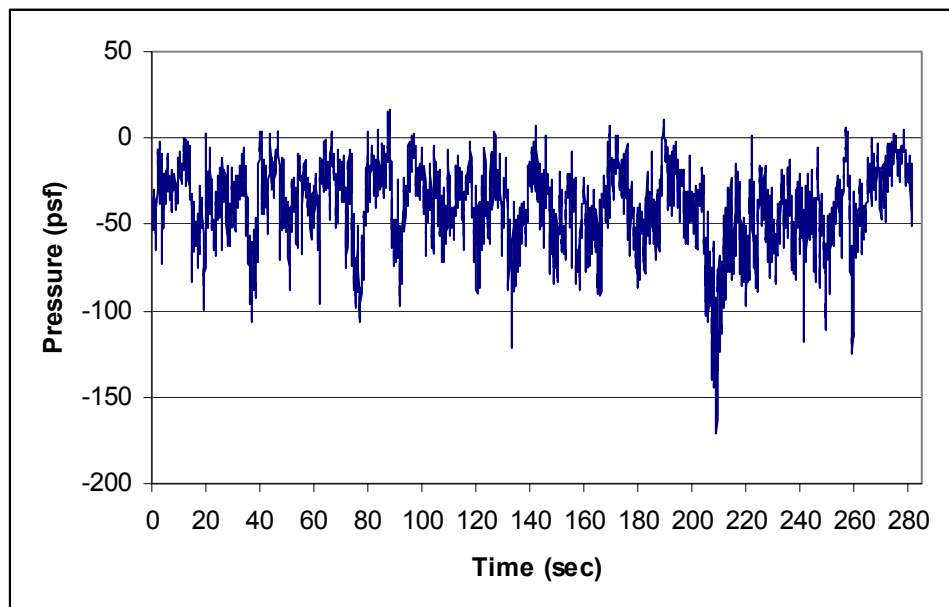


Figure A.19 – Peak loads for UWO data (Area 10)

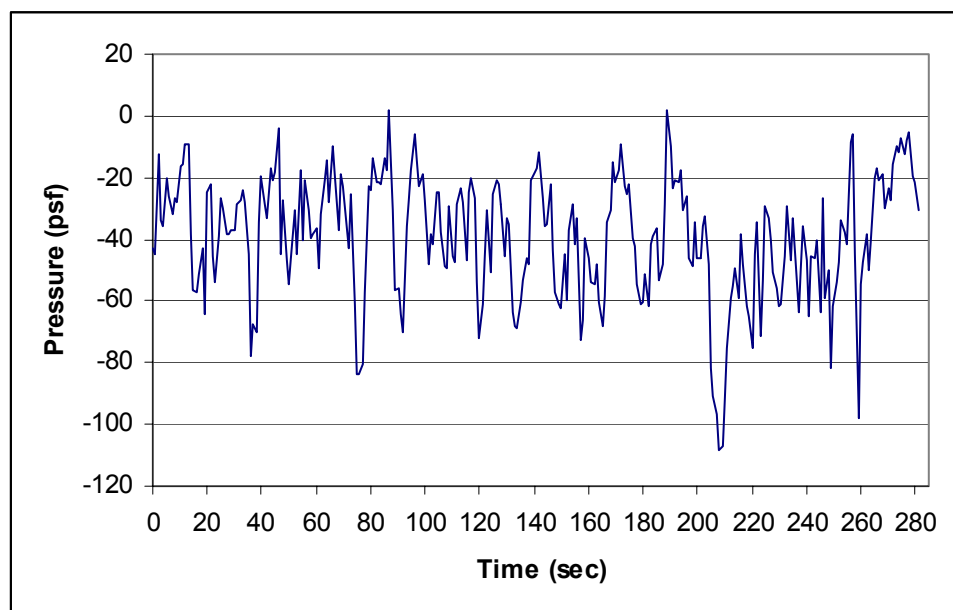


Figure A.20 – Peak loads for 20 point moving average data (Area 10)

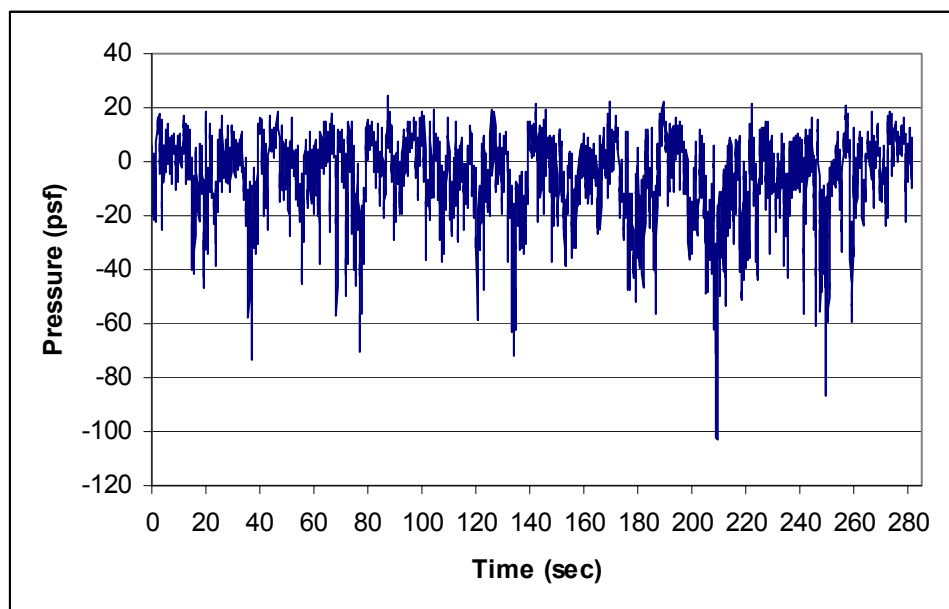


Figure A.21 – Peak loads for UWO data (Area 11)

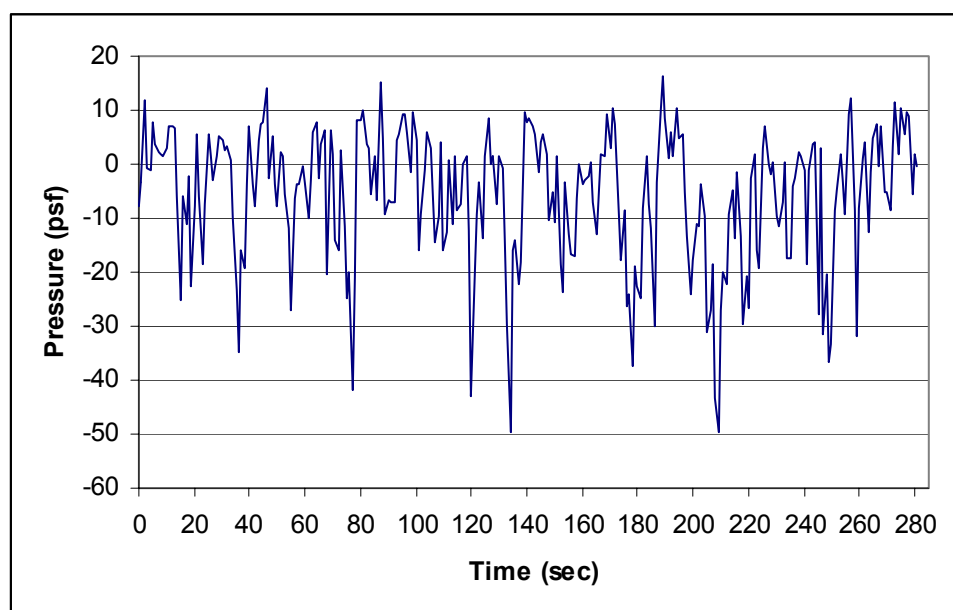


Figure A.22 – Peak loads for 20 point moving average data (Area 11)

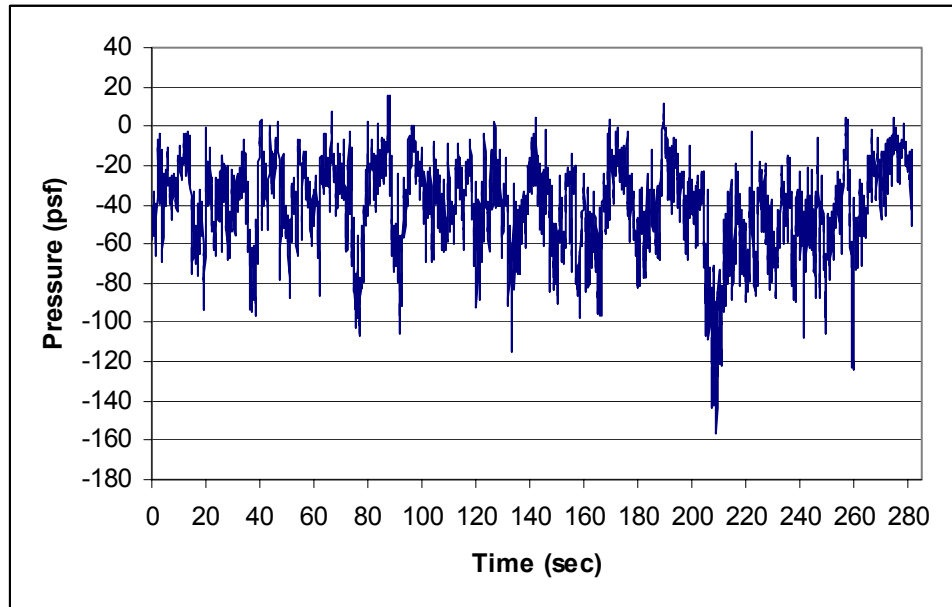


Figure A.23 – Peak loads for UWO data (Area 12)

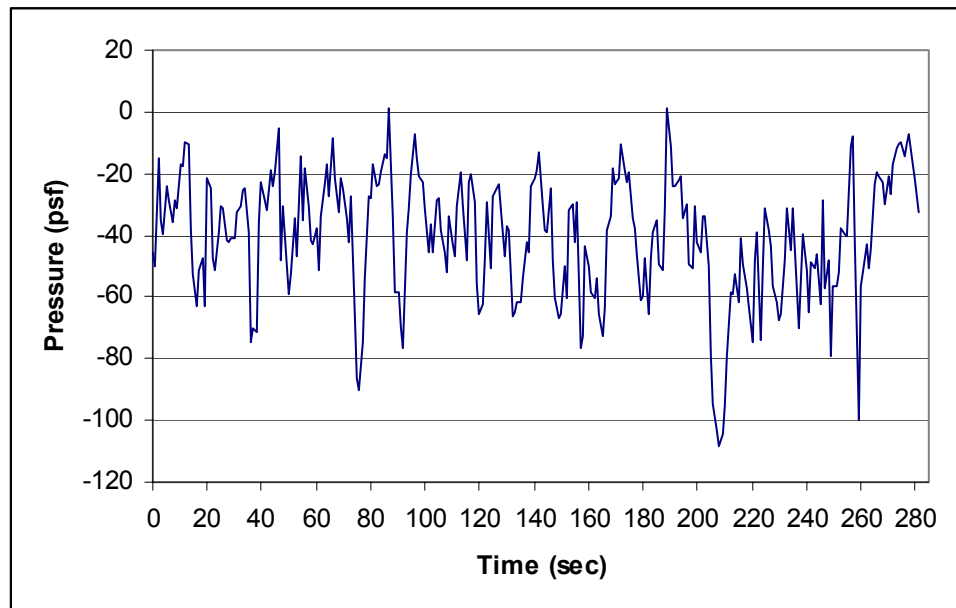


Figure A.24 – Peak loads for 20 point moving average data (Area 12)

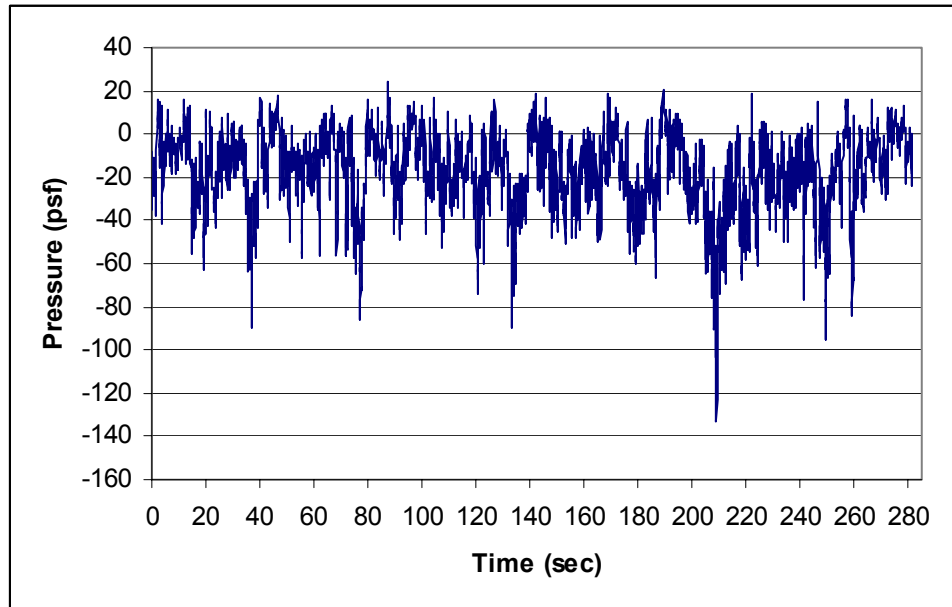


Figure A.25 – Peak loads for UWO data (Area 13)

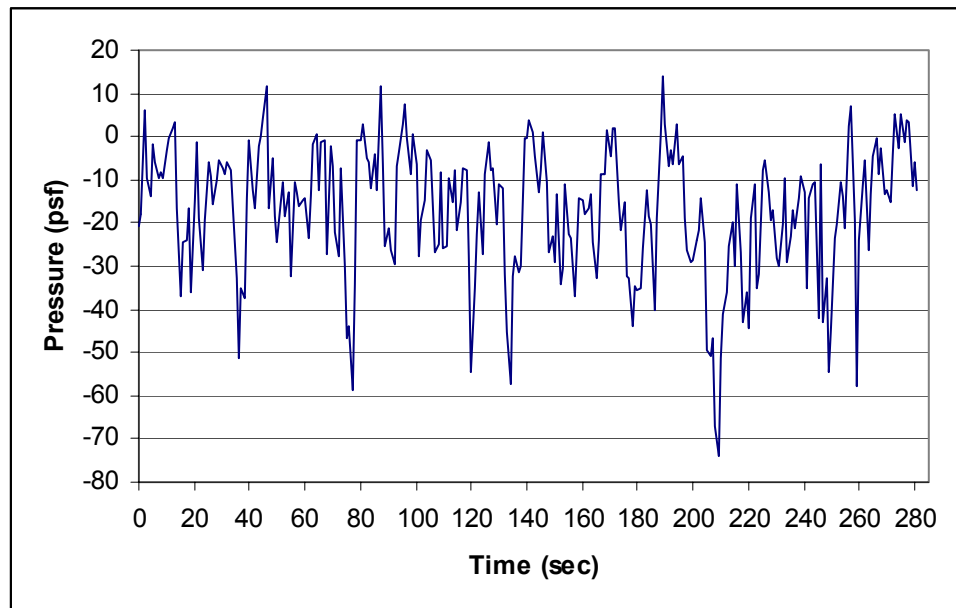


Figure A.26 – Peak loads for 20 point moving average data (Area 13)

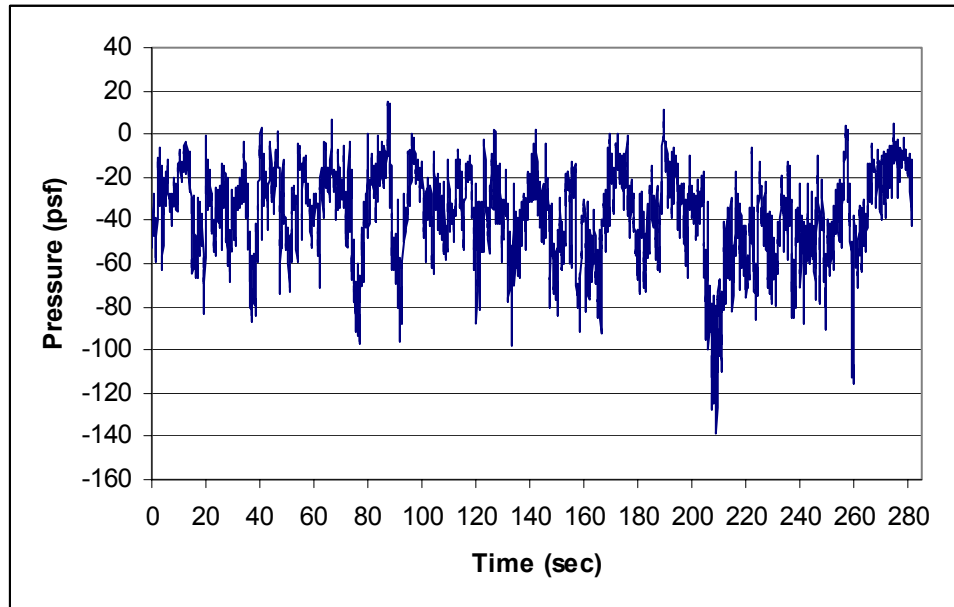


Figure A.27 – Peak loads for UWO data (Area 14)

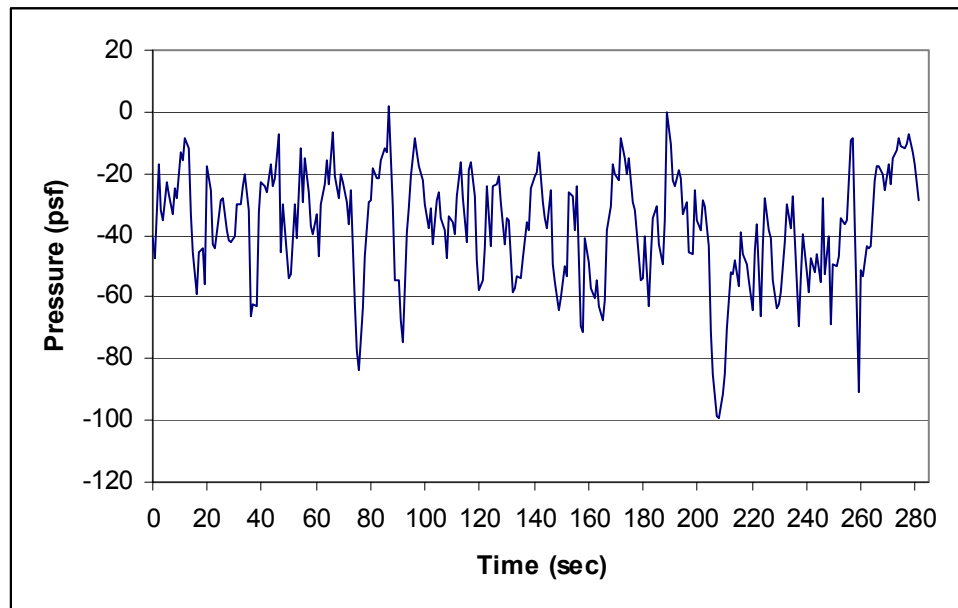


Figure A.28 – Peak loads for 20 point moving average data (Area 14)



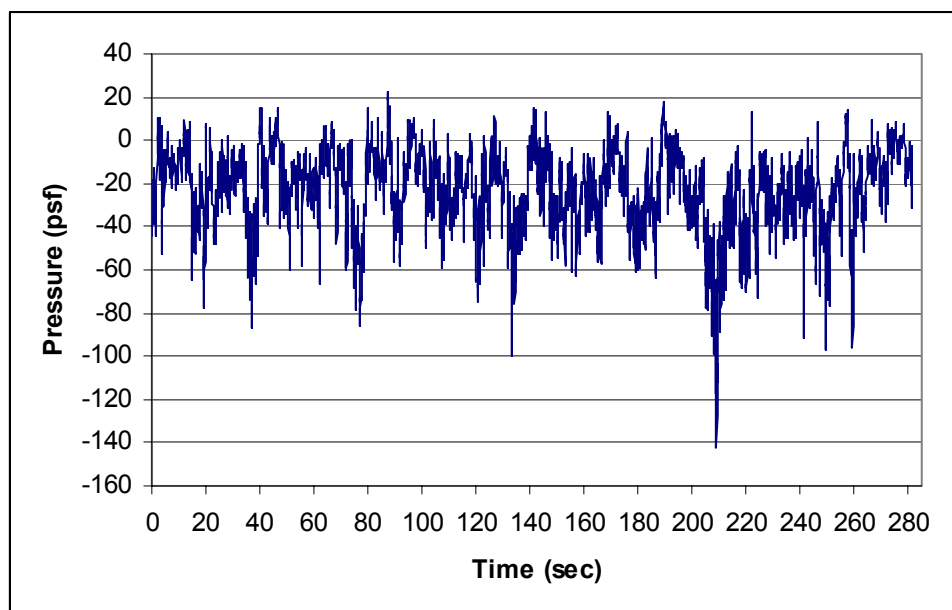


Figure A.29 – Peak loads for UWO data (Area 15)

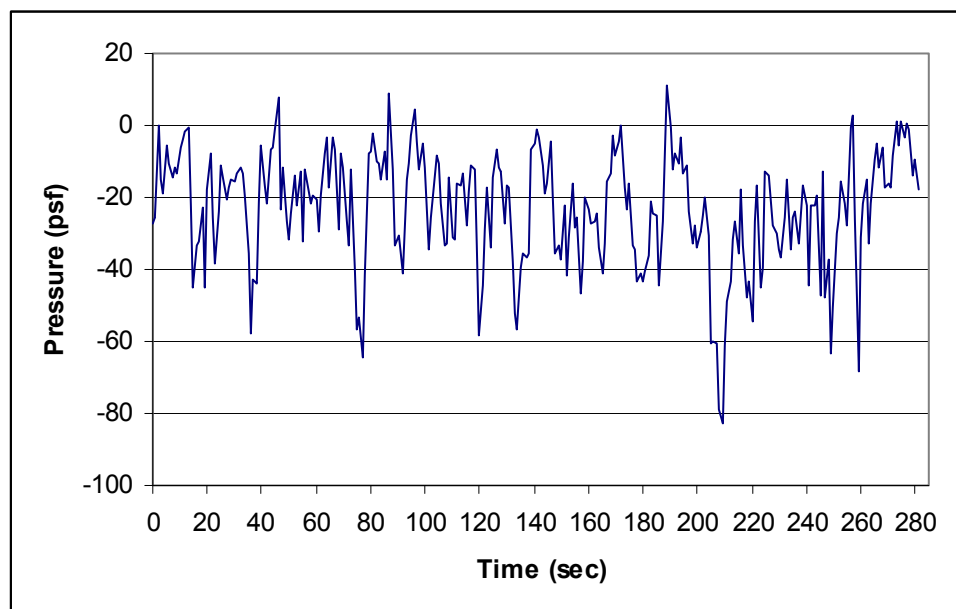


Figure A.30 – Peak loads for 20 point moving average data (Area 15)

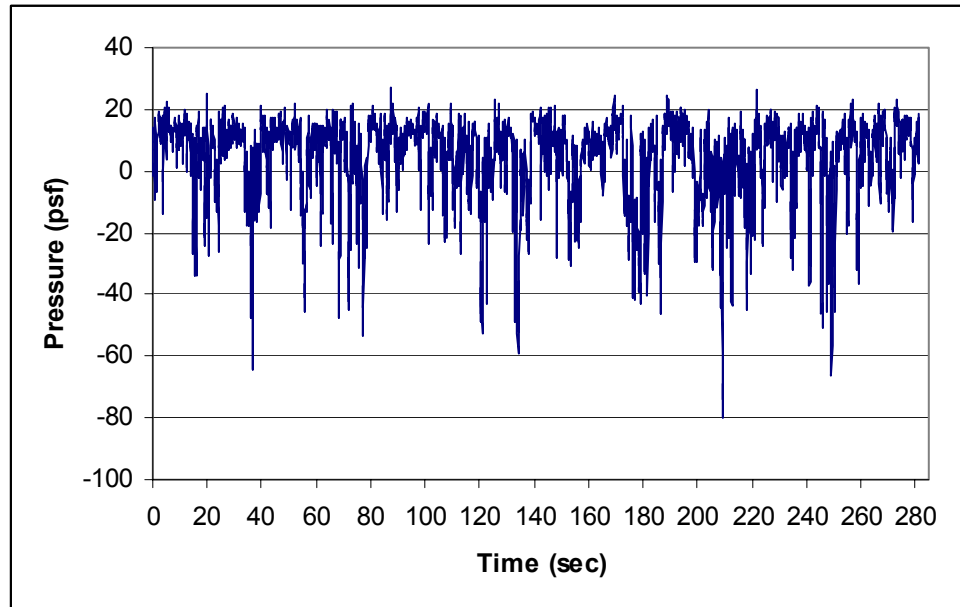


Figure A.31 – Peak loads for UWO data (Area 16)

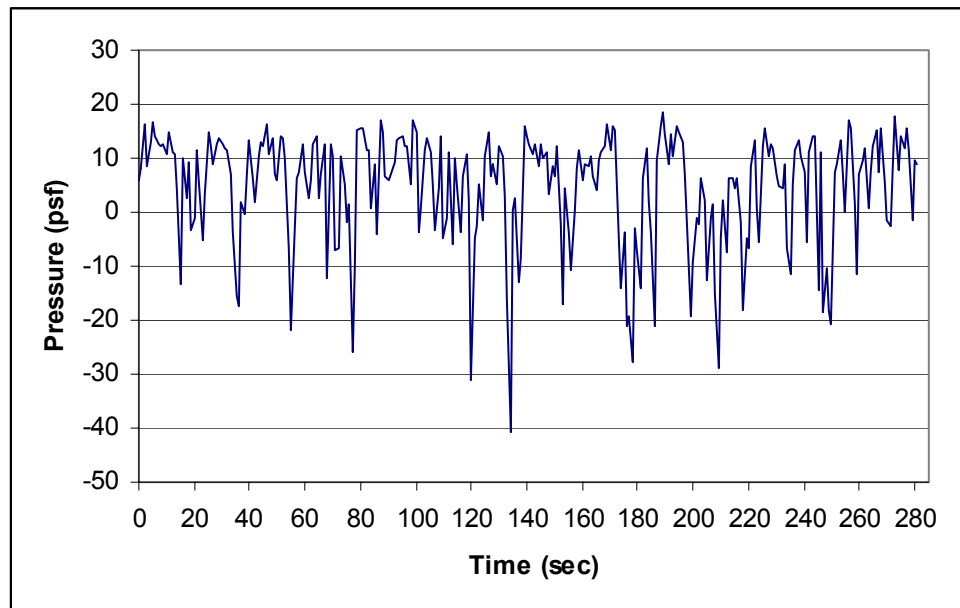


Figure A.32 – Peak loads for 20 point moving average data (Area 16)

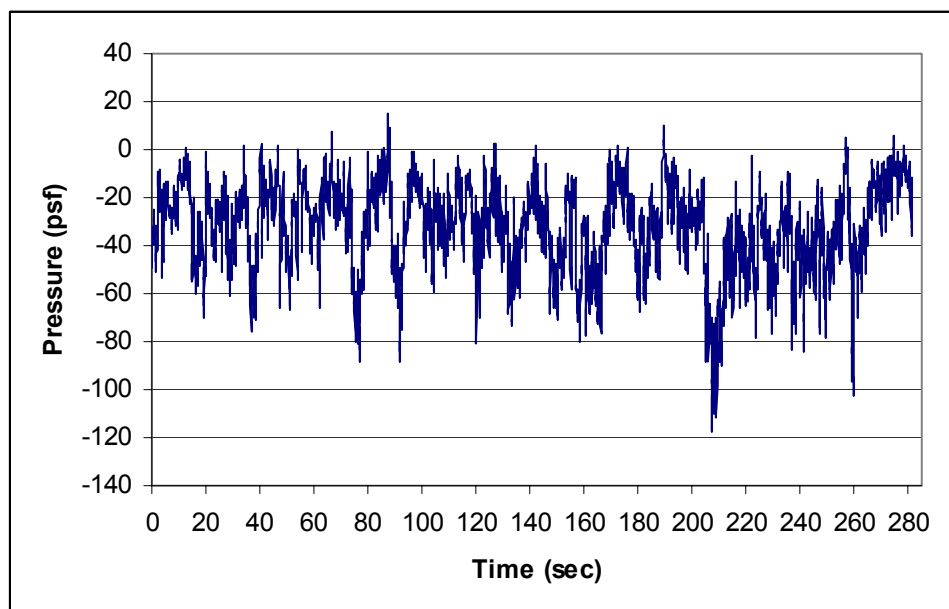


Figure A.33 – Peak loads for UWO data (Area 17)

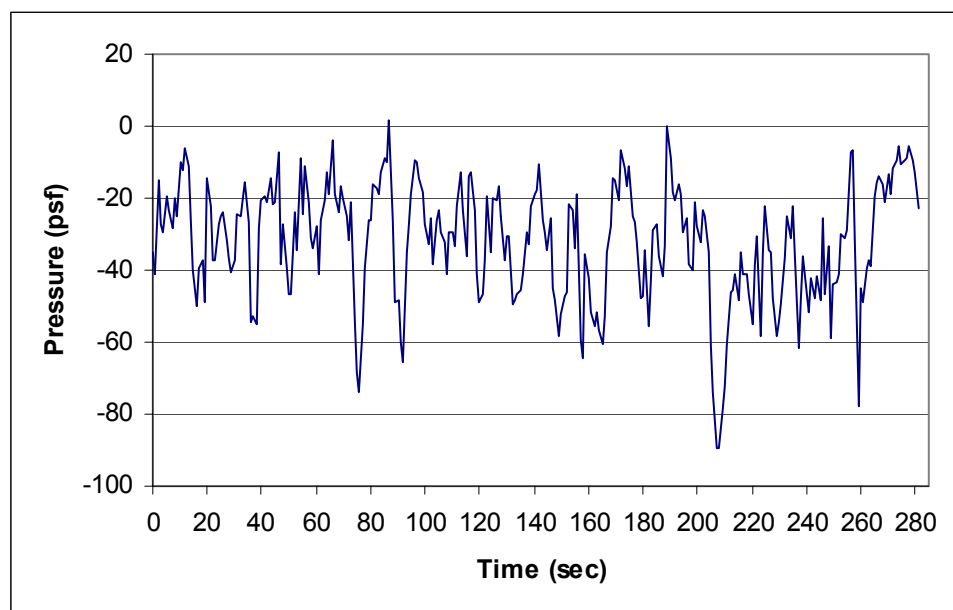


Figure A.34 – Peak loads for 20 point moving average data (Area 17)

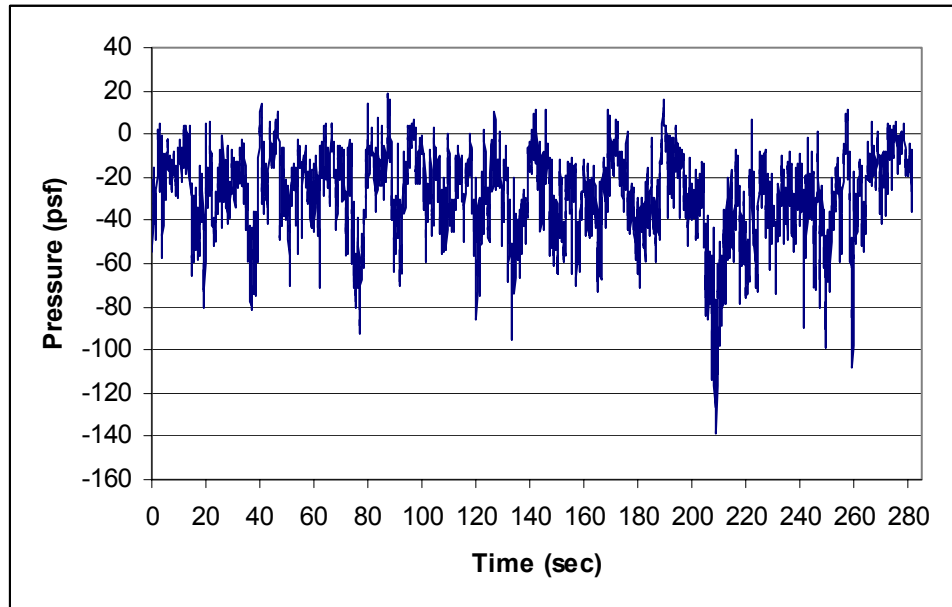


Figure A.35 – Peak loads for UWO data (Area 18)

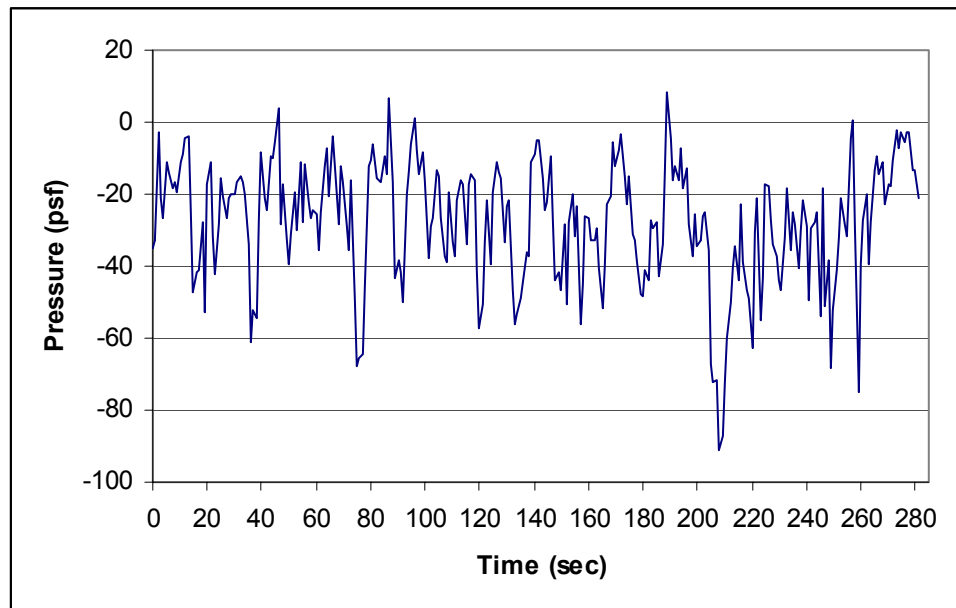


Figure A.36 – Peak loads for 20 point moving average data (Area 18)

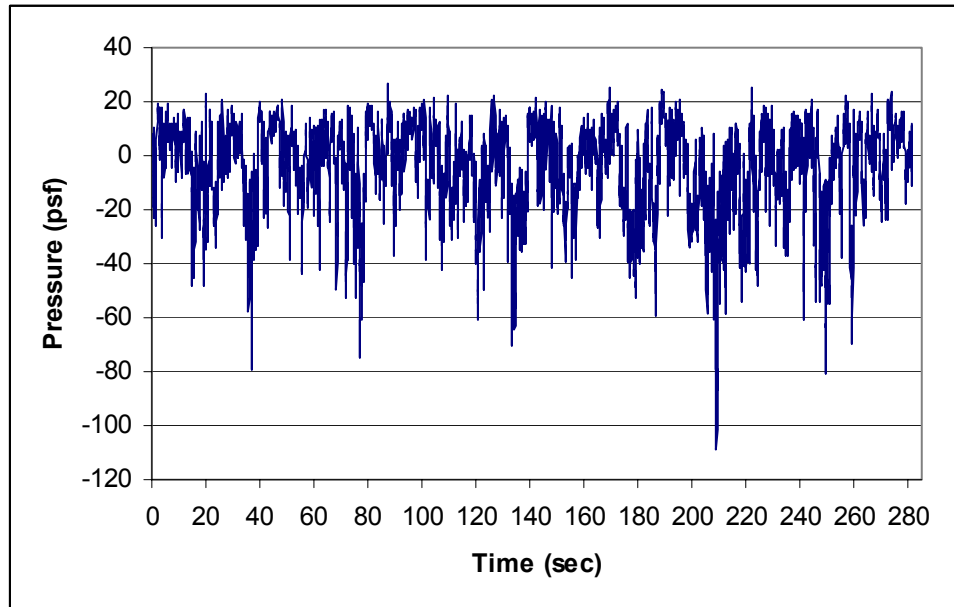


Figure A.37 – Peak loads for UWO data (Area 19)

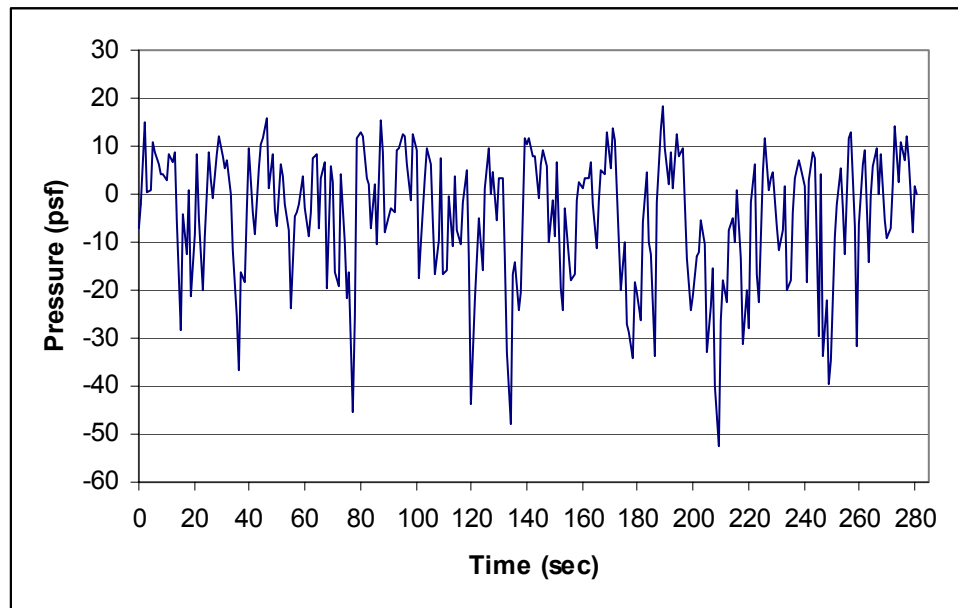


Figure A.38 – Peak loads for 20 point moving average data (Area 19)

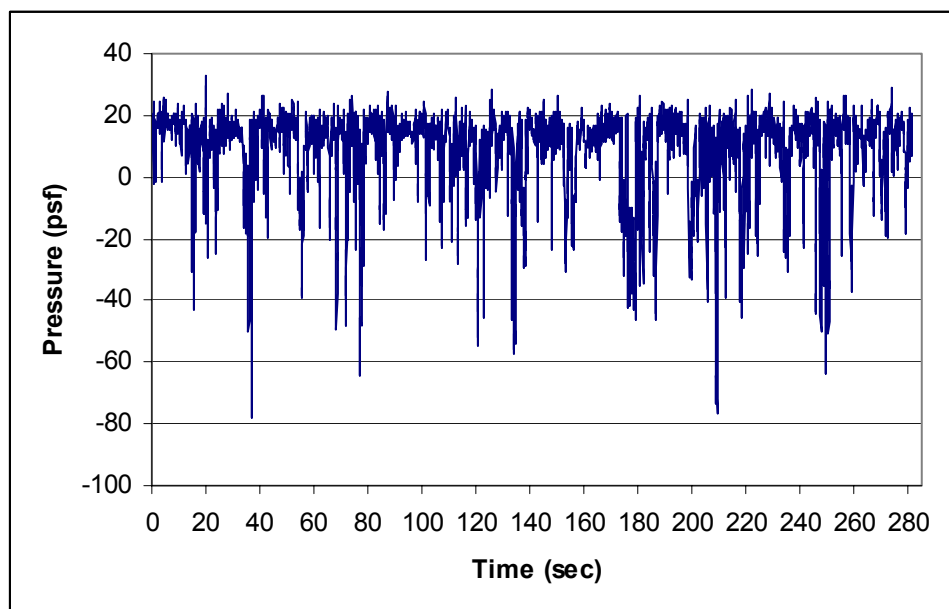


Figure A.39 – Peak loads for UWO data (Area 20)

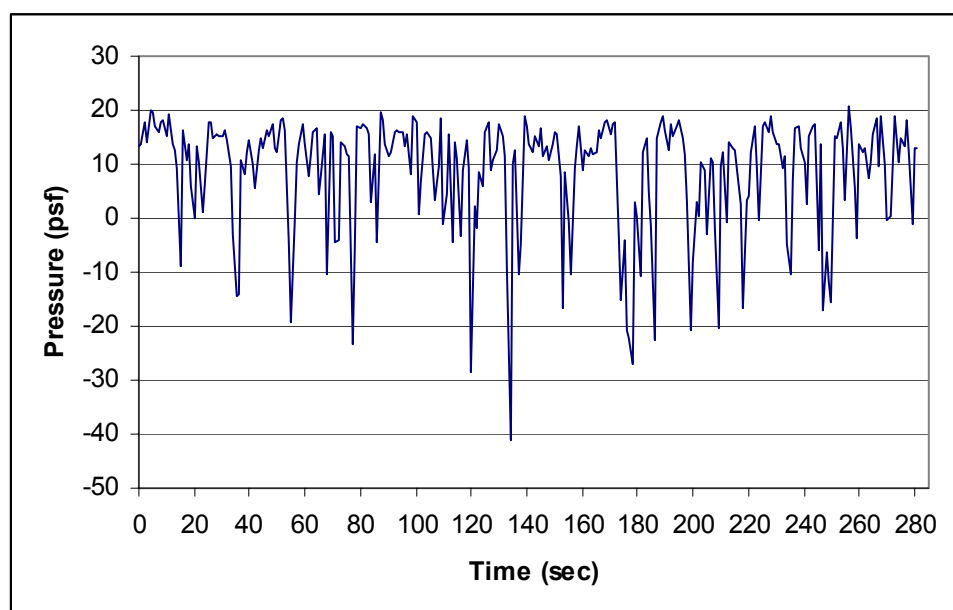


Figure A.40 – Peak loads for 20 point moving average data (Area 20)

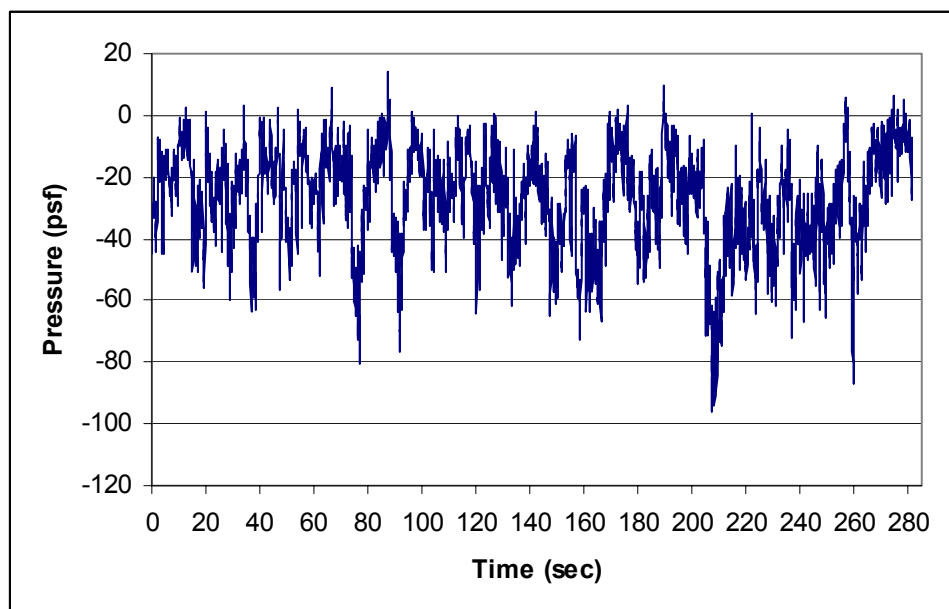


Figure A.41 – Peak loads for UWO data (Area 21)

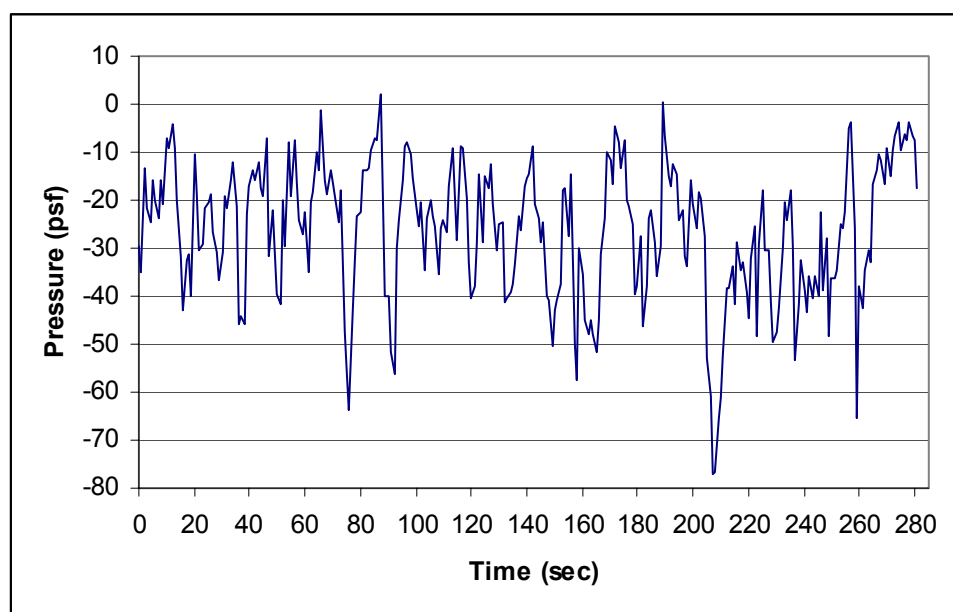


Figure A.42 – Peak loads for 20 point moving average data (Area 21)

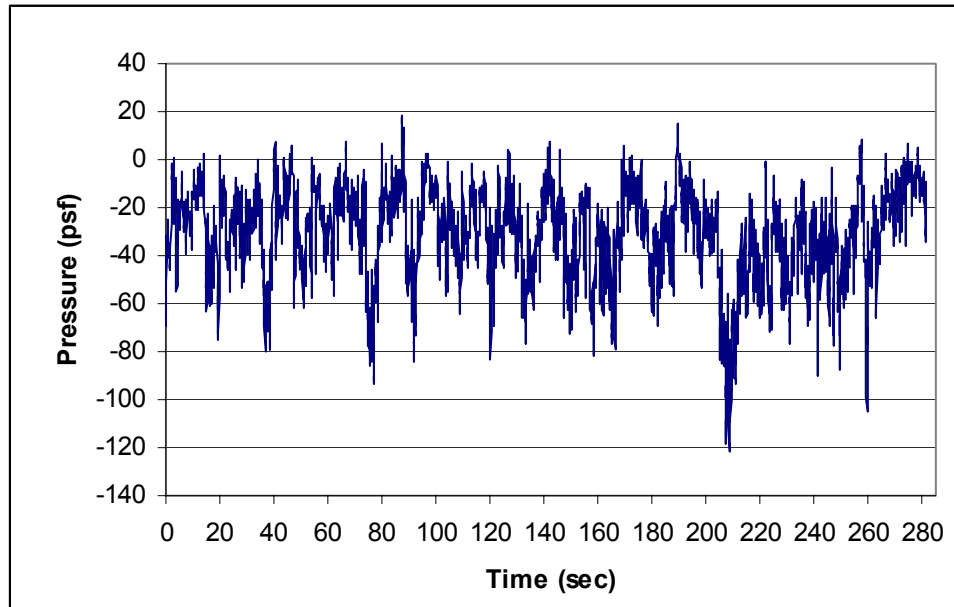


Figure A.43 – Peak loads for UWO data (Area 22)

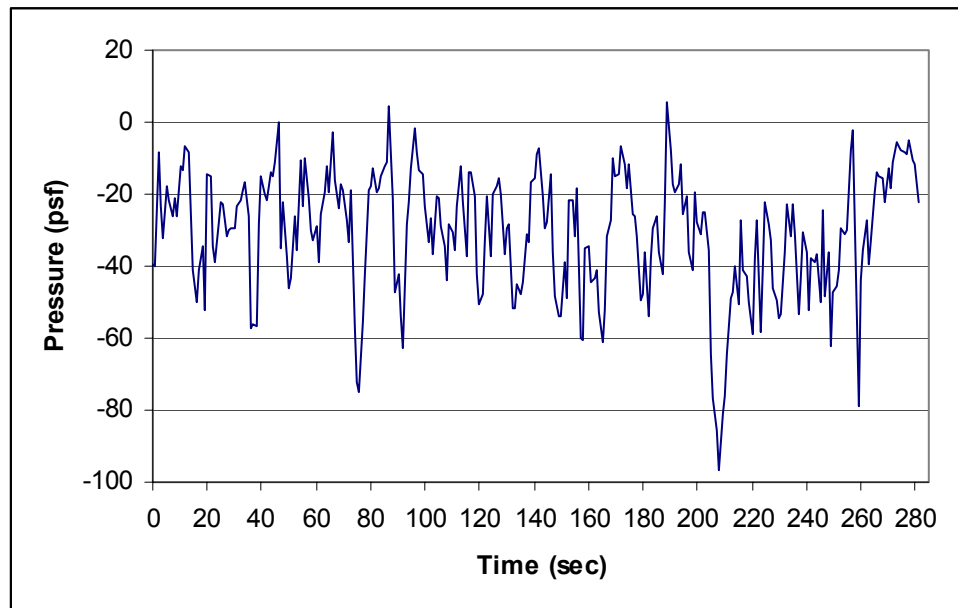


Figure A.44 – Peak loads for 20 point moving average data (Area 22)



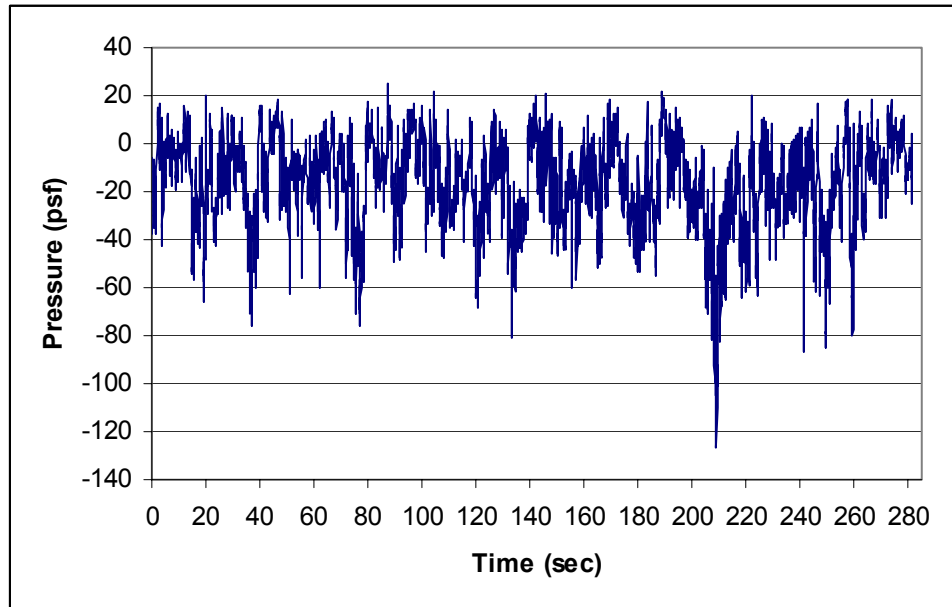


Figure A.45 – Peak loads for UWO data (Area 23)

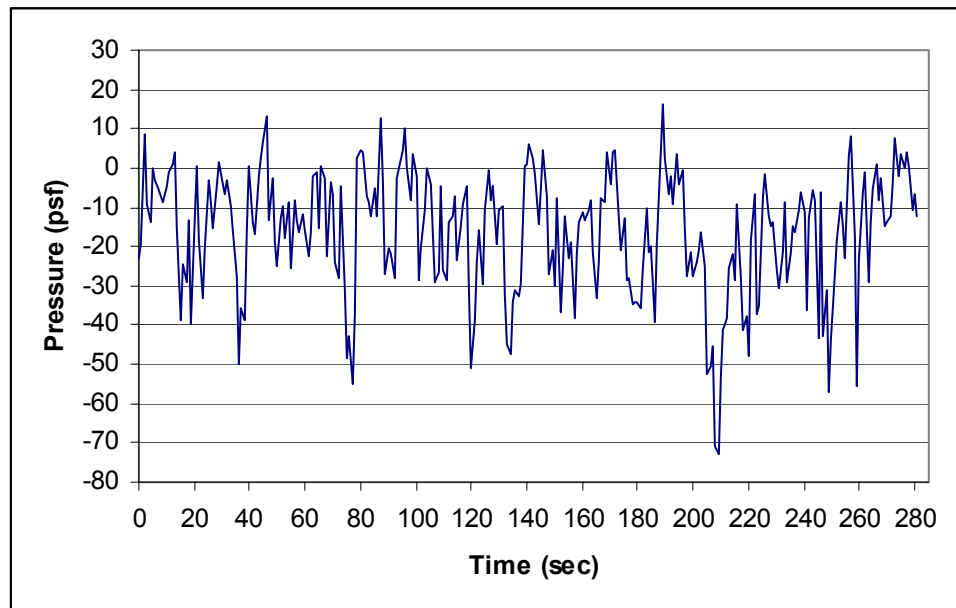


Figure A.46 – Peak loads for 20 point moving average data (Area 23)

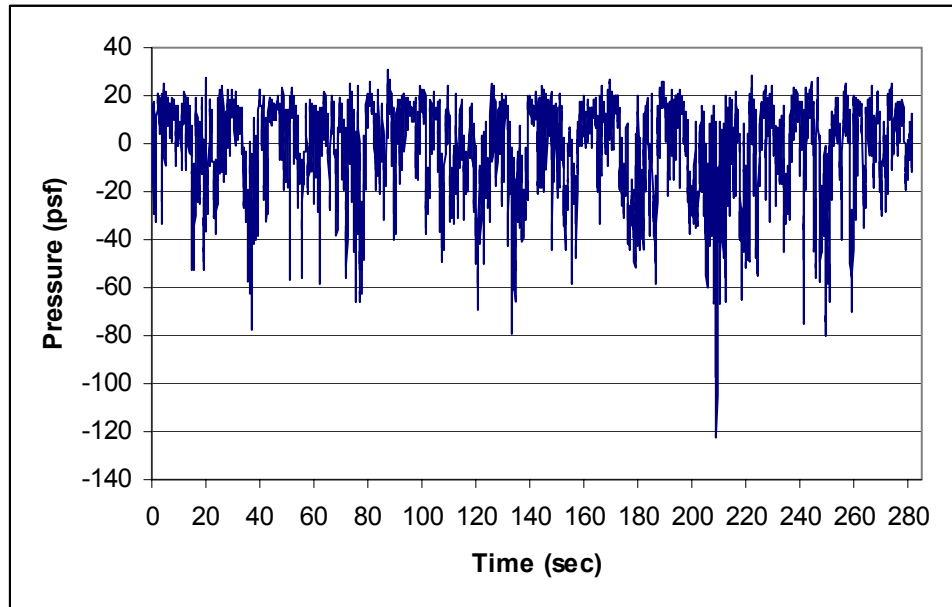


Figure A.47 – Peak loads for UWO data (Area 24)

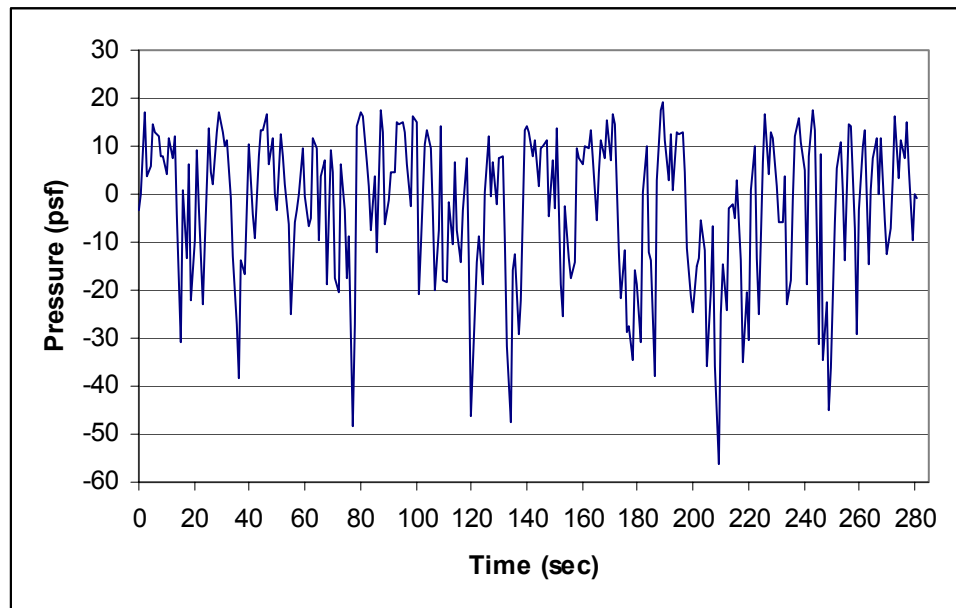


Figure A.48 – Peak loads for 20 point moving average data (Area 24)

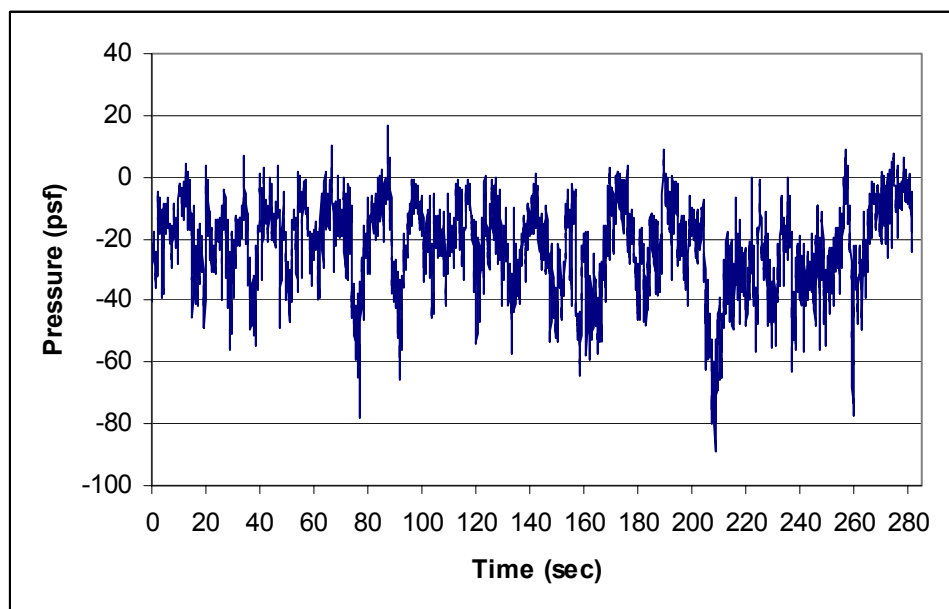


Figure A.49 – Peak loads for UWO data (Area 25)

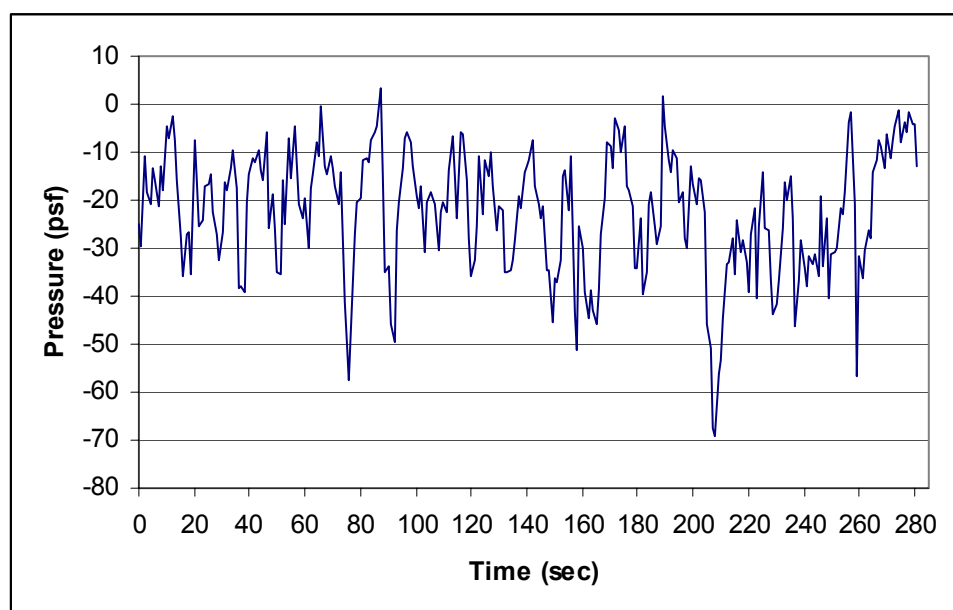


Figure A.50 – Peak loads for 20 point moving average data (Area 25)

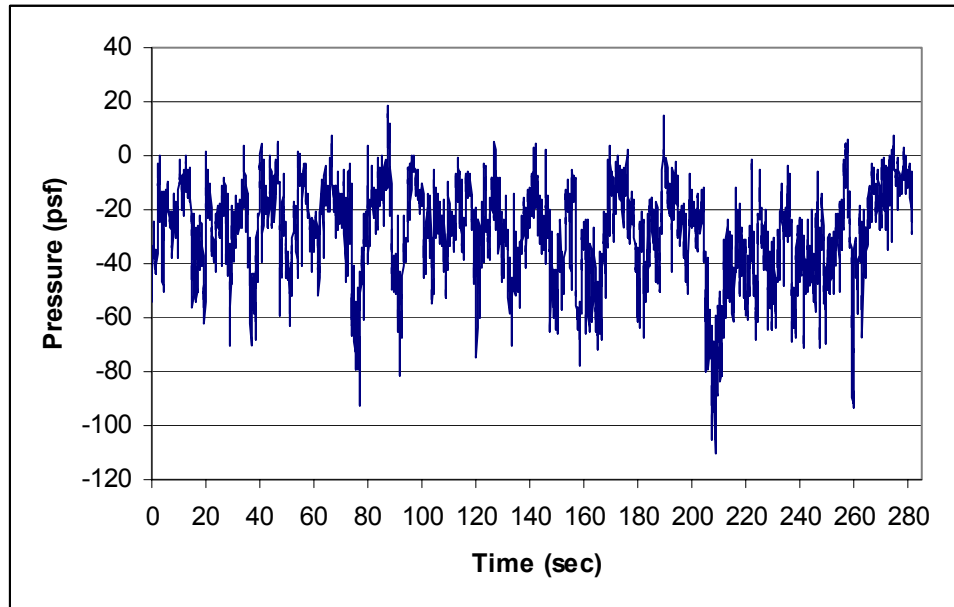


Figure A.51 – Peak loads for UWO data (Area 26)

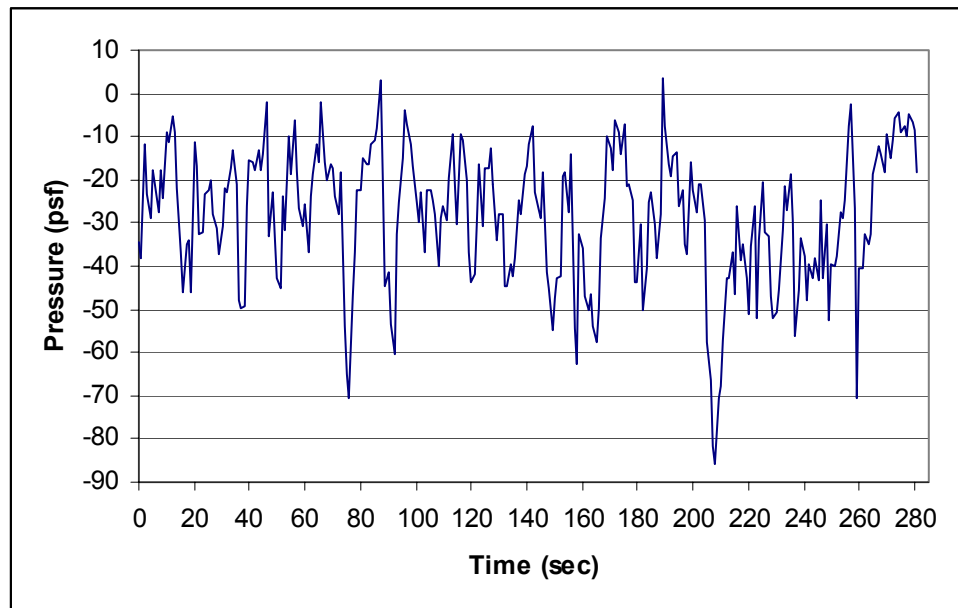


Figure A.52 – Peak loads for 20 point moving average data (Area 26)

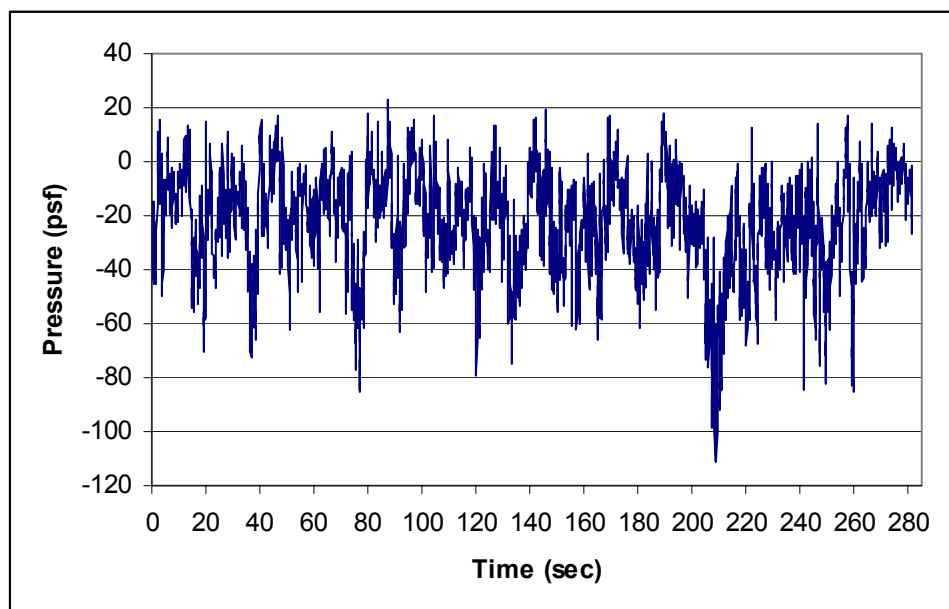


Figure A.53 – Peak loads for UWO data (Area 27)

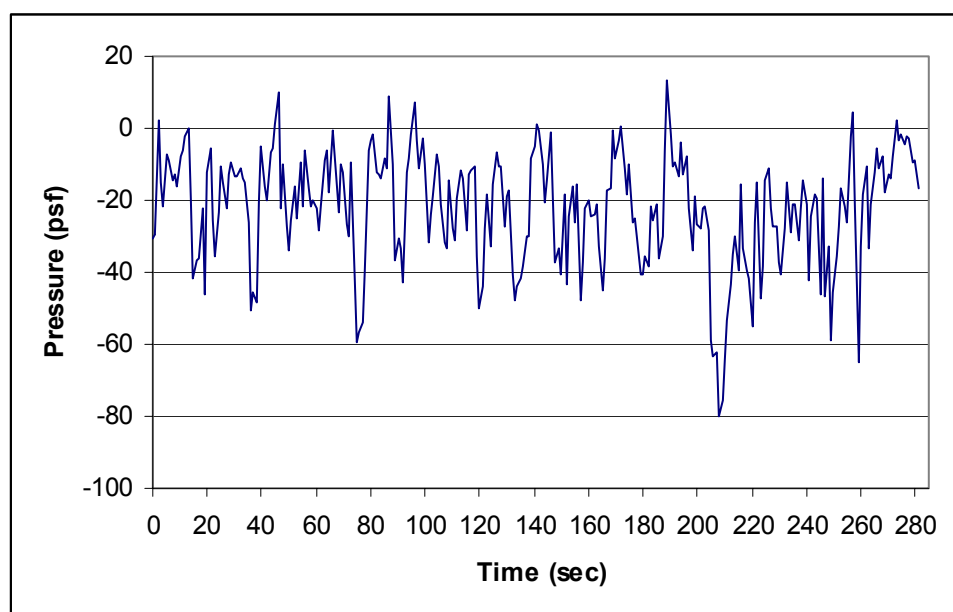


Figure A.54 – Peak loads for 20 point moving average data (Area 27)

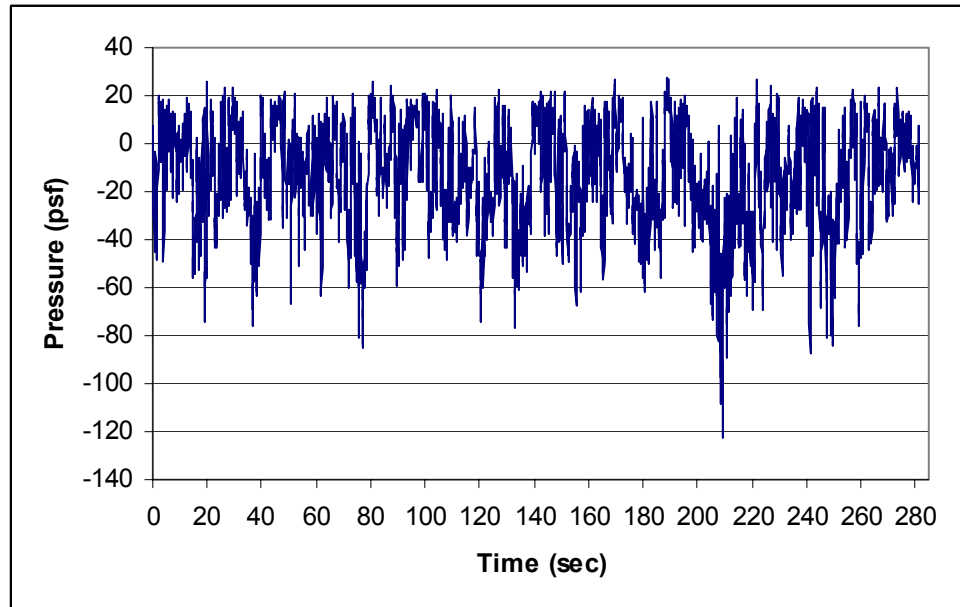


Figure A.55 – Peak loads for UWO data (Area 28)

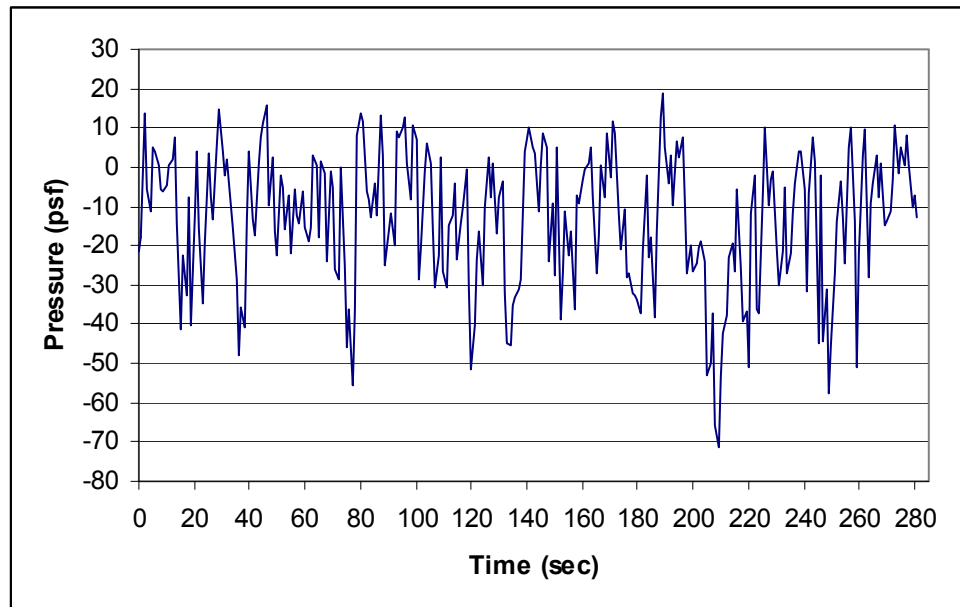


Figure A.56 – Peak loads for 20 point moving average data (Area 28)

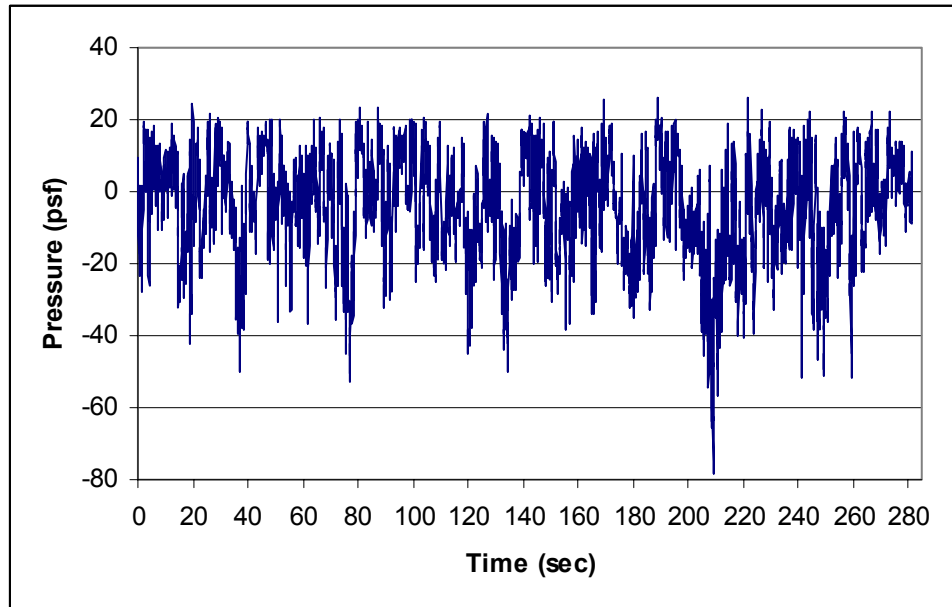


Figure A.57 – Peak loads for UWO data (Area 29)

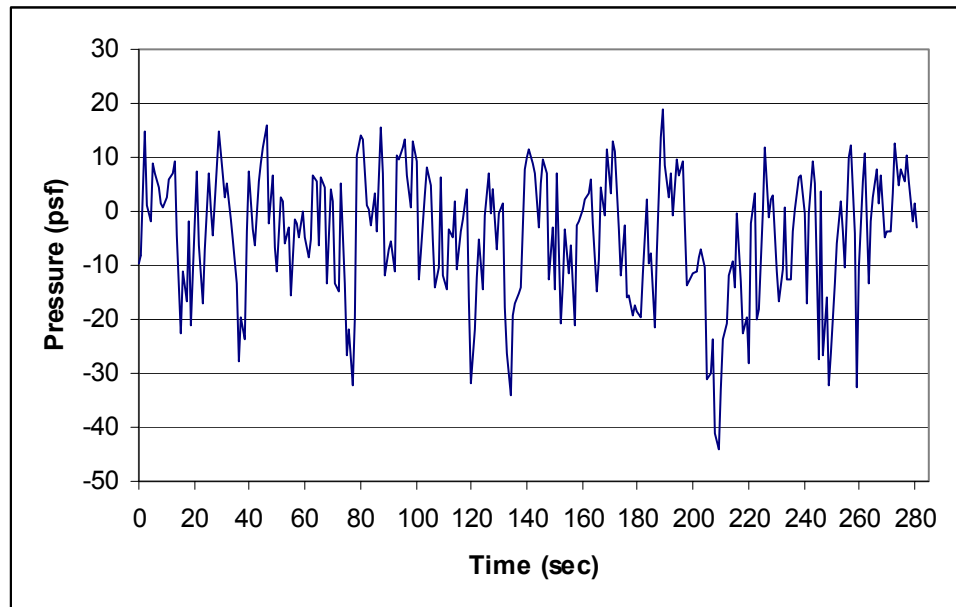


Figure A.58 – Peak loads for 20 point moving average data (Area 29)

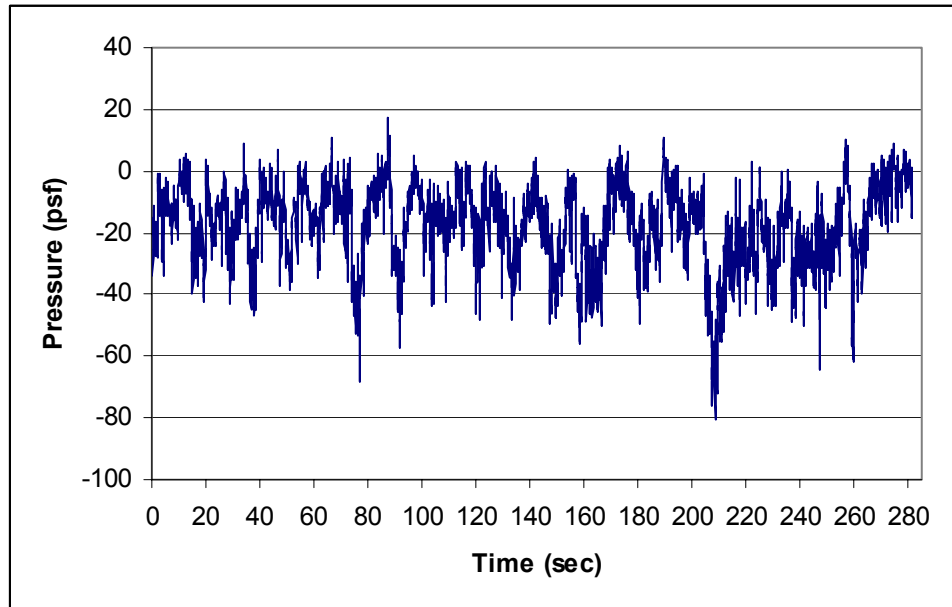


Figure A.59 – Peak loads for UWO data (Area 30)

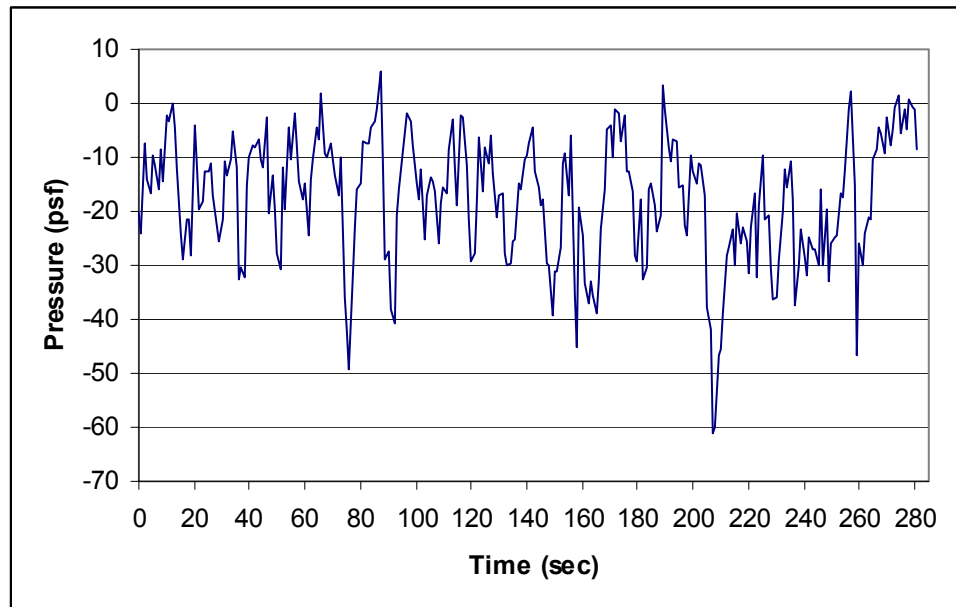


Figure A.60 – Peak loads for 20 point moving average data (Area 30)



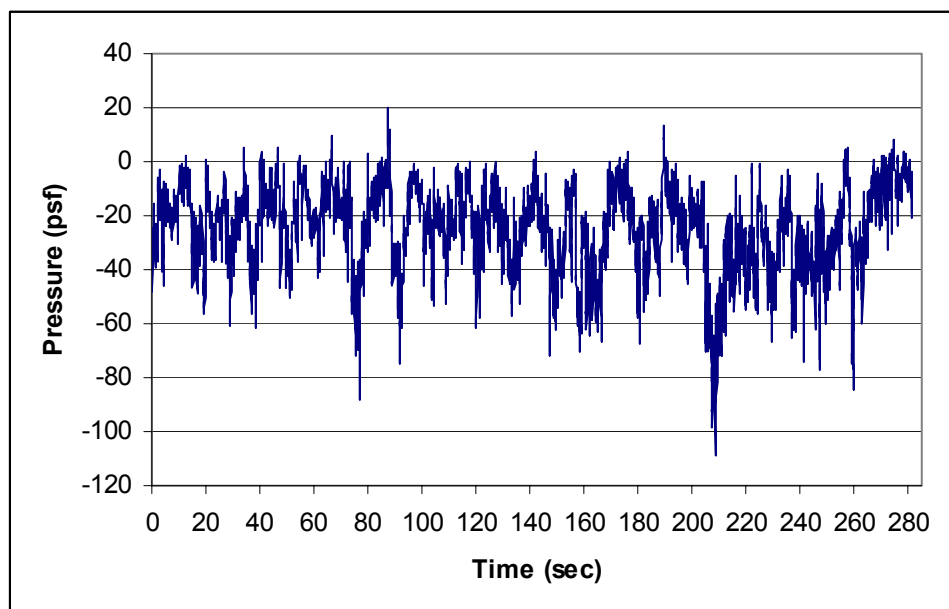


Figure A.61 – Peak loads for UWO data (Area 31)

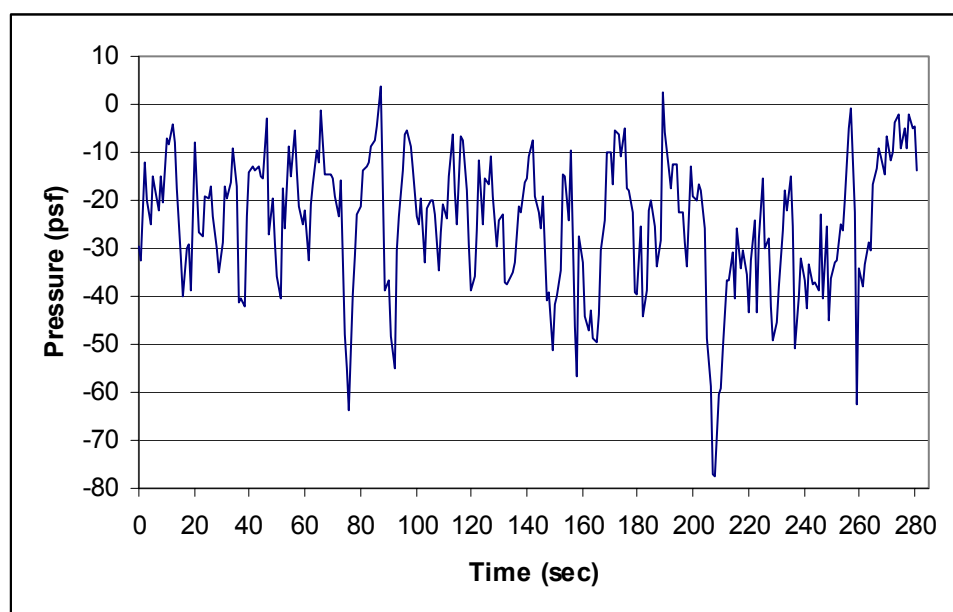


Figure A.62 – Peak loads for 20 point moving average data (Area 31)

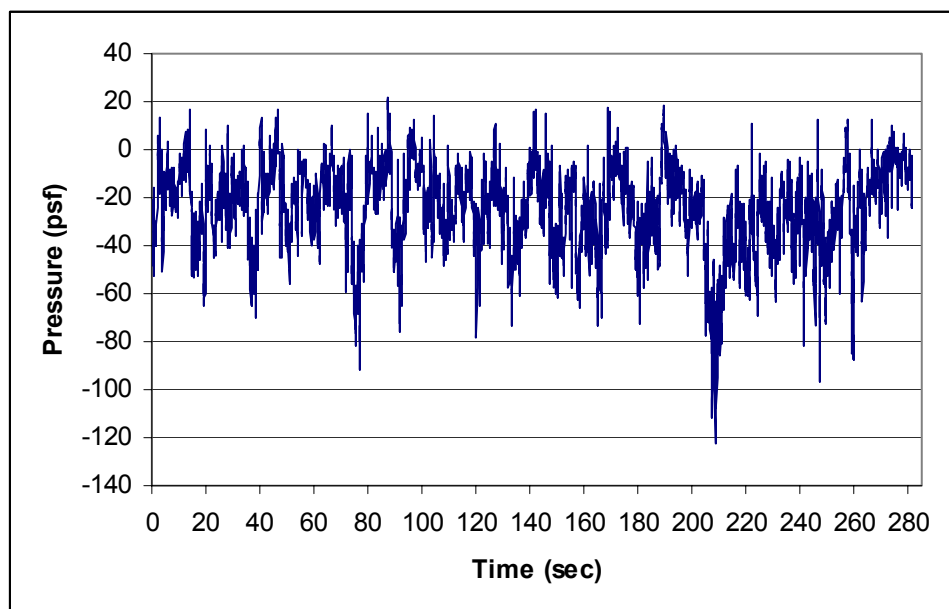


Figure A.63 – Peak loads for UWO data (Area 32)

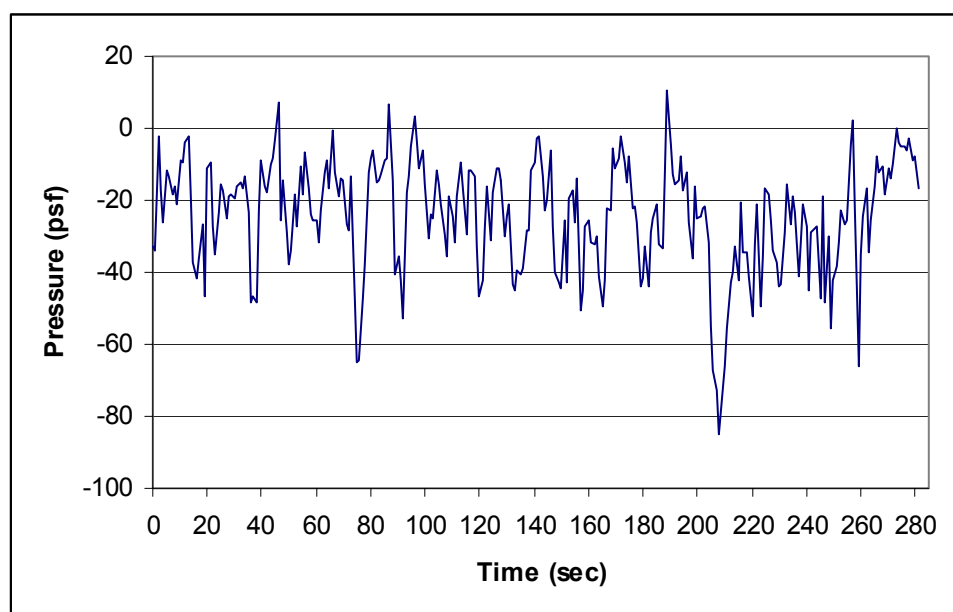


Figure A.64 – Peak loads for 20 point moving average data (Area 32)

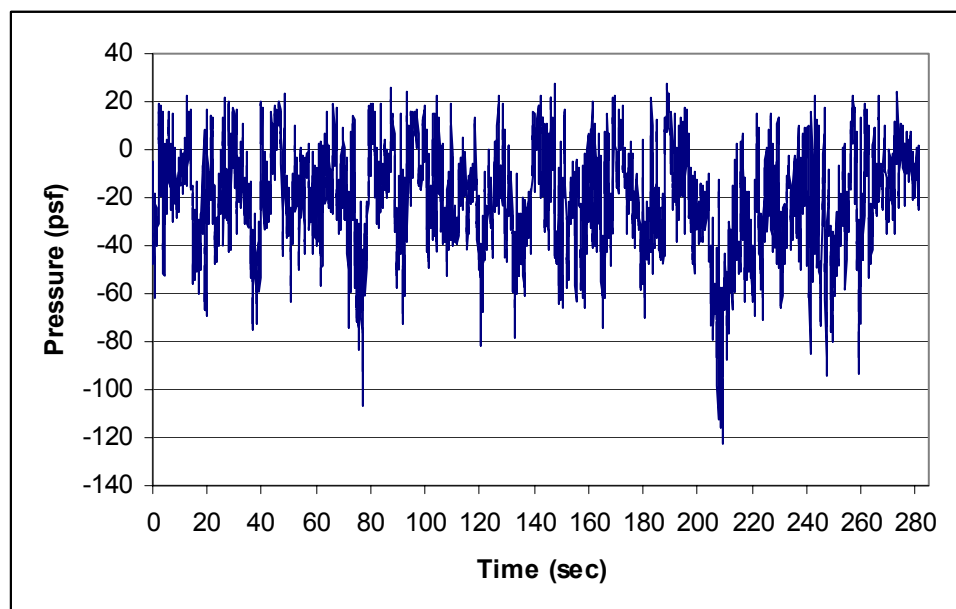


Figure A.65 – Peak loads for UWO data (Area 33)

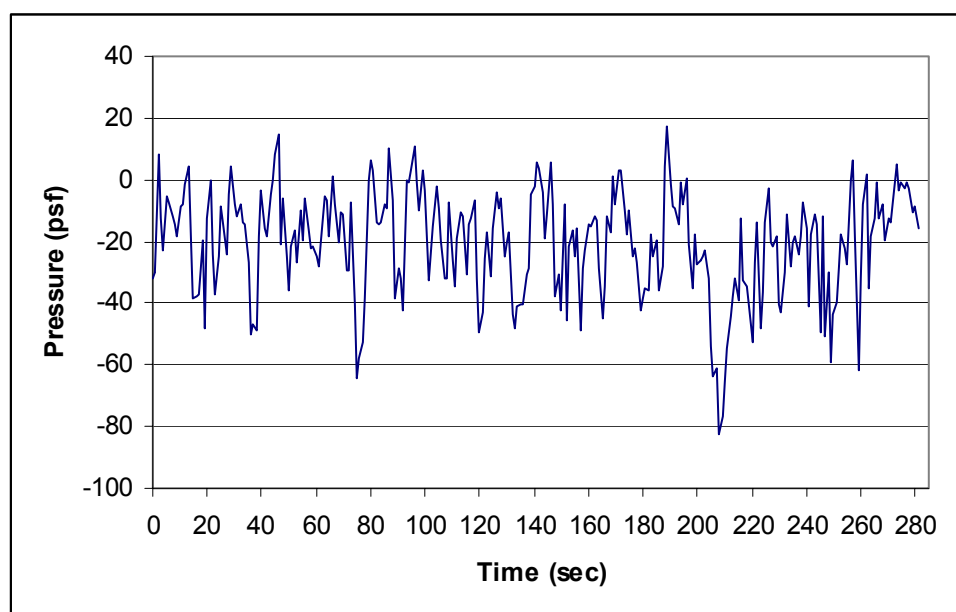


Figure A.66 – Peak loads for 20 point moving average data (Area 33)

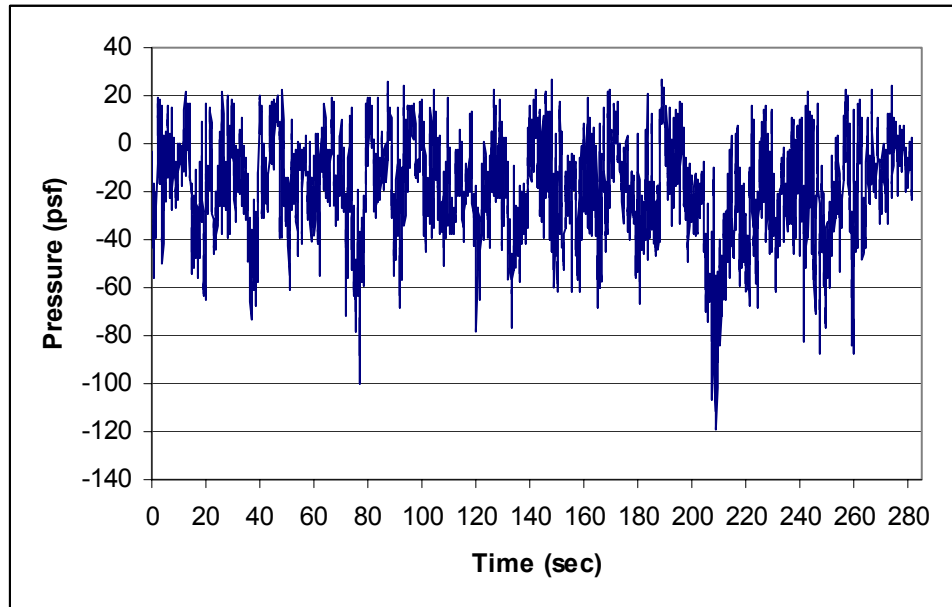


Figure A.67 – Peak loads for UWO data (Area 34)

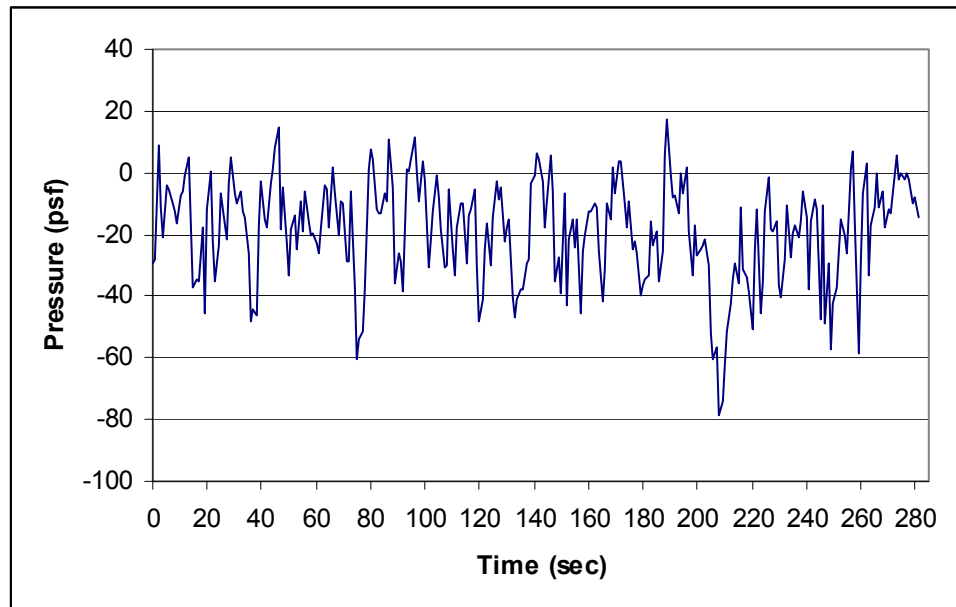


Figure A.68 – Peak loads for 20 point moving average data (Area 34)

APPENDIX B  
SENSITIVITY CHARTS

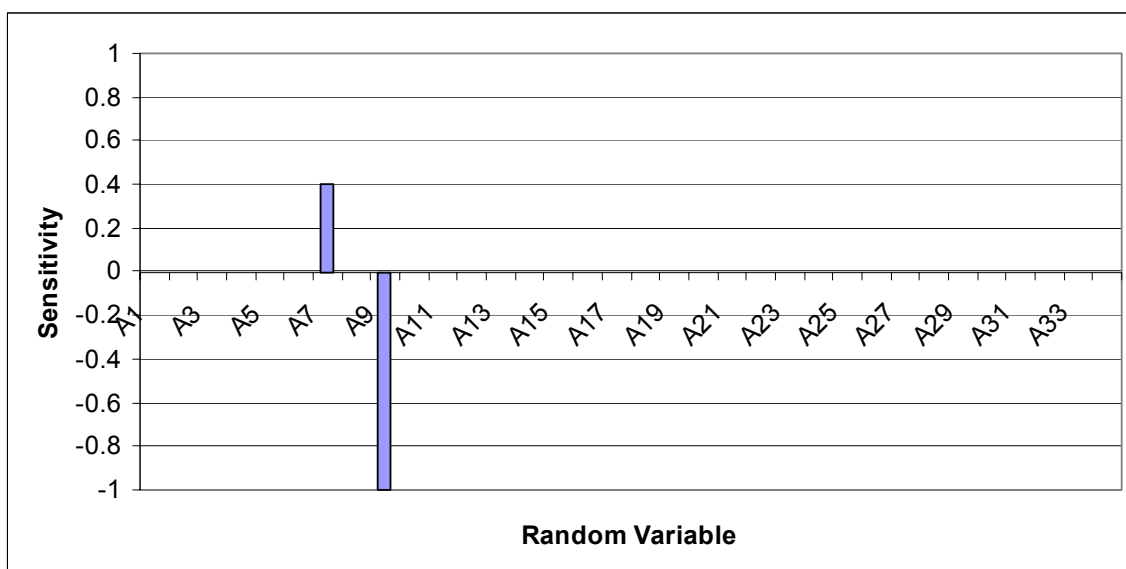


Figure B.1 – Sensitivity with respect to standard deviation for Panel #1

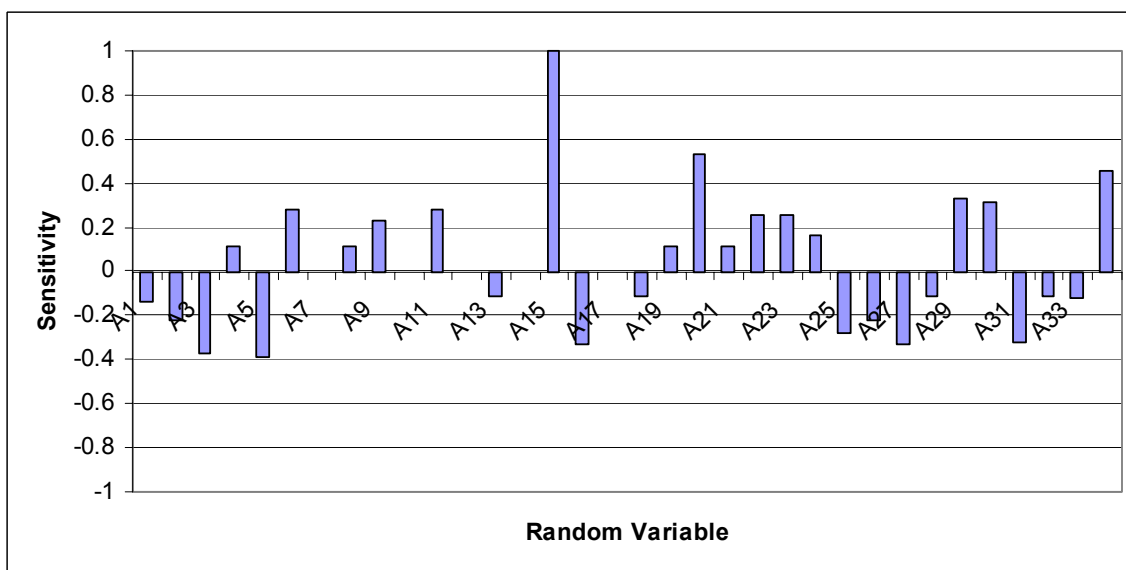


Figure B.2 – Sensitivity with respect to standard deviation for Panel #2

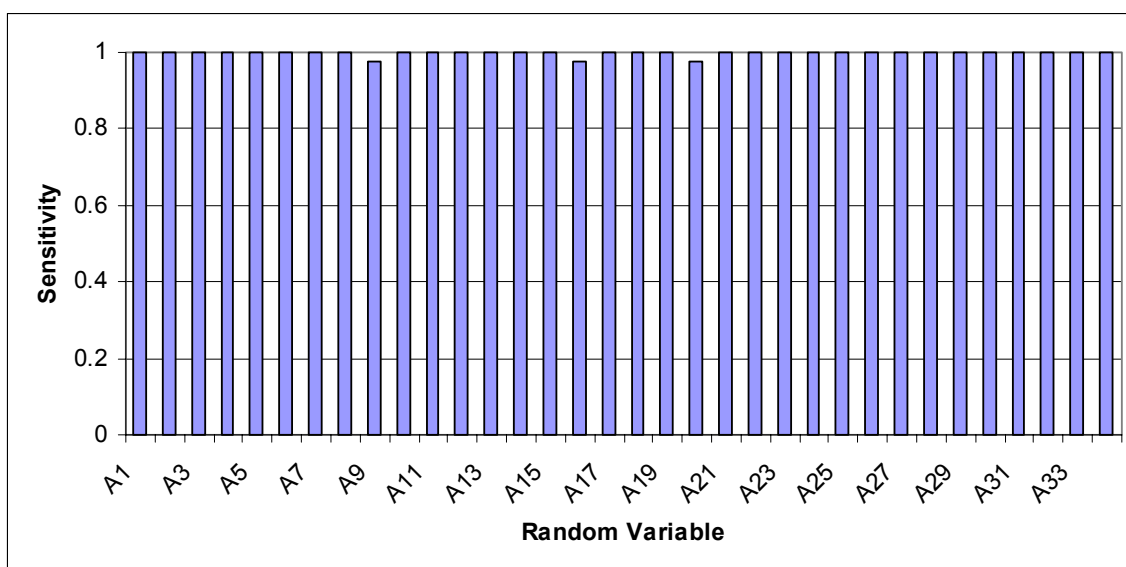


Figure B.3 – Sensitivity with respect to standard deviation for Panel #3

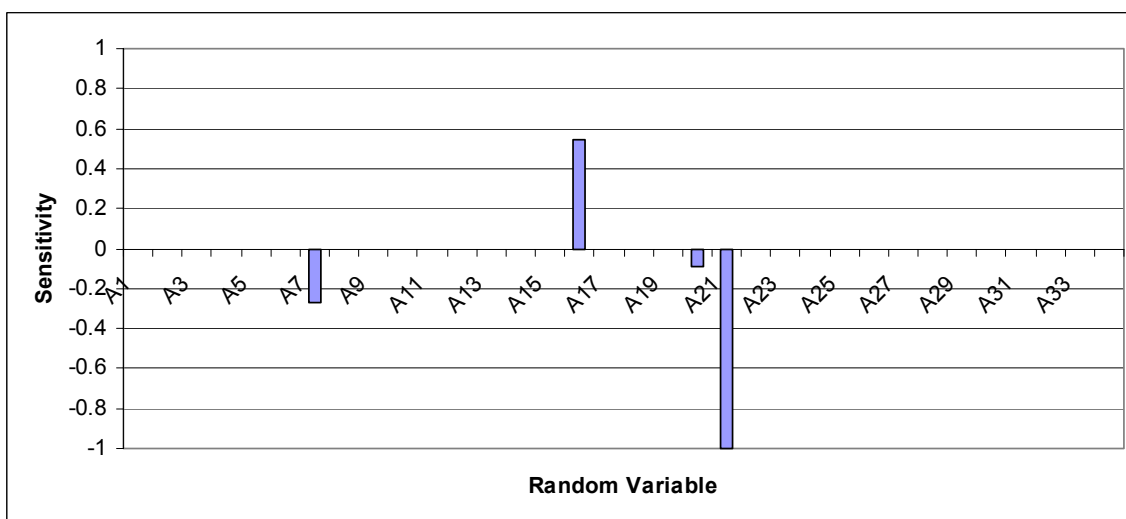


Figure B.4 – Sensitivity with respect to standard deviation for Panel #4

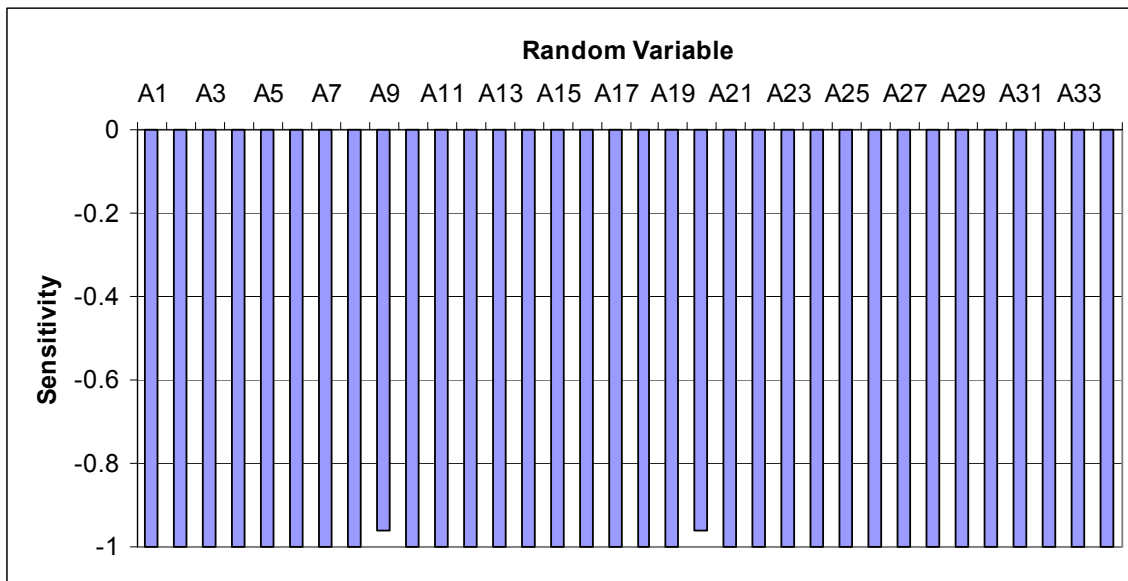


Figure B.5 – Sensitivity with respect to standard deviation for Panel #5

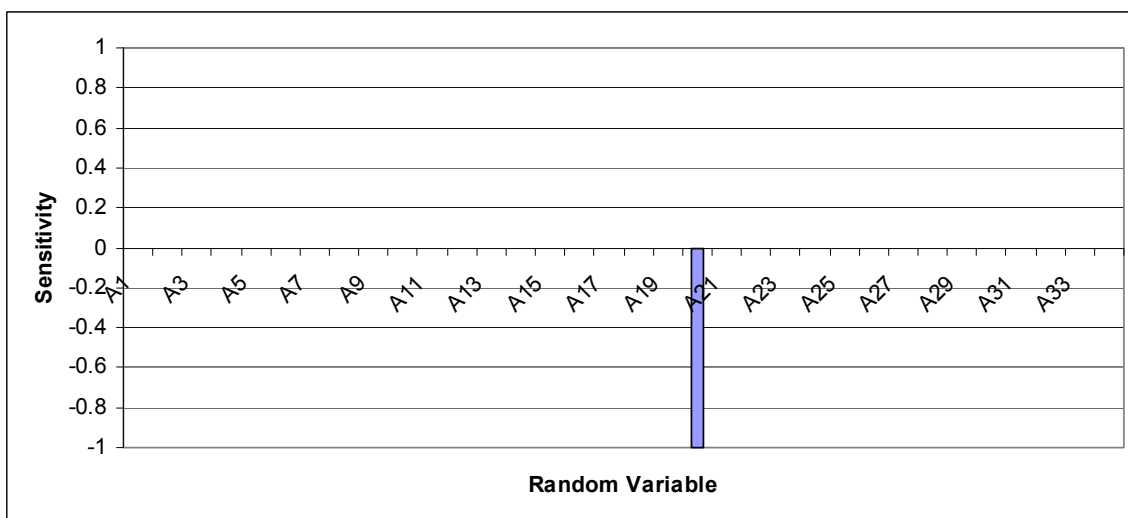


Figure B.6 – Sensitivity with respect to standard deviation for Panel #6



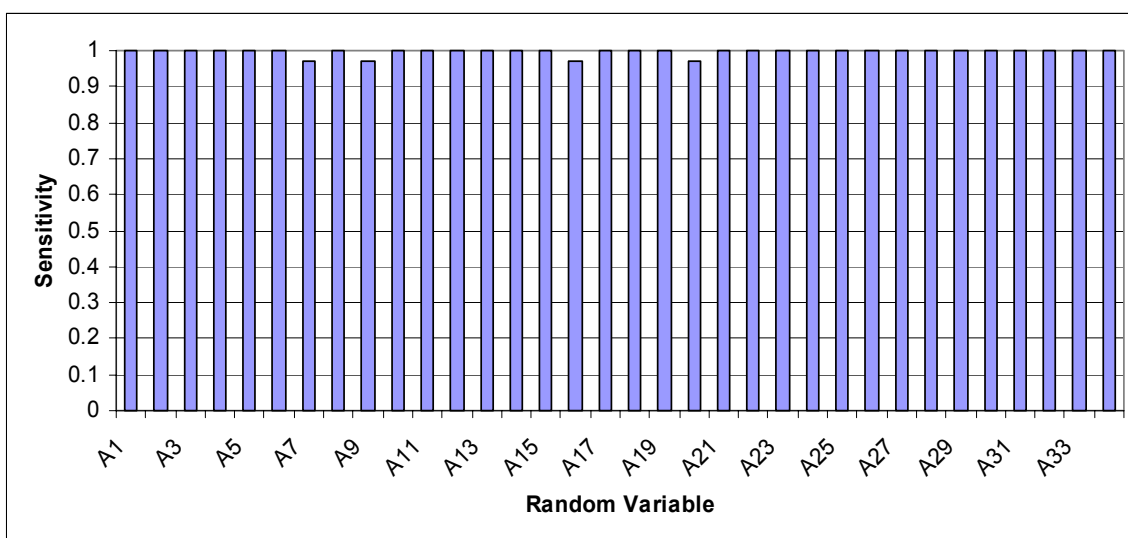


Figure B.7 – Sensitivity with respect to standard deviation for Panel #7

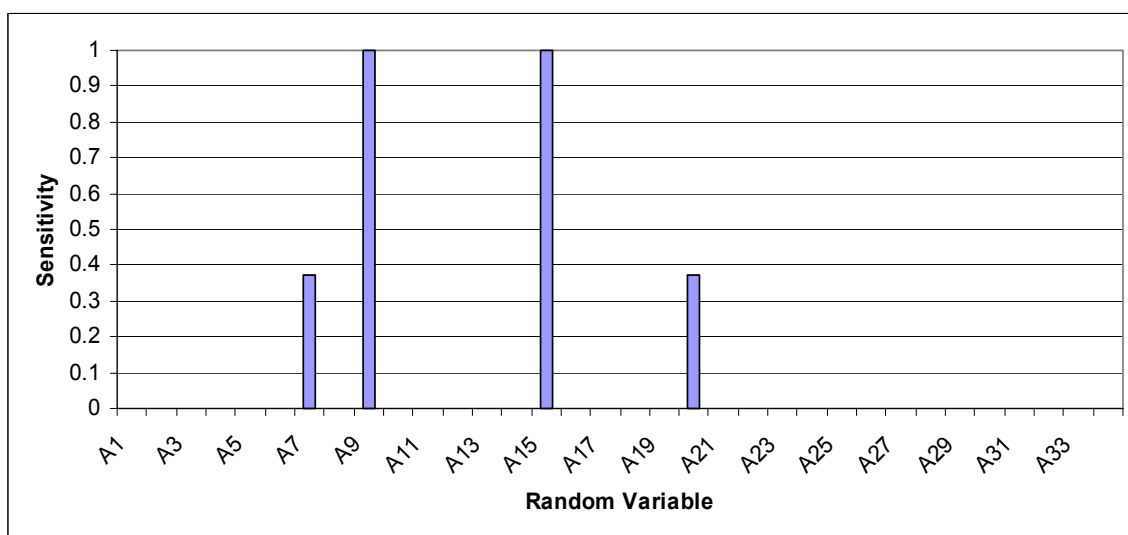


Figure B.8 – Sensitivity with respect to standard deviation for Panel #8

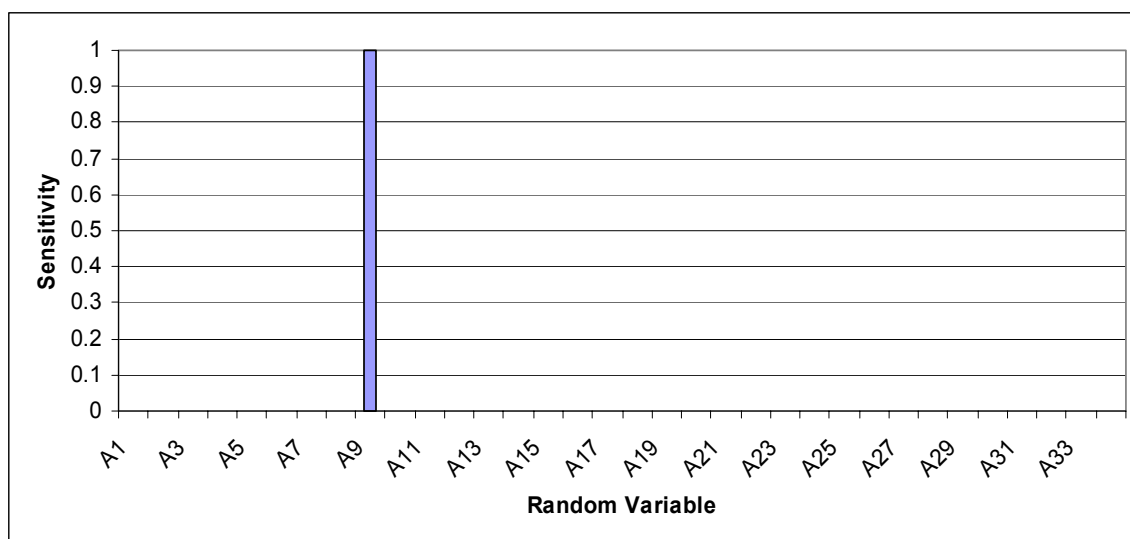


Figure B.9 – Sensitivity with respect to standard deviation for Panel #9

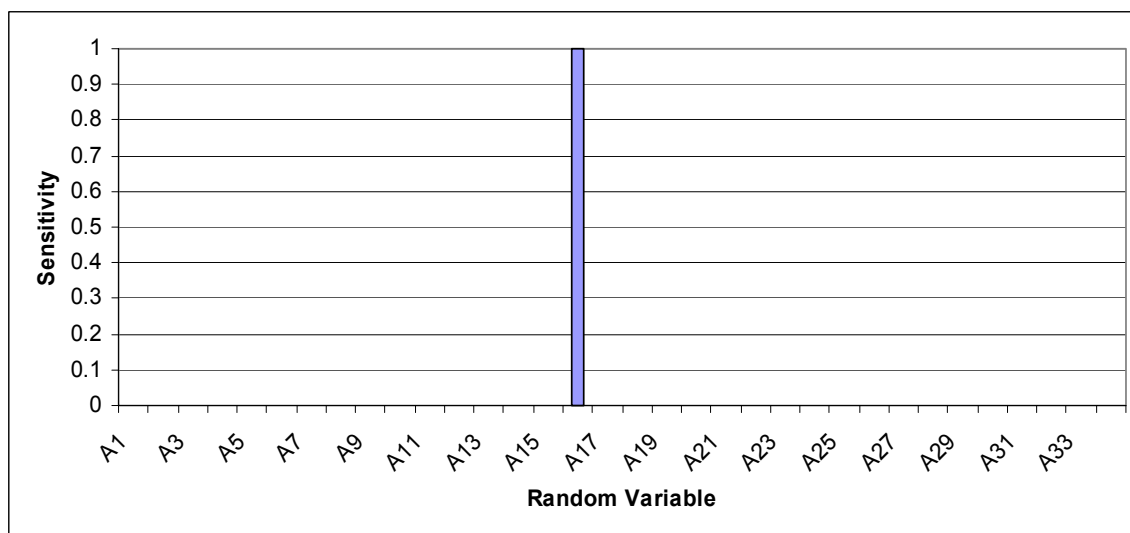


Figure B.10 – Sensitivity with respect to standard deviation for Panel #10

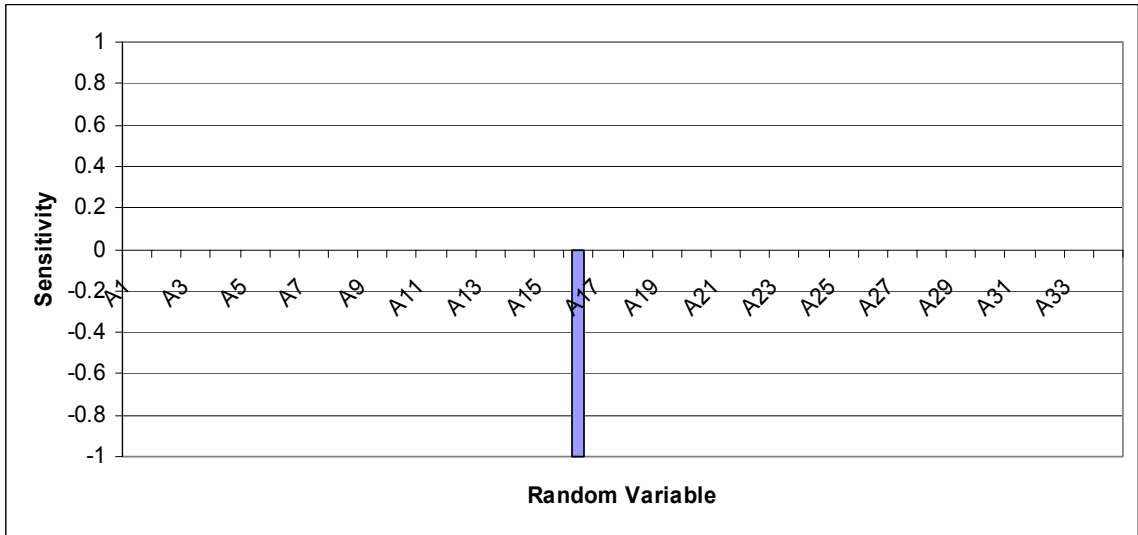


Figure B.11 – Sensitivity with respect to standard deviation for Panel #11

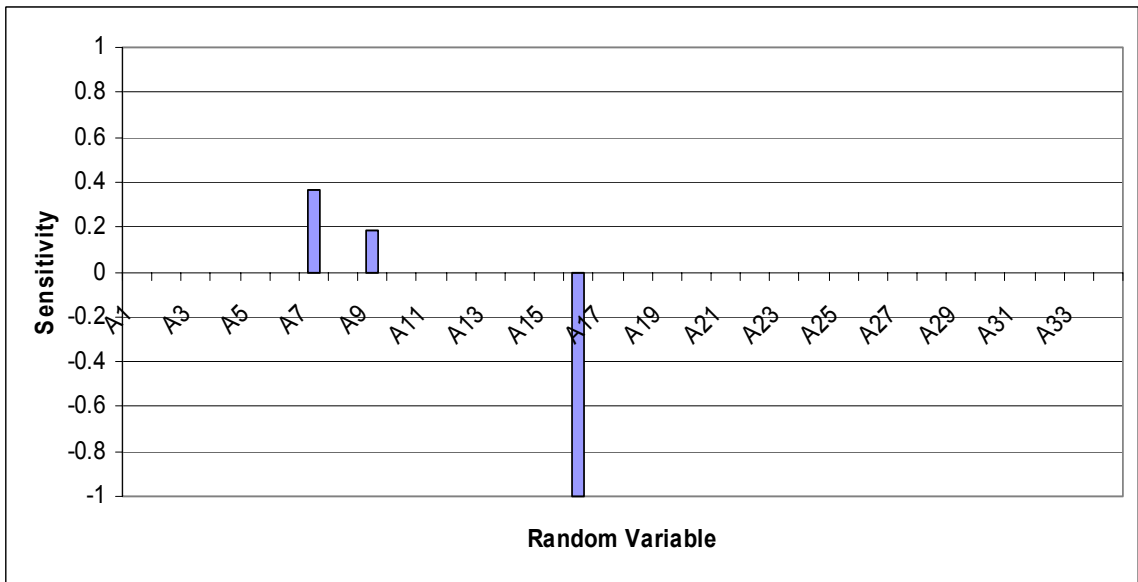


Figure B.12 – Sensitivity with respect to standard deviation for Panel #12

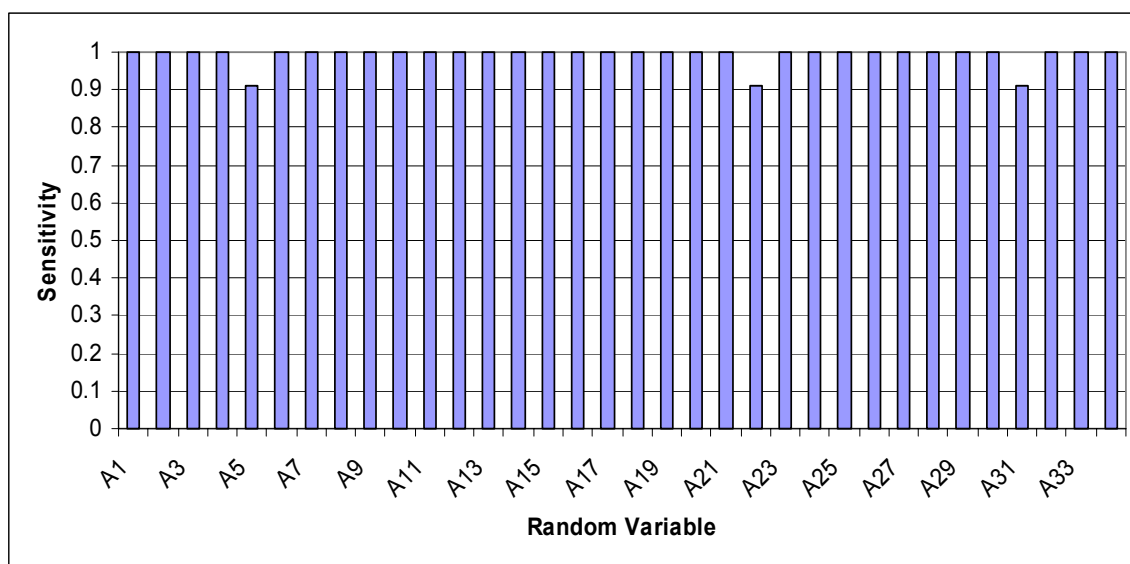


Figure B.13 – Sensitivity with respect to standard deviation for Panel #13

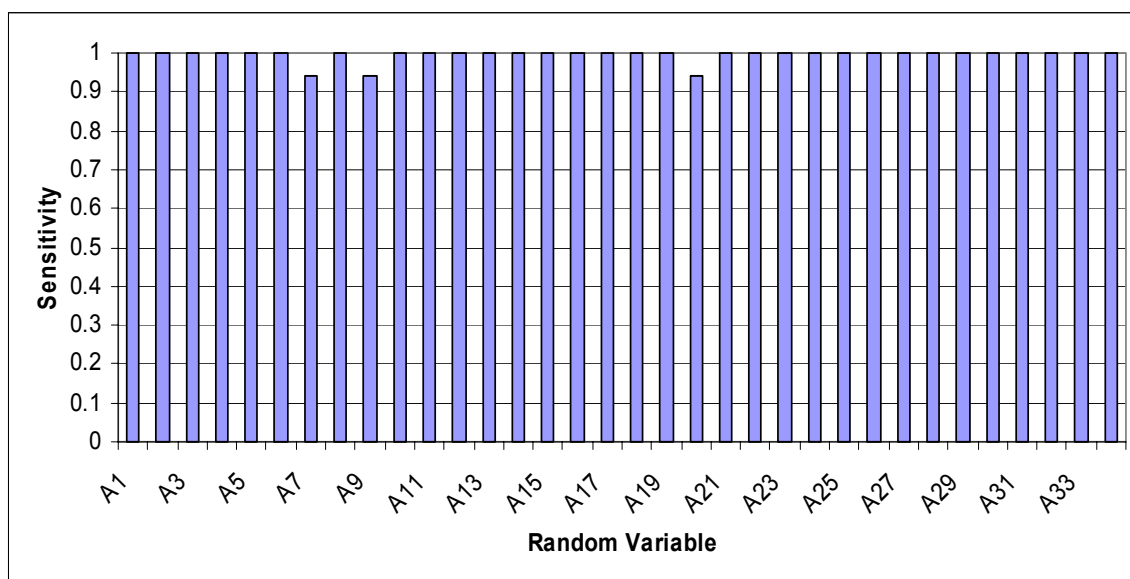


Figure B.14 – Sensitivity with respect to standard deviation for Panel #14

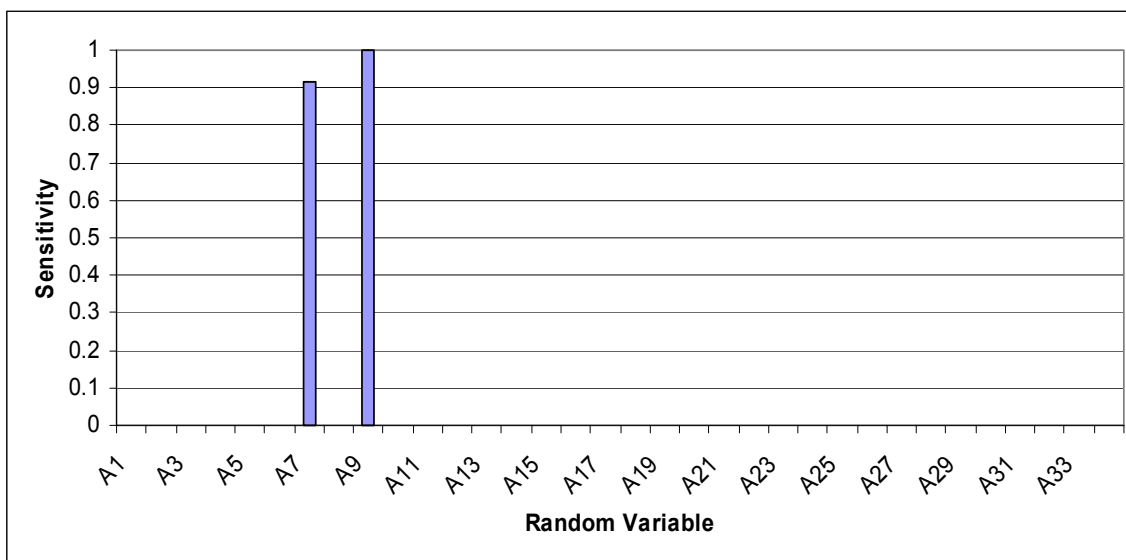


Figure B.15 – Sensitivity with respect to standard deviation for Panel #15

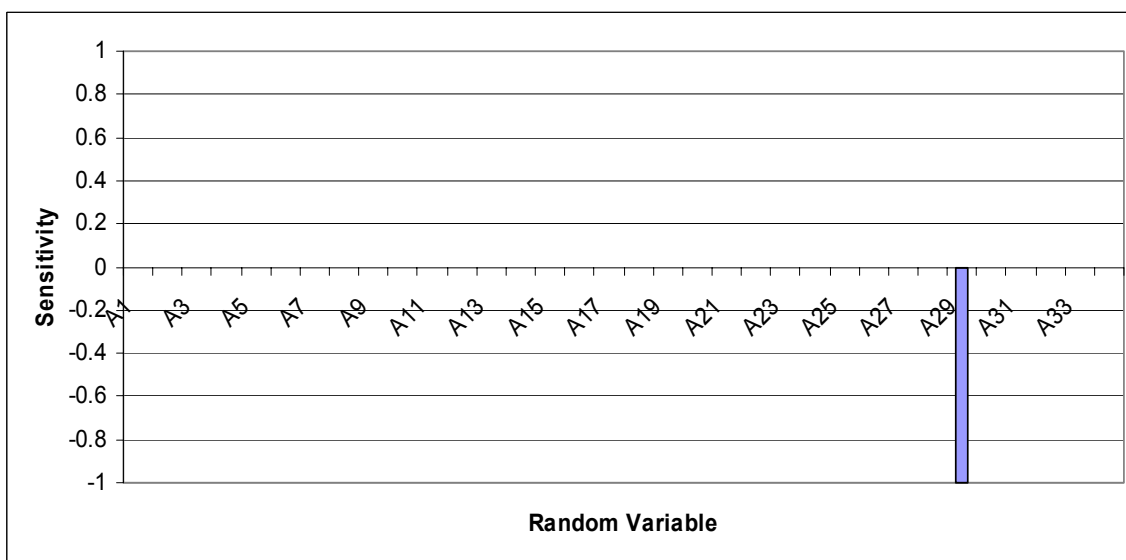


Figure B.16 – Sensitivity with respect to standard deviation for Panel #16

APPENDIX C  
NESSUS SAMPLE IMPUT FILE

```

*NESSUS
# Generated by NESSUS GUI, version: 8.1.0 (Build 190)
# Date generated: Sun Jun 19 19:25:49 CDT 2005

*TITLE test file
*DESCRIPTION
Use NASTRAN interaction to calculate reliability of Uniform based on
strain criteria.
*END DESCRIPTION

#
# Problem Statement:
#   g = R-0.01347822*Q
#   Q = FEA(M1, M2, M3, M4, M5, M6, M7, M8, M9, M10, M11, M12,
#   M13, M14, M15, M16, M17, M18, M19, M20, M21, M22, M23, M24,
#   M25, M26, M27, M28, M29, M30, M31, M32, M33, M34)

#
# Z-function definitions
#
*ZFDEFINE
  *MODEL analytical_1
#   g = R-0.01347822*Q
  *TYPE ANALYTICAL
    R Q
  *END TYPE
  *CVARIABLE g
  *END CVARIABLE g
  *END MODEL analytical_1
  *MODEL FEA
#   Q = FEA(M1, M2, M3, M4, M5, M6, M7, M8, M9, M10, M11, M12,
#   M13, M14, M15, M16, M17, M18, M19, M20, M21, M22, M23, M24,
#   M25, M26, M27, M28, M29, M30, M31, M32, M33, M34)
  *TYPE USER_DEFINED
    M1 M2 M3 M4 M5 M6 M7 M8 M9 M10 M11 M12 M13 M14 M15 M16 M17
M18 M19
    M20 M21 M22 M23 M24 M25 M26 M27 M28 M29 M30 M31 M32 M33 M34
  *END TYPE
  *COMMAND INTERACTIVE
# Include commands for executing the external program.
# Note that the input and output files defined below
# must be consistent with the execution command.
/home/dmr71/newpanel
#nastran ctest.bdf scr=yes news=no bat=no old=no
  *END COMMAND
  *ADVANCED_OPTIONS
    BATCH_INPUT true
    NORESTART true
  *END ADVANCED_OPTIONS
  *INPUTS
#   Label Destination
    input-1 magload.txt
  *END INPUTS
  *OUTPUTS

```

```

        panelmaxout.txt
*END OUTPUTS
*CARIABLE Q
    EXTERNAL_RESULTS FILE
    LINE_NUMBER 2
    START_COLUMN 9
    END_COLUMN 18
*END CVARIABLE Q
*END MODEL FEA
*END ZFDEFINE

#
# Variable definitions and mappings
#
*RVDEFINE
    *DEFINE g
    *END DEFINE g
    *DEFINE R
#       Mean           Stdev           Type
        4192.0         586.88         Normal
    *END DEFINE R
    *DEFINE Q
    *END DEFINE Q
    *DEFINE M1
#       Mean           Stdev           Type
        -20.71        -8.49          Lognormal
    *MAPPING FEA
        *BLOCK input-1
            *LOCATION
                *COLUMNS
#                   Start End Format
                    1 7 F7.1
                *END COLUMNS
#                   Start End Offset Skip
                *LINES 1 1 1 1
1.0
            *END LOCATION
        *END BLOCK input-1
    *END MAPPING FEA
*END DEFINE M1
*DEFINE M2
#       Mean           Stdev           Type
        -8.67         -3.56          Lognormal
    *MAPPING FEA
        *BLOCK input-1
            *LOCATION
                *COLUMNS
#                   Start End Format
                    1 7 F7.1
                *END COLUMNS
#                   Start End Offset Skip
                *LINES 2 2 1 1
1.0

```



```

                                *END LINES
                                *END LOCATION
                                *END BLOCK input-1
                                *END MAPPING FEA
                                *END DEFINE M2
                                *DEFINE M3
#                               Mean           Stdev           Type
                                -12.74        -5.22            Lognormal
                                *MAPPING FEA
                                *BLOCK input-1
                                *LOCATION
                                *COLUMNS
#                               Start End Format
                                1 7 F7.1
                                *END COLUMNS
#                               Start End Offset Skip
                                *LINES 3 3 1 1
1.0
                                *END LINES
                                *END LOCATION
                                *END BLOCK input-1
                                *END MAPPING FEA
                                *END DEFINE M3
                                *DEFINE M4
#                               Mean           Stdev           Type
                                -11.3         -4.63            Lognormal
                                *MAPPING FEA
                                *BLOCK input-1
                                *LOCATION
                                *COLUMNS
#                               Start End Format
                                1 7 F7.1
                                *END COLUMNS
#                               Start End Offset Skip
                                *LINES 4 4 1 1
1.0
                                *END LINES
                                *END LOCATION
                                *END BLOCK input-1
                                *END MAPPING FEA
                                *END DEFINE M4
                                *DEFINE M5
#                               Mean           Stdev           Type
                                -11.69        -4.79            Lognormal
                                *MAPPING FEA
                                *BLOCK input-1
                                *LOCATION
                                *COLUMNS
#                               Start End Format
                                1 7 F7.1
                                *END COLUMNS
#                               Start End Offset Skip
                                *LINES 5 5 1 1
1.0

```

```

                                *END LINES
                                *END LOCATION
                                *END BLOCK input-1
                                *END MAPPING FEA
                                *END DEFINE M5
                                *DEFINE M6
#                               Mean           Stdev           Type
                                -32.11        -13.17           Lognormal
                                *MAPPING FEA
                                *BLOCK input-1
                                *LOCATION
                                *COLUMNS
#                               Start End Format
                                1 7 F7.1
                                *END COLUMNS
#                               Start End Offset Skip
                                *LINES 6 6 1 1
1.0
                                *END LINES
                                *END LOCATION
                                *END BLOCK input-1
                                *END MAPPING FEA
                                *END DEFINE M6
                                *DEFINE M7
#                               Mean           Stdev           Type
                                5.81          2.38            Lognormal
                                *MAPPING FEA
                                *BLOCK input-1
                                *LOCATION
                                *COLUMNS
#                               Start End Format
                                1 7 F7.1
                                *END COLUMNS
#                               Start End Offset Skip
                                *LINES 7 7 1 1
1.0
                                *END LINES
                                *END LOCATION
                                *END BLOCK input-1
                                *END MAPPING FEA
                                *END DEFINE M7
                                *DEFINE M8
#                               Mean           Stdev           Type
                                -38.23        -15.67          Lognormal
                                *MAPPING FEA
                                *BLOCK input-1
                                *LOCATION
                                *COLUMNS
#                               Start End Format
                                1 7 F7.1
                                *END COLUMNS
#                               Start End Offset Skip
                                *LINES 8 8 1 1
1.0

```

```

                                *END LINES
                                *END LOCATION
                                *END BLOCK input-1
                                *END MAPPING FEA
                                *END DEFINE M8
                                *DEFINE M9
#                               Mean           Stdev           Type
                               5.63           2.31             Lognormal
                                *MAPPING FEA
                                *BLOCK input-1
                                *LOCATION
                                *COLUMNS
#                               Start End Format
                               1 7 F7.1
                                *END COLUMNS
#                               Start End Offset Skip
                                *LINES 9 9 1 1
1.0
                                *END LINES
                                *END LOCATION
                                *END BLOCK input-1
                                *END MAPPING FEA
                                *END DEFINE M9
                                *DEFINE M10
#                               Mean           Stdev           Type
                               -39.26        -16.1            Lognormal
                                *MAPPING FEA
                                *BLOCK input-1
                                *LOCATION
                                *COLUMNS
#                               Start End Format
                               1 7 F7.1
                                *END COLUMNS
#                               Start End Offset Skip
                                *LINES 10 10 1 1
1.0
                                *END LINES
                                *END LOCATION
                                *END BLOCK input-1
                                *END MAPPING FEA
                                *END DEFINE M10
                                *DEFINE M11
#                               Mean           Stdev           Type
                               -5.73          -2.35            Lognormal
                                *MAPPING FEA
                                *BLOCK input-1
                                *LOCATION
                                *COLUMNS
#                               Start End Format
                               1 7 F7.1
                                *END COLUMNS
#                               Start End Offset Skip
                                *LINES 11 11 1 1
1.0

```

```

                                *END LINES
                                *END LOCATION
                                *END BLOCK input-1
                                *END MAPPING FEA
                                *END DEFINE M11
                                *DEFINE M12
#                               Mean           Stdev           Type
                               -40.66         -16.67           Lognormal
                                *MAPPING FEA
                                *BLOCK input-1
                                *LOCATION
                                *COLUMNS
#                               Start End Format
                               1 7 F7.1
                                *END COLUMNS
#                               Start End Offset Skip
                                *LINES 12 12 1 1
1.0
                                *END LINES
                                *END LOCATION
                                *END BLOCK input-1
                                *END MAPPING FEA
                                *END DEFINE M12
                                *DEFINE M13
#                               Mean           Stdev           Type
                               -17.16         -7.03            Lognormal
                                *MAPPING FEA
                                *BLOCK input-1
                                *LOCATION
                                *COLUMNS
#                               Start End Format
                               1 7 F7.1
                                *END COLUMNS
#                               Start End Offset Skip
                                *LINES 13 13 1 1
1.0
                                *END LINES
                                *END LOCATION
                                *END BLOCK input-1
                                *END MAPPING FEA
                                *END DEFINE M13
                                *DEFINE M14
#                               Mean           Stdev           Type
                               -37.18         -15.24           Lognormal
                                *MAPPING FEA
                                *BLOCK input-1
                                *LOCATION
                                *COLUMNS
#                               Start End Format
                               1 7 F7.1
                                *END COLUMNS
#                               Start End Offset Skip
                                *LINES 14 14 1 1
1.0

```

```

                *END LINES
            *END LOCATION
        *END BLOCK input-1
    *END MAPPING FEA
*END DEFINE M14
*DEFINE M15
#       Mean           Stdev           Type
      -23.13         -9.48         Lognormal
    *MAPPING FEA
        *BLOCK input-1
            *LOCATION
                *COLUMNS
#                   Start End Format
                   1 7 F7.1
            *END COLUMNS
#                   Start End Offset Skip
            *LINES 15 15 1 1
1.0
                *END LINES
            *END LOCATION
        *END BLOCK input-1
    *END MAPPING FEA
*END DEFINE M15
*DEFINE M16
#       Mean           Stdev           Type
      4.53           1.68         Lognormal
    *MAPPING FEA
        *BLOCK input-1
            *LOCATION
                *COLUMNS
#                   Start End Format
                   1 7 F7.1
            *END COLUMNS
#                   Start End Offset Skip
            *LINES 16 16 1 1
1.0
                *END LINES
            *END LOCATION
        *END BLOCK input-1
    *END MAPPING FEA
*END DEFINE M16
*DEFINE M17
#       Mean           Stdev           Type
      -32.13        -13.17        Lognormal
    *MAPPING FEA
        *BLOCK input-1
            *LOCATION
                *COLUMNS
#                   Start End Format
                   1 7 F7.1
            *END COLUMNS
#                   Start End Offset Skip
            *LINES 17 17 1 1
1.0

```

```

*END LINES
*END LOCATION
*END BLOCK input-1
*END MAPPING FEA
*END DEFINE M17
*DEFINE M18
#      Mean          Stdev          Type
      -27.68         -11.35         Lognormal
*MAPPING FEA
  *BLOCK input-1
    *LOCATION
      *COLUMNS
#              Start End Format
              1 7 F7.1
    *END COLUMNS
#              Start End Offset Skip
    *LINES 18 18 1 1
1.0

*END LINES
*END LOCATION
*END BLOCK input-1
*END MAPPING FEA
*END DEFINE M18
*DEFINE M19
#      Mean          Stdev          Type
      -4.59          -1.88         Lognormal
*MAPPING FEA
  *BLOCK input-1
    *LOCATION
      *COLUMNS
#              Start End Format
              1 7 F7.1
    *END COLUMNS
#              Start End Offset Skip
    *LINES 19 19 1 1
1.0

*END LINES
*END LOCATION
*END BLOCK input-1
*END MAPPING FEA
*END DEFINE M19
*DEFINE M20
#      Mean          Stdev          Type
      8.64           3.54          Lognormal
*MAPPING FEA
  *BLOCK input-1
    *LOCATION
      *COLUMNS
#              Start End Format
              1 7 F7.1
    *END COLUMNS
#              Start End Offset Skip
    *LINES 20 20 1 1
1.0

```

```

                *END LINES
            *END LOCATION
        *END BLOCK input-1
    *END MAPPING FEA
*END DEFINE M20
*DEFINE M21
#           Mean           Stdev           Type
           -26.67         -10.9           Lognormal
    *MAPPING FEA
        *BLOCK input-1
            *LOCATION
                *COLUMNS
#                   Start End Format
                   1 7 F7.1
            *END COLUMNS
#                   Start End Offset Skip
            *LINES 21 21 1 1
1.0
                *END LINES
            *END LOCATION
        *END BLOCK input-1
    *END MAPPING FEA
*END DEFINE M21
*DEFINE M22
#           Mean           Stdev           Type
           -30.76         -12.61          Lognormal
    *MAPPING FEA
        *BLOCK input-1
            *LOCATION
                *COLUMNS
#                   Start End Format
                   1 7 F7.1
            *END COLUMNS
#                   Start End Offset Skip
            *LINES 22 22 1 1
1.0
                *END LINES
            *END LOCATION
        *END BLOCK input-1
    *END MAPPING FEA
*END DEFINE M22
*DEFINE M23
#           Mean           Stdev           Type
           -16.35          -6.7            Lognormal
    *MAPPING FEA
        *BLOCK input-1
            *LOCATION
                *COLUMNS
#                   Start End Format
                   1 7 F7.1
            *END COLUMNS
#                   Start End Offset Skip
            *LINES 23 23 1 1
1.0

```

```

                *END LINES
            *END LOCATION
        *END BLOCK input-1
    *END MAPPING FEA
*END DEFINE M23
*DEFINE M24
#       Mean           Stdev           Type
      -2.67           -1.09           Lognormal
    *MAPPING FEA
        *BLOCK input-1
            *LOCATION
                *COLUMNS
#                   Start End Format
                   1 7 F7.1
            *END COLUMNS
#                   Start End Offset Skip
            *LINES 24 24 1 1
1.0

                *END LINES
            *END LOCATION
        *END BLOCK input-1
    *END MAPPING FEA
*END DEFINE M24
*DEFINE M25
#       Mean           Stdev           Type
      -22.51          -9.23           Lognormal
    *MAPPING FEA
        *BLOCK input-1
            *LOCATION
                *COLUMNS
#                   Start End Format
                   1 7 F7.1
            *END COLUMNS
#                   Start End Offset Skip
            *LINES 25 25 1 1
1.0

                *END LINES
            *END LOCATION
        *END BLOCK input-1
    *END MAPPING FEA
*END DEFINE M25
*DEFINE M26
#       Mean           Stdev           Type
      -28.58          -11.72          Lognormal
    *MAPPING FEA
        *BLOCK input-1
            *LOCATION
                *COLUMNS
#                   Start End Format
                   1 7 F7.1
            *END COLUMNS
#                   Start End Offset Skip
            *LINES 26 26 1 1
1.0

```



```

                                *END LINES
                                *END LOCATION
                                *END BLOCK input-1
                                *END MAPPING FEA
                                *END DEFINE M26
                                *DEFINE M27
#                               Mean           Stdev           Type
                               -22.15        -9.08            Lognormal
                                *MAPPING FEA
                                *BLOCK input-1
                                *LOCATION
                                *COLUMNS
#                               Start End Format
                               1 7 F7.1
                                *END COLUMNS
#                               Start End Offset Skip
                                *LINES 27 27 1 1
1.0
                                *END LINES
                                *END LOCATION
                                *END BLOCK input-1
                                *END MAPPING FEA
                                *END DEFINE M27
                                *DEFINE M28
#                               Mean           Stdev           Type
                               -13.3         -5.45            Lognormal
                                *MAPPING FEA
                                *BLOCK input-1
                                *LOCATION
                                *COLUMNS
#                               Start End Format
                               1 7 F7.1
                                *END COLUMNS
#                               Start End Offset Skip
                                *LINES 28 28 1 1
1.0
                                *END LINES
                                *END LOCATION
                                *END BLOCK input-1
                                *END MAPPING FEA
                                *END DEFINE M28
                                *DEFINE M29
#                               Mean           Stdev           Type
                               -4.38         -1.8             Lognormal
                                *MAPPING FEA
                                *BLOCK input-1
                                *LOCATION
                                *COLUMNS
#                               Start End Format
                               1 7 F7.1
                                *END COLUMNS
#                               Start End Offset Skip
                                *LINES 29 29 1 1
1.0

```

```

*END LINES
*END LOCATION
*END BLOCK input-1
*END MAPPING FEA
*END DEFINE M29
*DEFINE M30
#      Mean          Stdev          Type
      -17.64         -7.23          Lognormal
*MAPPING FEA
  *BLOCK input-1
    *LOCATION
      *COLUMNS
#              Start End Format
              1 7 F7.1
    *END COLUMNS
#              Start End Offset Skip
    *LINES 30 30 1 1
1.0

*END LINES
*END LOCATION
*END BLOCK input-1
*END MAPPING FEA
*END DEFINE M30
*DEFINE M31
#      Mean          Stdev          Type
      -24.83         -10.18         Lognormal
*MAPPING FEA
  *BLOCK input-1
    *LOCATION
      *COLUMNS
#              Start End Format
              1 7 F7.1
    *END COLUMNS
#              Start End Offset Skip
    *LINES 31 31 1 1
1.0

*END LINES
*END LOCATION
*END BLOCK input-1
*END MAPPING FEA
*END DEFINE M31
*DEFINE M32
#      Mean          Stdev          Type
      -24.43         -10.02         Lognormal
*MAPPING FEA
  *BLOCK input-1
    *LOCATION
      *COLUMNS
#              Start End Format
              1 7 F7.1
    *END COLUMNS
#              Start End Offset Skip
    *LINES 32 32 1 1
1.0

```

```

                *END LINES
            *END LOCATION
        *END BLOCK input-1
    *END MAPPING FEA
*END DEFINE M32
*DEFINE M33
#       Mean           Stdev           Type
      -20.5           -8.4           Lognormal
    *MAPPING FEA
        *BLOCK input-1
            *LOCATION
                *COLUMNS
#                   Start End Format
                   1 7 F7.1
            *END COLUMNS
#                   Start End Offset Skip
            *LINES 33 33 1 1
1.0
                *END LINES
            *END LOCATION
        *END BLOCK input-1
    *END MAPPING FEA
*END DEFINE M33
*DEFINE M34
#       Mean           Stdev           Type
      -18.89          -7.74           Lognormal
    *MAPPING FEA
        *BLOCK input-1
            *LOCATION
                *COLUMNS
#                   Start End Format
                   1 7 F7.1
            *END COLUMNS
#                   Start End Offset Skip
            *LINES 34 34 1 1
1.0
                *END LINES
            *END LOCATION
        *END BLOCK input-1
    *END MAPPING FEA
*END DEFINE M34
*END RVDEFINE

#
# Probabilistic analysis settings
#
*PADEFINE
  *METHOD FPI # Advanced first order reliability method (FPI)
    *ADVANCED_OPTIONS
  *END ADVANCED_OPTIONS
*END METHOD FPI
*ANALYSIS_TYPE ZLEVEL
  0.0
*END ANALYSIS_TYPE

```

```
*END PADEFINE

#
# Model definitions
#
*MODELDEFINE
*MODEL analytical_1
*INPUT a1
R-0.01347822*Q
*END INPUT a1
*END MODEL analytical_1
*MODEL FEA
*INPUT_IMPORT input-1
FEA/run/magload.txt
*END INPUT_IMPORT input-1
*END MODEL FEA
*END MODELDEFINE

*END NESSUS
#-----END OF FILE-----
```

APPENDIX D  
MONTE CARLO SIMULATION RESULTS

The AFORM solution procedure described in Chapter V was not able to provide a solution for panel #2. In order to obtain a full set of results, panel #2 was analyzed using a 2000 samples Monte Carlo Simulation (MCS). The results of the analysis were plotted so an estimate of the probability of failure ( $P_f$ ) and the reliability index ( $\beta$ ) could be obtained. A MCS analysis for panel #3 was also performed so comparison could be made with the results obtained from the AFORM solution. The results are presented in figures D.1 and D.2.

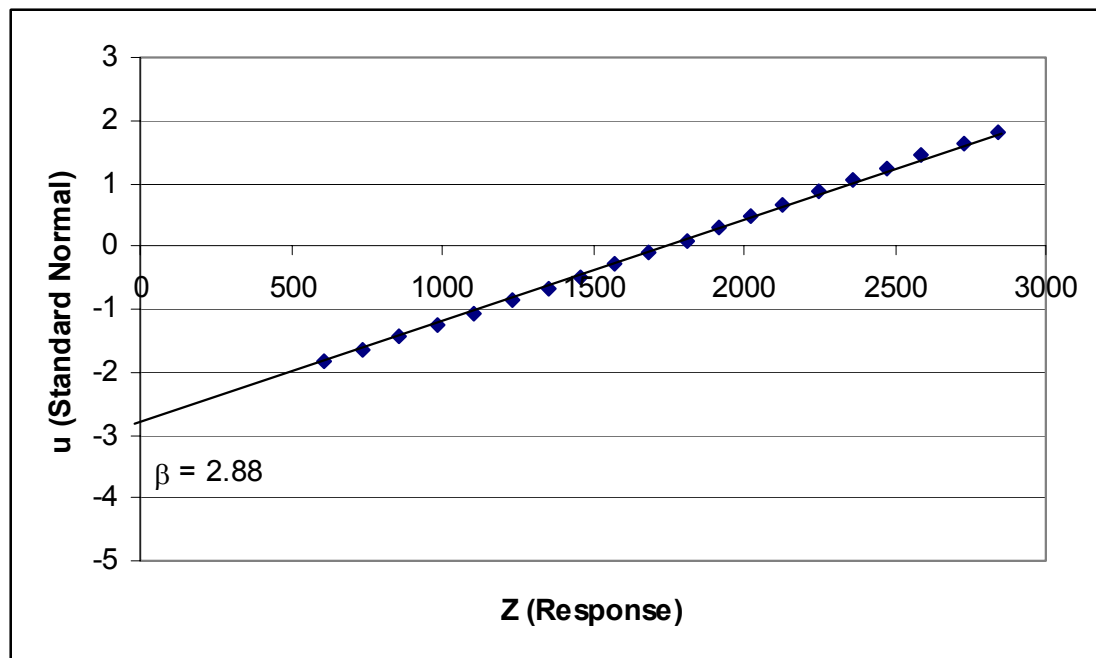


Figure D.1 – MCS results for panel #2

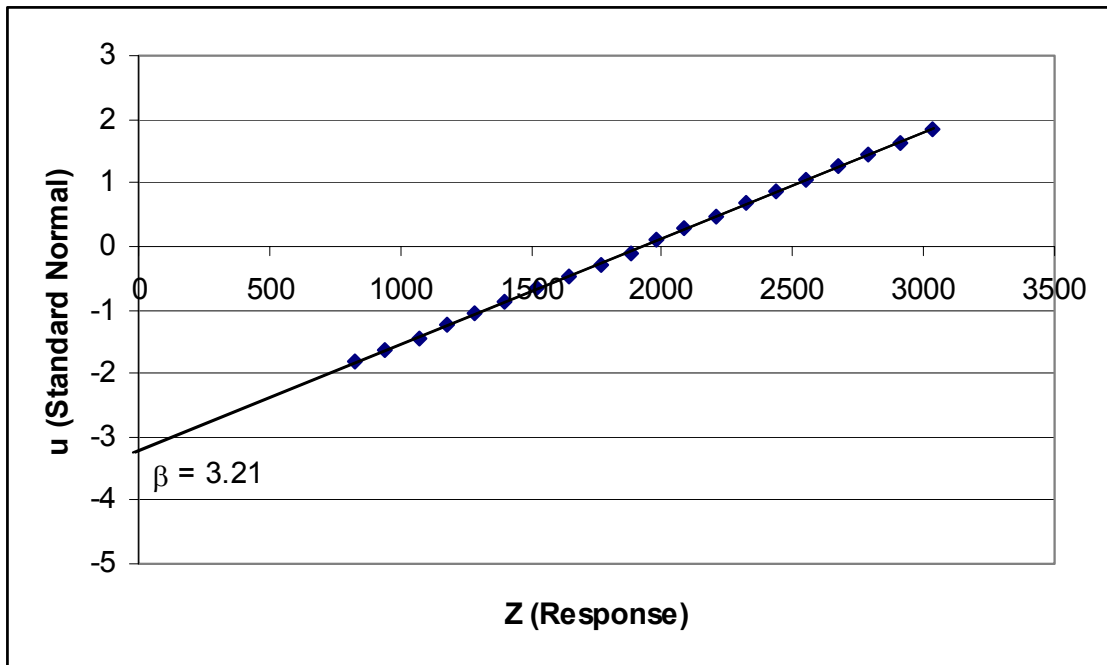


Figure D.2 – MCS results for panel #3

The results for panel #3 show that the AFORM solution overestimates the reliability index, as expected, but it provides results comparable to a MCS simulation.